

**A POLY (OCTANEDIOL CITRATE)/GALLIUM-CONTAINING
BIOGLASS COMPOSITE FOR BONE TISSUE REGENERATION**

EHSAN ZEIMARAN

**FACULTY OF ENGINEERING
UNIVERSITY OF MALAYA
KUALA LUMPUR**

2016

**A POLY (OCTANEDIOL CITRATE)/GALLIUM-
CONTAINING BIOGLASS COMPOSITE FOR BONE
TISSUE REGENERATION**

EHSAN ZEIMARAN

**THESIS SUBMITTED IN FULFILMENT OF THE
REQUIREMENTS FOR THE DEGREE OF DOCTOR OF
PHILOSOPHY**

**FACULTY OF ENGINEERING
UNIVERSITY OF MALAYA
KUALA LUMPUR**

2016

UNIVERSITY OF MALAYA

ORIGINAL LITERARY WORK DECLARATION

Name of Candidate: **Ehsan Zeimaran**

Registration/Matric No: **KHA120159**

Name of Degree: **Doctor of Philosophy**

Title of Project Paper/Research Report/Dissertation/Thesis (“this Work”):

A poly (octanediol citrate)/gallium-containing bioglass composite for bone tissue regeneration

Field of Study: **Biomedical Engineering (Biomaterials and Tissue Engineering)**

I do solemnly and sincerely declare that:

- (1) I am the sole author/writer of this Work;
- (2) This Work is original;
- (3) Any use of any work in which copyright exists was done by way of fair dealing and for permitted purposes and any excerpt or extract from, or reference to or reproduction of any copyright work has been disclosed expressly and sufficiently and the title of the Work and its authorship have been acknowledged in this Work;
- (4) I do not have any actual knowledge nor do I ought reasonably to know that the making of this work constitutes an infringement of any copyright work;
- (5) I hereby assign all and every right in the copyright to this Work to the University of Malaya (“UM”), who henceforth shall be owner of the copyright in this Work and that any reproduction or use in any form or by any means whatsoever is prohibited without the written consent of UM having been first had and obtained;
- (6) I am fully aware that if in the course of making this Work I have infringed any copyright whether intentionally or otherwise, I may be subject to legal action or any other action as may be determined by UM.

Candidate’s Signature

Date:

Subscribed and solemnly declared before,

Witness’s Signature

Date:

Name:

Designation

ABSTRACT

Bone can be affected by osteosarcomae requiring surgical excision of the tumor as part of a treatment regime. Complete removal of cancerous cells is difficult and conventionally requires the removal of a margin of safety around the tumor to offer improved patient prognosis. Gallium has been shown to be clinically effective, both against bone resorption and for the treatment of cancer-related hypercalcemia. This work considers a novel series of composite scaffolds based on poly (octanediol citrate) (POC) impregnated with a gallium-containing bioactive glass (0.48SiO₂-0.12CaO-0.32ZnO-0.08Ga₂O₃, molar fraction) microparticles for possible incorporation into bone following tumor removal. The objective of this research was to fabricate and characterize these scaffolds and subsequently report on their mechanical, thermal, structural and biological properties. The porous microcomposite scaffolds, with various concentrations of bioactive glass (10, 20, 30 wt%) incorporated, were fabricated using a salt leaching technique. The scaffolds exhibited compression moduli in the range of 0.3-7 MPa. The addition of bioactive glass increased the mechanical properties even though porosity increased. Furthermore, increasing the concentration of bioactive glass had a significant influence on glass transition temperature from 2.5 °C for the pure polymer to approximately 25 °C for 30 % bioactive glass-containing composite. The ion release study revealed that composites containing 30 % bioactive glass had the highest ion release ratio after 28 days of soaking in phosphate buffered saline (PBS). The interaction of the bioactive glass phase with POC led to the formation of additional ionic crosslinks, aside from the covalent crosslinks, which further resulted in increased stiffness and decreased weight loss. The antibacterial activity of these scaffolds was investigated against both Gram-positive (*Staphylococcus aureus*) and Gram-negative (*Escherichia coli*) bacteria in vitro. The ability of the scaffolds to release ions and the subsequent ingress of these ions into

hard tissue was evaluated using a bovine bone model. Scaffolds containing bioactive glass exhibited antibacterial activity which increased with higher bioactive glass loads; viable cells decreased to about 20 % for the composite scaffold containing 30 % bioactive glass. The Ga^{3+} release rate increased as a function of time and Zn^{2+} was shown to incorporate into the surrounding bone. The effect of composite scaffolds on growth and osteogenic differentiation of human osteoblast-like cells and human bone marrow-derived mesenchymal stem cells (hBMSCs) was investigated. The osteoblast-like cells were well attached and growth on composites and collagen synthesis increased particularly with the 10 % bioactive glass concentration. All the scaffolds were able to support the growth of hBMSCs and guide their osteogenic differentiation without osteogenic media stimulation. The expression of bone-associated genes (collagen I, osteonectin and osteocalcin, bone morphogenetic protein 2, runt-related transcription factor 2) was significantly increased by a culture time for of up to 2 weeks, particularly for the composite scaffolds loaded with 10 % bioactive glass. The composite scaffolds significantly stimulated alkaline phosphatase (ALP) activity compared to the pure POC scaffolds. Cellular mineralization of the secreted extracellular matrix illustrated a higher calcium level on the composites than pure POC, and increased with culture time. These results suggest that composite scaffolds of POC and a bioactive glass doped with therapeutic elements provides favourable conditions for osteogenic differentiation of hBMSCs and can potentially be used to induce bone healing and regeneration.

ABSTRAK

Tulang yang terjejas oleh “osteosarcomae” memerlukan pembedahan untuk membuang tumor sebagai sebahagian daripada kaedah rawatan. Pembuangan sepenuhnya sel-sel kanser adalah sukar dan secara konvensional melibatkan penyingkiran sel-sel yang sihat di sekeliling ketumbuhan menawarkan penambahan baik prognosis pesakit. Secara klinikal, Gallium telah terbukti berkesan terhadap penerapan semula tulang dan rawatan yang berkaitan dengan kanser hyperkalsemia. Penyelidikan ini dianggap novel dalam bidang perancah komposit di mana poli (octanediolsitrat) (POC) diresapi dengan gallium-biogelas bersaiz mikro untuk kemungkinan penggabungan ke dalam tulang untuk penyingkiran ketumbuhan. Objektif kajian ini adalah untuk membuat dan mencirikan perancah ini dan seterusnya melaporkan sifat mekanik, haba, struktur dan biologi mereka. Perancah berliang dengan pelbagai kepekatan biogelas (10, 20, 30 % berat) telah dimasukkan dengan menggunakan teknik larut lesap garam (salt leaching). Perancah ini mempunyai modulus mampatan dalam lingkungan 0,3-7 MPa. Penambahan kaca bioaktif meningkatkan sifat mekanik walaupun keliangan meningkat. Selain itu, peningkatan kepekatan kaca bioaktif mempunyai pengaruh yang besar ke atas suhu peralihan kaca dari 2.5°C untuk polimer tulen ke kira-kira 25 °C untuk komposit yang mengandungi 30 % kaca bioaktif. Kajian terhadap pembebasan ion mendedahkan bahawa komposit yang mengandungi 30 % kaca bioaktif mempunyai nisbah tertinggi selepas 28 hari terendam dalam larutan fosfat (PBS). Interaksi di antara biogelas dengan POC membawa pembentukan penyilangan ionic tambahan di samping penyilangan kovalen dan seterusnya meningkatkan kekerasan dan pengurangan berat. Aktiviti antibakteria perancah ini telah disiasat terhadap kedua-dua jenis bakteria iaitu Gram-positif (*Staphylococcus aureus*) dan Gram-negatif (*Escherichia coli*). Keupayaan perancah untuk membebaskan dan menyerap ion ke dalam tisu keras dinilai dengan

menggunakan model tulang lembu. Perancah yang mengandungi kaca bioaktif menunjukkan aktiviti anti-bakteria dan meningkat banyak dalam in vitro dengan gelas bioaktif yang lebih tinggi; sel-sel hidup menurun ke kira-kira 20 % untuk perancah komposit yang mengandungi 30% gelas bioaktif. Kadar pelepasan ion Ga^{3+} meningkat berkadaran terus dengan masa dan ion Zn^{2+} telah diserap ke dalam sekitaran tulang. Kesan perancah komposit dalam pertumbuhan dan pembezaan osteogenik sel osteoblast seperti manusia dan sel-sel mesenchymal stem sumsum yang diperolehi daripada tulang manusia (hBMSCs) telah dikaji. Sel-sel seperti osteoblast melekat dan bertumbuh pada komposit dan sintesis kolagen meningkat terutamanya dengan 10 % kepekatan kaca bioaktif. Semua perancah dapat menyokong pertumbuhan hBMSCs dan membimbing pembezaan osteogeniknya tanpa rangsangan media osteogenik. Kehadiran gen yang berkaitan dengan tulang (kolagen I, osteonectin dan osteocalcin, tulang morphogenetic protein 2, faktor transkripsi 2 yang berkaitan runt) telah meningkat dengan ketara sehingga 2 minggu, terutamanya bagi perancah komposit yang mengandungi 10 % kaca bioaktif. Perancah komposit merangsang aktiviti phosphatase alkali (ALP) dengan signifikan berbanding dengan perancah POC tulen. Mineral selular daripada rembesan matriks extracellular telah menggambarkan tahap kalsium yang lebih tinggi pada komposit berbanding dengan POC tulen dan meningkat dengan masa kultur. Keputusan ini menunjukkan bahawa perancah komposit POC dan gelas bioaktif yang didopkan dengan unsur-unsur terapeutik menyediakan keadaan yang baik bagi pembezaan osteogenik hBMSCs dan berpotensi dapat digunakan untuk mendorong penyembuhan dan pertumbuhan semula tulang.

ACKNOWLEDGEMENTS

I owe thanks to a great many people who so generously contributed to the work presented in this thesis.

Special mention goes to my enthusiastic supervisors, Prof. Mark Towler and Assoc. Prof. Belinda Pinguan-Murphy whose encouragement, guidance and support from the initial to the final level enabled me to develop an understanding of the subject. I acknowledge my sincere thanks to Assoc. Prof. Nahrizul Adib Kadri for his generous support, both financial and moral.

I wish to express my gratitude to members of National Orthopaedic Centre of Excellence in Research and Learning (NOCERAL), Prof. Tunku Kamarul, Dr. Hanumantha Rao Balaji Raghavendran, Dr. Malliga Raman Murali and Saktiswaren Mohan for their help and advice on this research.

I am greatly indebted to the University of Malaya for its financial support under the High Impact Research (HIR), grant number: UM.C/HIR/MOHE/ENG/58 and University of Malaya Research Grant (UMRG), grant number: RG156-12AET.

Last but by no means least; I would like to thank my family for unbelievable support and encouragement. My special thanks go to my wife and colleague, Sara Pourshahrestani, for her incredible help, patience and understanding throughout this project.

TABLE OF CONTENTS

ABSTRACT	III
ABSTRAK	V
ACKNOWLEDGEMENTS	VII
TABLE OF CONTENTS	VIII
LIST OF FIGURES	XIII
LIST OF TABLES	XIX
LIST OF SYMBOLS AND ABBREVIATIONS	XX
CHAPTER 1: INTRODUCTION	1
1.1 Background of study	1
1.2 Rational	6
1.3 Objectives of the study	9
1.4 Thesis outline	10
CHAPTER 2: LITERATURE REVIEW.....	11
2.1 Introduction	11
2.2 Bioglass materials: the general concept and performance	13
2.3 Cellular response to bioglass materials	16
2.4 Antibacterial activity of bioglass materials	18
2.5 Silicon and calcium functions in human body	19
2.6 Gallium-doped bioactive glasses	20
2.7 Zinc-doped bioactive glasses	23
2.8 Scaffold-guided tissue engineering and scaffold materials	26
2.8.1 Polymers: general requirements for bone regeneration	26
2.8.2 Elastomers as biomimetic scaffold materials	29
2.9 Elastomer/bioglass composite scaffolds	32

2.9.1 Composite scaffolds: fabrication techniques	37
2.9.2 Thermoplastic elastomer/bioglass composites	41
2.9.2.1 Poly (α -caprolactone) based thermoplastic elastomers	41
2.9.2.2 Poly (hydroxyalkanoates) (PHA) based composites	46
2.9.2.2.1 Poly (3-hydroxybutyrate)	46
2.9.2.2.2 Poly (3-hydroxybutyrate-co-3-hydroxyvalerate) ..	47
2.9.2.3 Composite of polyurethane/bioglass	48
2.9.3 Thermoset polyester/bioglass elastomer composites	51
2.9.3.1 Poly (diol citrate)	51
2.9.3.2 Poly (glycerol sebacate)	56
2.10 Composite materials from natural elastomers and bioglass	57
2.11 The effect of filler size: polymer / bioglass nano- and micro- composites	61
CHAPTER 3: EXPERIMENTAL.....	64
3.1 Introduction	64
3.2 Synthesis of bioactive glass	64
3.3 Synthesis of POC	65
3.4 Fabrication of POC/bioglass film	66
3.5 Fabrication of POC/Bioglass scaffolds	66
3.6 Characterization	67
3.6.1 Morphological and structural characterization of the bioglass	67
3.6.2 Field emission scanning electron microscopy (FESEM)	67
3.6.3 Fourier transform infrared spectroscopy (FTIR)	68
3.6.4 Thermal analysis	68
3.6.5 Mechanical tests	68
3.6.6 Porosity estimation	69
3.6.7 <i>In vitro</i> degradation test	70

3.6.8	Acidity measurement	70
3.6.9	Contact angle measurements	71
3.6.10	Swelling studies	71
3.6.11	Ion release studies	71
3.6.12	Acellular <i>in vitro</i> tests in SBF	72
3.6.13	<i>In vitro</i> tests to evaluate ion penetration into bone tissue matrix	72
3.6.14	Scanning electron microscopy and energy disperse spectrometric analysis	73
3.6.15	Antibacterial tests	73
3.6.16	Osteoblast responses to the scaffolds	74
3.6.16.1	Cell culture, attachment, morphology and viability of osteoblasts.....	74
3.6.16.2	RNA isolation and cDNA synthesis and qPCR microarrays .	75
3.6.16.3	Indirect Immunostaining	78
3.6.17	hBMSC responses to the scaffolds	79
3.6.17.1	Cell culture and seeding	79
3.6.17.2	Cell adhesion and morphology	80
3.6.17.3	Cell distribution and density	80
3.6.17.4	Cell proliferation	81
3.6.17.5	ALP activity	81
3.6.17.6	RNA isolation and cDNA synthesis and qPCR microarrays .	82
3.6.17.7	Determination of calcium content	83
3.6.18	Statistical analysis	84

CHAPTER 4: RESULTS AND DISCUSSION 85

4.1	Introduction	85
4.2	Morphological and structural characterization of the bioglass	85
4.3	Surface morphology of scaffolds by FESEM	86
4.4	FTIR analysis	89

4.5	Thermal analysis	90
4.6	Mechanical properties and porosity	92
4.7	<i>In vitro</i> degradation study	95
4.8	Water in air contact angle	96
4.9	Swelling experiment	97
4.10	Ion release study	99
4.11	Acellular <i>in vitro</i> tests performed in SBF	100
4.12	<i>In vitro</i> bone tests for ion penetration into bone tissue matrix	105
4.13	Antibacterial tests	109
4.14	Osteoblast-scaffold interaction	115
	4.14.1 Cell morphology and viability	115
	4.14.2 Real-time PCR	117
	4.14.3 Indirect Immunostaining	118
4.15	Stem cell-scaffold interaction	120
	4.15.1 hBMSCs adhesion and proliferation	120
	4.15.2 Cell proliferation	121
	4.15.3 ALP activity	122
	4.15.4 Quantitative RT-PCR	123
	4.15.5 Calcium content	124
4.16	Discussion	125
 CHAPTER 5: CONCLUSIONS AND FUTURE DIRECTIONS		132
5.1	Introduction	132
5.2	Summary and conclusions	132
5.3	Direction for future research	134

REFERENCES.....	136
LIST OF PUBLICATIONS AND PAPERS PRESENTED	164

University of Malaya

LIST OF FIGURES

Figure 1.1: The illustration schematically shows the types of bone grafts; autograft, allograft, xenograft and synthetic bone graft substitutes.....	2
Figure 2.1: Sequence of interfacial reactions involved in forming a bond between tissue and bioactive ceramics.....	15
Figure 2.2: SEM micrographs of MC3T3-E1 cells cultured on 13–93 glass fiber scaffolds for: (A) 4 days; and (B) 6 days. The micrographs show increased cell density during the 6 day incubation and well-attached morphology.....	17
Figure 2.3: Possible structure of surface Ga sites; (A) Ga act as network modifier, and (B) Ga acts as network former.....	23
Figure 2.4: SEM images of apatite growth on the surface of (a) 58S (b) 58S-0.5% Zn (c) 58S-4% Zn after 1 day soaking in SBF.....	25
Figure 2.5: Classification of elastomers accompanied by examples of each group: ^a Poly (ϵ -caprolactone/glycolide); ^b Poly (ϵ -caprolactone/lactide); ^c polyester urethane urea; ^d Poly(1,3-trimethylene carbonate); ^e Poly(1,3-trimethylene carbonate/caprolactone); ^f Poly(1,3-trimethylene carbonate/D,L-lactide); ^g Poly (3-hydroxybutyrate); ^h Poly (3-hydroxybutyrate-co-3-hydroxyvalerate); ⁱ Poly(glycerol sebacate); ^j Poly (1,8-octanediol) citrate.....	30
Figure 2.6: Schematic diagram of some common methods for fabrication of composite scaffolds including standard synthesis conditions; A) Solvent casting-particulate leaching (SC/PL) B) Solid–liquid phase separation (SLPS) C) Thermally induced phase separation (TIPS) D) Melt-molding E) Electrospinning F) Rapid prototyping techniques. ^a Thermoset elastomer; ^b Thermoplastic elastomer.....	38

Figure 2.7: SEM images of the radial cross-sections of PLGA disks (13 × 6 mm) during the 6 weeks degradation in vitro. (a and c) Salt-leached scaffolds; (b and d) TIPS scaffolds.....	40
Figure 2.8: SEM images of PCL/glass fiber composite after 5 weeks immersion in deionized water.....	43
Figure 2.9: Optical micrographs of the newly formed bone (NB) in the vicinity of the defect center with a higher magnification: (a) empty defect; (b) pure PCL membrane; and (c) PCL/nanofiber bioglass composite membrane	44
Figure 2.10: SEM images of composite with 20 % bioglass after immersion in SBF for 3 days.....	48
Figure 2.11: SEM images of porous samples of (a) pure polyurethane and (b) composite containing 20 % bioglass.....	49
Figure 2.12: (a) Tensile stress–strain curves of PU/PVA blend, composites PU/PVA with 10 and 25 % of BGNP; and (b) Compressive stress–strain curves of foams PU/PVA and PU/PVA with 10% of BGNP, essayed successive referred as 1, 2, and 3 tests, respectively.....	50
Figure 2.13: SEM images shows the morphology of: a) neat PU scaffold; b) composite scaffold.....	50
Figure 2.14: Comparison of mass loss of: (a) Bioglass-coated and uncoated PUR; and (b) PUR/PDLLA scaffolds during immersion in SBF for up to 21 days.....	51
Figure 2.15: General structure of PDC.....	53
Figure 2.16: Apatite mineralization in SBF after 15 days of incubation at 37 °C for A) POC B) POC-HA composite with 40 wt% HA and C) POC-HA composite with 65 wt% HA.....	53
Figure 2.17: SEM images of POC–HA composites. (A) 40nano, (B) 60nano, (C) 40micro, and (D) 60micro. An increase in nanoparticle content enhanced	

surface homogeneity, whereas an increase in microparticle content enhanced heterogeneity. SB for all POC–HA composites (A,B,C,D) = 50 μm	55
Figure 2.18: Digital images showed new cartilage layer formed over POC-HA (a) nanocomposite; (b) microcomposite; implanted 6 weeks in New Zealand rabbit knee.....	56
Figure 2.19: SEM images of: (A) gelatin/bioglass scaffold; and (B) bioglass particles with apatite on the surface after immersion of 3 days in SBF.....	59
Figure 2.20: Alkaline phosphatase staining image obtained from microscope for: left-Composite and right-control.....	60
Figure 2.21: Modulus comparison for various concentrations of m-BG and n-BG particles in P(3HB)/bioactive glass composites.....	62
Figure 3.1: Schematic diagram of melt-quench technique for synthesizing bioglass....	65
Figure 3.2: Schematic diagram of the method of synthesizing POC pre- polymer.....	65
Figure 3.3: Schematic diagram of composite scaffold fabrication.....	67
Figure 3.4: Digital photographs of representative cell-seeded scaffolds before and after fixation.....	80
Figure 4.1: (a) FESEM micrograph showing the irregular shape of the glass particles; (b) EDS spectrum of bioactive glass showing the peaks of Si, Ca, Zn, Ga and O; and (c) XRD pattern of the bioactive glass particles showing the typical amorphous halo.....	86
Figure 4.2: Digital photographs of representative POC-BG scaffolds: (a) demonstration of elastomeric nature of POC-BG-10% scaffold; (b) frontal and cross-sectional view of the POC-BG-30% scaffold prepared for cell culture. (c, d) Microstructure of scaffolds observed by FESEM: (c, d) POC-BG-20%; (e) POC; (f) POC-BG-30%; (g) POC-BG-20%; and (h) POC-BG-10%.....	88

Figure 4.3: Representative ATR-FTIR spectrum of POC-BG composite; insert showing expanded spectral region for: pure POC (black); POC-BG-10% (red); POC-BG-20% (green); and POC-BG-30% (blue).....	90
Figure 4.4: TGA curves measured for POC-BG composites in comparison to pure POC (Control).....	91
Figure 4.5: DMA analysis of composite scaffolds illustrating the typical plots of Tan delta ($\tan\delta$) and storage modulus (E') under bending mode.....	94
Figure 4.6: <i>In vitro</i> degradation profiles of composite scaffolds (PBS; 37 °C).....	96
Figure 4.7: Swelling ratio in water and PBS of: pure POC (black-◆); POC-BG-10% (red-■); POC-BG-20% (green-▲); and POC-BG-30% (blue-●). The images show films of POC and POC-BG-30% after soaking in water (left) and PBS (right) for 4 h.....	98
Figure 4.8: Ion release kinetics from composite scaffolds in PBS: AES plots of elemental concentrations of Si, Ca, Ga and Zn after 28 days of scaffolds immersion.....	100
Figure 4.9: <i>In vitro</i> ion release kinetics for composite scaffolds in SBF: ICP plots of elemental concentration of Ca^{2+} , PO_4^{3-} , Ga^{3+} and Zn^{2+} vs. immersion time for the investigated composites.....	102
Figure 4.10: (left): SEM images confirm CaP layer deposition (arrows) on the composite scaffolds during immersion in SBF and (right): EDS profiles of the composite scaffolds after being soaked in SBF for 28 days.....	103
Figure 4.11: (a) Digital image and (b) SEM image of POC scaffold implanted into bone specimen.....	107
Figure 4.12: Normal atomic % EDS data for Ca, P and Zn content as well as Ca/P ratio at scaffold-bone interface at various distances 0, 200, 1500 and 4500 μm	107

Figure 4.13: Effect of the composite scaffolds on the growth of <i>E. coli</i> and <i>S. aureus</i> ; measured by monitoring the optical density at 595 nm.....	110
Figure 4.14: The viable <i>E. coli</i> and <i>S. aureus</i> recovered from agar plates after 10 h of incubation at 37 °C.....	111
Figure 4.15: Plate assay of <i>E. coli</i> and <i>S. aureus</i> using (a) LB broth; (b) POC; (c) POC- BG-10%; (d) POC-BG-20%; (e) POC-BG-30% at 10 hours.....	112
Figure 4.16: FESEM images of cell attachment of human osteoblast cells after 7 days in culture: (a) POC control; (b) POC-BG-10%; (c) POC-BG-20%; and (d) cell proliferation examined by MTT assay after 1, 7, 14 and 28 days culture; normalized to pure POC; (*P< 0.05) significantly different in comparison to respective pure POC.....	116
Figure 4.17: Gene expression of collagen I and collagen III on composite scaffolds in comparison to POC scaffold used as control after 7 days in culture; (*P< 0.05) significantly different in comparison to respective pure POC.....	117
Figure 4.18: Fluorescent images of indirect immunostaining of collagen synthesis type I collagen and type III collagen on composite scaffolds after 7 days in culture: (a, b) pure POC; (c, d) POC-BG-10%; (e, f) POC-BG-20%; and (g, h) POC- BG-30%.....	119
Figure 4.19: FESEM micrographs of hBMSCs for 2 weeks on (a, e) pure POC; (b, f) POC-10%BG; (c, g) POC-20%BG; (d, h) POC-30%BG scaffolds at various magnifications. (i, j, k, l) Fluorescence microscopy of the cells attached to the scaffolds on day 14 – Hoechst’s staining.....	121
Figure 4.20: Proliferation of hBMSC on POC, POC-10%BG, POC-20%BG and POC30%BG scaffolds evaluated by AlamarBlue® assay on days 1, 3, 7, and 14; (*P< 0.05) significantly different in comparison to respective pure POC.....	122

Figure 4.21: ALP activity of the hBMSC on the scaffolds was measured with the pNPP assay at 3, 7, and 14 days of culture; (*P< 0.05) significantly different in comparison to respective pure POC.....123

Figure 4.22: RT-PCR results showing transcript levels associated to osteoblastic marker expression of RUNX2, COL I, BMP2, SPARC, and BGLAP at 7 and 14 days after hBMSCs growth on the scaffolds. Data have been normalized to the gene expression levels on day 0; (*P< 0.05) significantly different in comparison to respective pure POC.....124

Figure 4.23: Calcium content measurements of hBMSC on the scaffolds during culture for 14 days; (*P< 0.05) significantly different in comparison to respective pure POC.....125

University of Malaya

LIST OF TABLES

Table 2.1: Composition of selected bioglasses and the common method of synthesis.....	14
Table 2.2: Elastomer/bioglass composite materials.....	34
Table 2.3: Benefits and drawbacks of common techniques for composite scaffolds fabrication (Boccaccini et al., 2003; Cannillo et al., 2010; Cao et al., 2006; Fabbri et al., 2010; W.-J. Li & Cooper Jr, 2011; Liebschner et al., 2003; Mano et al., 2007; Narayan, 2009; Peltola et al., 2008; Puppi et al., 2010; Subia et al., 2010).....	39
Table 3.1: Components and the required volumes of each component for preparation of 2X RT master mixtures.....	77
Table 3.2: Thermal cycling conditions used for RT-PCR experiment.....	77
Table 3.3: The reaction components, required volumes of each component and their final concentrations used in RT-PCR experiment.....	78
Table 3.4: Thermal cycling conditions used for RT-PCR experiment.....	78
Table 3.5: Primer sequences of Collagen type I and III genes used for RT-qPCR.....	78
Table 3.2: Primer sequences of RUNX2, COL I, SPARC, BMP2, and BGLAP genes used for RT-qPCR.....	83
Table 4.1: Comparison of theoretical and experimental bioglass content using total weight loss of the materials obtained by TGA.....	91
Table 4.2: The thermal and mechanical properties of POC-BG scaffolds.....	92

LIST OF SYMBOLS AND ABBREVIATIONS

%	:	Percentage
wt%	:	Weight percent
mol%	:	Mole percent
g	:	Gram
μg	:	Microgram
μm	:	Micrometer
nm	:	Nanometer
MPa	:	Megapascal
kPa	:	Kilopascal
GPa	:	Gigapascal
$^{\circ}$:	Degree
h	:	Hour
$^{\circ}\text{C}$:	Degree <i>Celsius</i>
ml	:	Millilitre
min	:	Minute
mm	:	Millimetre
cm	:	Centimetre
mg	:	Milligram
Hz	:	Hertz
KN	:	Kilonewton
kV	:	Kilovolt
μL	:	Microliter
rpm	:	Revolutions per minute
Θ	:	Theta

M	:	Molar
ppm	:	Part per million
E'	:	Storage modulus
E''	:	Loss modulus
tan δ	:	Tan delta
μ M	:	Micromole
N	:	Normality
MSCs	:	Mesenchymal stem cells
hMSCs	:	Human mesenchymal stem cells
ECM	:	Extracellular matrix
3D	:	Three dimensional
FDA	:	Food and drug administration
BG	:	Bioactive glass
Ag	:	Silver
Ca	:	Calcium
P	:	Phosphorous
PO ³⁻⁴	:	Phosphate
Si	:	Silicon
Ga	:	Gallium
Zn	:	Zinc
Cu	:	Copper
Mg	:	Magnesium
Sr	:	Strontium
Na	:	Sodium
K	:	Potassium
Ti	:	Titanium

Al	:	Aluminium
Fe	:	Iron
BO ₃ ³⁻	:	Boron
PDC	:	Poly (diol citrate)
POC	:	Poly (octanediol citrate)
PLLA	:	Poly (L-lactic acid)
PLA	:	Poly (lactic acid)
PGA	:	Poly (glycolic acid)
PLGA	:	Poly (lactic-co-glycolic acid)
PGS	:	Poly (glycerol sebacate)
HA	:	Hydroxyapatite
HCA	:	Hydroxyl carbonate apatite
CaP	:	Calcium phosphate
hFOB	:	Human osteoblast-like cells
hBMSCs	:	Human bone marrow mesenchymal stem cells
DMEM	:	Dulbecco's modified Eagle's medium
FBS	:	Fetal bovine serum
MTT	:	(3-(4,5-dimethylthiazol-2-yl)-2,5-diphenyltetrazolium bromide)
SBF	:	Simulated body fluid
PBS	:	Phosphate buffered saline
MQ	:	Melting-quench technique
SG	:	Sol-gel technique
VEGF	:	Vascular endothelial growth factor
bFGF	:	Basic fibroblast growth factor
ALP	:	Alkaline phosphatase activity
DNA	:	Deoxyribonucleic acid

RNA	:	Ribonucleic acid
MG-63	:	Human osteosarcoma cells
MC3T3-E1	:	Mouse osteoblastic cells
BAE-1	:	Bovine aortic endothelial cells
SaOS-2	:	Human osteogenic sarcoma cells
HDPSCs	:	Human dental pulp stems cells
hPDLF	:	Human Periodontal Ligament Fibroblast
Tg	:	Glass transition temperatures
TPEs	:	Thermoplastic elastomers
-OH	:	Hydroxyl
-COOH	:	Carboxyl
TSEs	:	Thermoset elastomers
PCL	:	Poly (α -caprolactone)
PDLLA	:	Poly (D,L-lactide)
P(CL/DL-LA)	:	Poly (ϵ -caprolactone-co-D,L-lactide)
P(3HB)	:	Poly (3-hydroxybutyrate)
PHBV	:	Poly (3-hydroxybutyrate-co-3-hydroxyvalerate)
PU	:	Polyurethane
PUEs	:	Polyurethane elastomers
PVA	:	Poly (vinyl alcohol)
PHA	:	Poly (hydroxyalkanoates)
PPS	:	Poly (polyolsebacate)
SC/PL	:	Solvent casting/ particulate leaching
SLPS	:	Solid-liquid phase separation
TIPS	:	Thermally induced phase separation
SFF	:	Rapid prototyping or Solid freeform

NaCl	:	Sodium chloride
NaHCO ₃	:	Sodium bicarbonate
CA	:	Citric acid
OD	:	1, 8-octanediol
XRD	:	X-ray powder diffraction
FTIR	:	Fourier transform infrared spectroscopy
DSC	:	Differential scanning calorimetry
DMA	:	Dynamic mechanical analysis
TGA	:	Thermogravimetric analysis
FESEM	:	Field Emission Scanning Electron Microscopy
MP–AES	:	Plasma–atomic emission spectrometer
ICP-MS	:	Inductively Coupled Plasma Mass Spectrometry
EDS	:	Energy dispersive spectrometer
SEM	:	Scanning electron microscope
LB	:	Luria-Bertani
E. coli	:	Escherichia coli
S. aureus	:	Staphylococcus aureus
OD	:	Optical density
DEPC-dH ₂ O	:	Diethyl pyrocarbonate-treated distilled water
EDTA	:	Ethylenediaminetetraacetic acid
RT-PCR	:	Reverse transcription polymerase chain reaction
FITC	:	Fluorescein isothiocyanate
<i>p</i> NPP	:	<i>p</i> -nitrophenol phosphate
<i>p</i> NP	:	<i>p</i> -nitrophenol
HCl	:	Hydrochloric acid
UV-VIS	:	Ultraviolet–visible

CHAPTER 1: INTRODUCTION

1.1 Background of study

Bone is one of the most commonly transplanted tissues of the body with over 2 million grafting procedures annually worldwide (N. L. Leong et al., 2006). Bone defects caused by tumor reconstruction, chronic infection or traumatic bone loss create a major surgical problem (Zhou et al., 2006). The majority of fractures heal well under standard conservative or surgical therapy. However, extended bone defects following trauma or cancer resection or non-unions of fractures may require more sophisticated treatments (Kneser et al., 2006). The accepted clinical standard for bone defect treatment and nonunion is autologous bone grafting (Figure 1.1). This treatment presents serious problems with donor site morbidity, prolonged operation time, and the limited availability of graft materials (X. Wu, 2012). Allograft bone also has concerns related to disease transmission risk and infection, explaining why synthetic bone grafts are increasingly being employed in the clinical field (Zhou et al., 2006). Certain biomaterials can repair or replace damaged or diseased tissue by mimicking the natural extracellular matrix (Puppi et al., 2010). Bio-resorbable scaffolds can be formulated to degrade *in-situ* and minimize the need for additional surgery to remove the implant (Akmaz et al., 2004). The ideal scaffold should degrade at a rate comparable with the rate of bone growth, physically creating open space for new bone formation until full regeneration is achieved. From a mechanical viewpoint, an ideal bone scaffold must provide sufficient mechanical support for preserving tissue volume and consequently promotion of tissue regeneration (Alvarez & Nakajima, 2009).

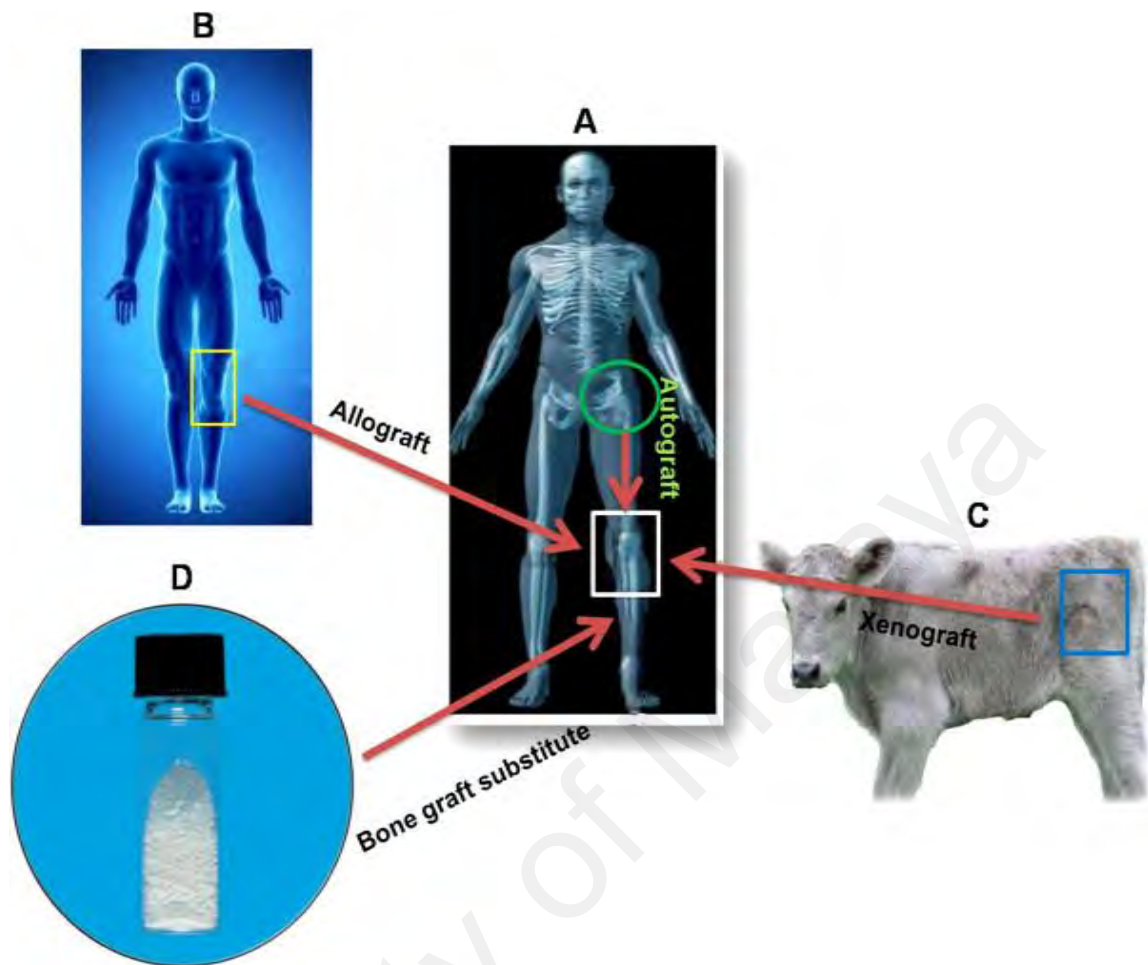


Figure 1.1: The illustration schematically shows the types of bone grafts; autograft, allograft, xenograft and synthetic bone graft substitutes [Reprinted with permission from (Oryan et al., 2014)].

A crucial factor identified in the failure of many tissue-engineered constructs is inadequate tissue regeneration around the biomaterial immediately after implantation (Marolt et al., 2010). Since the interaction of cells with biomaterials is a fundamental parameter in the evaluation of a scaffold, a number of recent contributions to the literature have focused on the design and development of biomaterial structures that facilitate favourable interactions and augment tissue regeneration. *In vivo* bone formation involves osteogenic reparative cells originating from mesenchymal stem cells (MSCs) in bone marrow, the presence of a regeneration template, and the provision of regulatory signals (Caplan, 2000). Human

mesenchymal stem cells (hMSCs) isolated from bone marrow serve as an ideal cell source for a wide variety of cell-therapy concepts due to their self-renewal ability, multilineage differentiation potential and immunomodulatory properties (Bianco et al., 2001). hMSCs are also able to secrete biomolecules such as cytokines, chemokines, growth factors, and extra cellular matrix (ECM) molecules, in a paracrine or even autocrine manner, which influence the surrounding environment to promote angiogenesis, reduce inflammation, and enhance tissue repair (Nawaz et al., 2015). Furthermore, hMSCs have a high ability to proliferate and retain their functionality after culture and cryopreservation (Marquez-Curtis et al., 2015). For the application of hMSCs to bone tissue regeneration, a better understanding of the interactions occurring between hMSCs and biological scaffold material is essential because the interaction at the cell-biomaterial interface play a major role in the bonding of implant materials to native bone tissue, and in inhibiting fibrous encapsulation.

The choice of scaffold material is a critical factor in the promotion of the development of competent tissues with the desired characteristics (Rohman et al., 2007). Synthetic biomaterials are now being designed with a combination of both resorbable and bioactive characteristics to stimulate regeneration of living tissue. So far, there is no single biomaterial that is able to satisfy all the requirements of an ideal bone graft. To help address the need for suitable bone substitutes, tissue engineers seek to create 3D scaffolds made up bioceramic and polymeric materials to facilitate normal bone growth.

Bioactive silicate glasses, as a highly bioactive material, have achieved great success in many clinical applications in comparison to other bioceramics such as synthetic hydroxyapatite due to their well-known osteoconductive and osteoinductive properties. Bioactive glasses are increasingly employed for bone void filling. The first commercially available bioactive glass, known as “45S5” ($45\text{SiO}_2\text{-}24.5\text{CaO-}24.5\text{Na}_2\text{O-}6\text{P}_2\text{O}_5$ wt%), has

shown positive interaction with both hard and soft tissue (Hench et al., 1971). However, the lack of versatility in material processing and the inherent brittleness of bioactive glasses limits their applicability in load bearing applications (Gerhardt & Boccaccini, 2010; Rezwan et al., 2006). Bioglasses can bond to both hard and soft tissue through rapid formation of hydroxyl carbonate-apatite on the glass surface upon implantation to promote cell migration and differentiation and able to release ions which further stimulate the healing process at the site of injury (I. D. Xynos et al., 2000; Xynos et al., 2001). Bioactive glasses can be doped with therapeutic elements to modulate the required tissue responses. For instance, incorporation of magnesium or potassium ions can tune bioactivity, and addition of silver, zinc (Zn) or gallium (Ga) ions to the glass network can impart antibacterial properties, while it is reported that doping strontium ions into bioactive glasses can enhance bone cell responses (Baino & Vitale-Brovarone, 2011; Hoppe et al., 2011). Although there have been many studies on the interaction of bioactive glasses with MSCs, very few have investigated the effect of bioactive glasses doped with therapeutic elements on MSCs responses. In order to utilize the potential of therapeutic ion-releasing bioglasses, they need to be delivered to the body in scaffolds in a controlled release dosage form. Composite materials including biodegradable polyesters are possible candidates for bioactive porous scaffolds. Research postulates that polymer/bioglass composite materials could combine the osteoconductive properties, stiffness and strength of bioactive glasses with the processability of biodegradable polymers in order to increase the applicability of glass-based materials for tissue augmentation (Boccaccini et al., 2010; Bretcanu et al., 2012).

Poly (octanediol citrate) (POC) has been widely investigated as a tissue engineering scaffold due to its biomimetic viscoelastic properties, linear degradation profile and non-toxic degradation products. The mechanical properties and biodegradation rate of POC can

be controlled by altering curing conditions (time and temperature) and the initial monomer molar ratio to mimic the pliancy of certain soft tissues such as blood vessels, urinary bladder smooth muscle and myocardium (Sharma et al., 2010). POC appears to have good compatibility with a number of cell types, including articular chondrocytes, endothelial cells, myoblasts and osteoblasts, without requiring any additional treatment (Y. Du et al., 2015; Kang et al., 2006; Prabhakaran et al., 2012; Yang et al., 2006). However, poor mechanical properties and limited osteogenic bioactivity retard its use in load bearing applications. Accordingly, many attempts have been made to manipulate the physicochemical properties of POC by synthesis and fabrication of co-polymers and composites suitable for hard tissue engineering (Dey et al., 2008; Qiu et al., 2006). Indeed, its low stiffness makes it a suitable material for loading a large amount of fillers without the detrimental effect of stress shielding (Chung, Qiu, et al., 2011). Several studies have been conducted to develop composites of POC and ceramic materials such as hydroxyapatite (HA) and calcium silicate with the aim of improving both mechanical properties and the osteoinductive potential of POC in bone tissue regeneration (Chung, Qiu, et al., 2011; Qiu et al., 2006; Shirazi et al., 2014). It has been shown that tissue ingrowth into POC-HA increased compared to ingrowth into PLLA, which highlights an additional benefit of these novel biomaterials. However, HA is more stable and exhibits a low dissolution rate, whereas bioactive glasses are more soluble and their degradation products are released into the surrounding environment, potentially inducing bioactivity (Rahaman et al., 2011). So far, no attempt has been made to produce composites of a therapeutic ion-releasing bioactive glass with biocompatible POC elastomers.

1.2 Rationale

Skeletal defects caused by tumor reconstruction, chronic infection or traumatic bone loss present the need for complex treatment (Dimitriou et al., 2011). Strategies for repairing segmental bone defects generally focus on preserving equivalent tissue engineering standards to heal large bony defects caused by trauma or disease. Current treatments for *large segmental bone defects* rely on the use of autografts, allografts, or metallic or ceramic implants, each of which have their own disadvantages such as donor site morbidity, disease transmission, and mismatch of mechanical properties with the native bone (Smith et al., 2009). Alongside current treatments, tissue engineering has emerged as an alternative approach to create *de novo* tissue by growing cells on 3D scaffolds (Rahman et al., 2015). An ideal bone graft substitute or tissue scaffold should provide the necessary support for cells to attach, proliferate, and facilitate ingrowth (Dhandayuthapani et al., 2011). In parallel with tissue formation, an ideal scaffold should degrade and create open space for new bone formation, until regeneration is achieved. Accordingly, a biodegradable scaffold can reduce the number of surgeries since there is no need for an additional operation to remove the implant. Furthermore, the mechanical properties of a hard tissue scaffold such as fatigue strength, stiffness, and strength should be matched with those of natural bone (Alvarez & Nakajima, 2009).

The mechanical properties of scaffolds are highly dependent on both fabrication technique and porosity; the latter being small enough to facilitate load bearing but large enough to encourage vascularization (Puppi et al., 2010). Stress shielding would occur when the transplanted bone stiffness is not matched to natural bone (Allo et al., 2012). Implants with higher stiffness can lead to stress concentration in the surrounding area and ultimately increase the likelihood of failure. Uneven load sharing between bone and scaffold that is

yielded due to stiffness inequality is known as stress shielding. The effect of this phenomenon appears in the bone remodeling process. The underloaded bone adapts to the low stress environment and becomes less dense and consequently weak (Tsaryk et al., 2007). To overcome the problems associated with modulus-mismatch between current implants and bone and to promote the formation of a physiological bond between the implant and host tissue, the concept of analogue biomaterials (using bioceramics as reinforcing phase in polymeric composites) was introduced by Bonfield *et al.* in the 1980s (Bonfield et al., 1981). Since bone tissue itself is a composite between collagen (a natural elastomer) and bone mineral, the composite materials produced from organic elastomers and inorganic components should be the first choice for effective engineering of bones. However, the geometry and anisotropic properties of natural bone makes the designing of an 'ideal bone scaffold' difficult (Bose et al., 2012; Olszta et al., 2007). Composites of polymers and bioactive glasses have been made with the aim of improving both the mechanical properties and the biological compatibility of materials. Polymers suffer from insufficient strength and poor bioactivity, whereas bioactive glasses suffer from low fracture toughness, brittleness, and low flexibility when used alone (Hacker & Mikos, 2009; Lü et al., 2009; Rezwan et al., 2006; Woodruff & Huttmacher, 2010). In order to achieve the goal, bioactive glasses can be combined with polymers (as fillers or coatings) resulting in composite materials with improved bone repair ability (Chen & Boccaccini, 2006; Roether et al., 2002).

The elastic nature of elastomers makes them useful material for biomedical applications compared to the more common biodegradable polymers. The major advantage of such materials is that elastomers can sustain and recover from deformations in highly dynamic environments such as the human body. However acidic degradation products and insufficient mechanical properties of elastomers constrict the application range. The properties of

elastomeric materials have resulted in their applicability for soft tissue applications. In addition, high elasticity provides a large capacity for filler loading which may be able to facilitate sufficient mechanical properties for hard tissue applications such as bone augmentation. Hence, combining elastomers and bioactive glasses can result in a composite with the synergistic advantages of both the organic and inorganic phases and is anticipated to provide a natural bone mimic from the standpoint of structure and composition.

Another essential factor identified in the failure of many tissue-engineered constructs is inadequate tissue regeneration around the biomaterial immediately after implantation (Marolt et al., 2010). Most current strategies for developing tissue-engineered constructs involve combining living cells with a scaffold. The ability of a biomaterial to mimic the structural and mechanical aspects of the cellular microenvironment is a key factor in determining the ultimate success or failure of such engineered devices when used clinically for tissue regeneration. Furthermore, engineered scaffolds for self-regenerative applications should not only provide a framework for tissue repair but should also act as carriers for antimicrobial agents. The scaffold should be designed to promote cell adhesion for target tissues whilst also preventing bacterial adhesion and biofilm formation. Infections associated with surgical implants require long periods of antibiotic therapy and usually implant removal and replacement is the only remedy once a mature bacterial biofilm is formed (Belt et al., 2001).

A unique macroporous scaffold of POC has been reported which has demonstrated good *in vitro* and *in vivo* biocompatibility (Kang et al., 2006). However, the scaffold is not strong enough to be used as a hard tissue replacement. In addition, due to acidic degradation by-products, the biocompatibility and osteoconductivity of such POC scaffolds should be improved. Although composite scaffolds have already been developed by incorporation of an inorganic phase (e.g. HA), the majority of inorganic fillers are non-biodegradable, and the

presence of an inorganic filler phase may compromise the 3-D geometry of a highly porous parent polymer structure. Furthermore, the scaffolds do not impart antibacterial activity. Therefore, it is necessary to develop a biodegradable POC-based composite scaffold, retaining the unique macroporous structure reported above, but with improved mechanical properties and biological performance.

1.3 Aims and objectives

The major objective of the current study is to produce a bone tissue engineering scaffold which has the ability to release therapeutic ions from a Si-Ca-Zn-Ga bioglass phase, offering a better clinical outcome particularly for sufferers of osteosarcomae. To address this, the project has five short-term objectives:

1. To synthesize a novel bioactive glass using a melt-quench technique.
2. To fabricate porous scaffolds of POC with different quantities of the bioglass by solvent-casting/particulate-leaching technique.
3. To characterize POC/bioglass scaffolds for their chemical structure, composite morphology and *in vitro* biodegradation and ion release kinetics.
4. To investigate the effect of released ions from composites scaffolds on *in vitro* bioactivity and antibacterial activity.
5. To evaluate the biocompatibility of composite scaffolds *in vitro* and the effect of materials on osteogenesis of human osteoblast-like cells (hFOB) and human bone marrow-derived mesenchymal stem cells (hBMSCs).

1.4 Thesis outline

This research exploited a new composite scaffold made from polymer and bioactive glass to be used for treatment of large bony defects. This thesis was written in 5 chapters:

Chapter 1 presents the background of study, the current challenges in this area, and objectives of this study.

Chapter 2 includes a literature review on three main parts: i) Bioactive glasses and their physicochemical and biological properties; ii) the required properties of polymeric scaffolds for bone tissue engineering and introducing different types of elastomeric materials and their properties; iii) a concise overview of composites made from elastomers and bioactive glasses.

Chapter 3 deals with the experimental procedures for sample preparation. All the methods employed to collect the data and generate the results are also reported in this chapter.

Chapter 4 focuses on the presentation of results and discussion on the impact of bioactive glass incorporation into POC scaffold and its concentration on the physicochemical properties, bioactivity, antibacterial activity and *in vitro* cellular responses.

Chapter 5 summarizes the outcomes of the research, and explores implications for future research.

CHAPTER 2: LITERATURE REVIEW

2.1 Introduction

Bone may undergo damage due to insult or bone disease such as osteoporosis or osteosarcoma (Hamed & Jasiuk, 2012). There are increasing numbers of patients with diseased and/or injured organs who require an organ transplant. However, transplantation is currently not the best therapy for many patients because the number requiring a transplant far exceeds the number of available organs (Watson & Dark, 2012). Additionally, due to physiological immunological response raising the possibility of rejection patients are required to adhere to a strict regimen of immunosuppressant drugs. For that reason the concept of tissue engineering could offer an effective solution to complicated procedures such as transplant surgery (X. Wu, 2012). Indeed, bone tissue engineering is identifying new methods to address bone defects, which conventional methods cannot treat suitably (Alvarez & Nakajima, 2009). Reconstruction of native tissue inside the body presents an attractive strategy based on the engineering and design of biodegradable materials. A common approach utilizes a biomaterial as a temporary porous 3D scaffold for the delivery and integration of cells and/or growth factors at the repair site (Velema & Kaplan, 2006).

Polymers have a wide range of applications in surgery including as scaffolds and fillers. The criteria for selection of polymeric materials for such applications are: material chemistry, molecular weight, solubility, shape, hydrophilicity/hydrophobicity, surface properties, water absorption, and degradation mechanism (Dhandayuthapani et al., 2011). There are many different groups of polymeric biomaterials, among which are “elastomers” which are gaining great attention due to their biocompatibility and mechano-compatibility with natural

extracellular matrix (ECM) proteins (Y. Li et al., 2012). Suitable elastomeric materials that have controllable mechanical properties are usually synthesized from biocompatible monomers such as citric acid, with ester bonds to promote hydrolysis degradation (Bettinger, 2011). However, elastomers lack sufficient mechanical properties, which consequently limits their applicability for bone tissue engineering (Chen et al., 2012).

Bioactive materials such as bioactive ceramics (*i.e.* amorphous hydroxyapatite (HA) and calcium phosphate) and bioactive glasses lack satisfactory fracture toughness and strength, which restricts their use in load bearing applications (Q. Fu et al., 2011; Rezwan et al., 2006). It is hypothesized that a composite which combines the outstanding properties of both polymers and bioglasses can address these concerns. In addition, the desired properties of bioglasses are gained by controlling the chemical composition of the material. This feature provides the ability to obtain a modulated degradation ratio and a specific therapeutic activity, which can be further tuned to match the mechanical integrity for engineering organs (Chen et al., 2012; Q. Fu et al., 2011). To date, bioactive glasses have been used only in non-load-bearing applications in the skeleton, due to their poor mechanical properties.

This chapter focuses mainly on bone tissue engineering scaffolds that have been produced from elastomer/bioglass composite materials. The basic criteria and the fabrication methods for composite scaffold fabrication are also reviewed in this study. For a review of all the other elastomeric materials used in tissue engineering, readers are referred to the recent review papers by Chen et al, Li et al, and You et al (Chen et al., 2013; Y. Li et al., 2012; You & Wang, 2011).

2.2 Bioglass materials: the general concept and performance

A “bioactive” material is generally defined as material with specific biological activity for a targeted tissue (Bohner & Lemaître, 2009). The meaning was amended when Kokubo and Takadama defined a bioactive material for tissue bonding and integration (Kokubo, 1998). One characteristic of bioactive glasses is their kinetics of surface modification as a function of time when implanted into the body. The bioactivity of glasses results from their ability to form hydroxyl carbonate apatite (HCA), which is responsible for bonding bioactive glass to human bone upon implantation in the body. It means that glasses with a higher capacity to be coated with HCA when in contact with physiological fluids have higher bioactivity (Larry L Hench, 1998; Kokubo, 1998; Salinas & Vallet-Regí, 2013). The *in vitro* apatite formation on the surface of bioactive glasses can be evaluated using simulated body fluid (SBF) which is prepared with an ionic composition equal to human blood plasma (Kokubo, 1998). This relatively simple experiment can be used to indicate the bioactive potential of materials *in vivo* (Rahaman et al., 2011). Ultimately all biomaterials should be tested *in vivo* for immunological response. Upon implantation, bioactivity can also be evaluated by the prevention of fibrous capsule formation. Table 2.1 displays the composition of bioactive glasses that showed promising performance in bone tissue regeneration. For example, silicate-based bioactive glasses are the most common glasses used for clinical applications. The first silicate-based bioactive glass was made by Hench (1969) and is known as 45S5 which, at that specific composition, can positively interact with bone and soft tissues (Hench et al., 1971). Nonetheless, the limitation associated with Si-based bioactive glasses is the slow rate of degradation and conversion to apatite which further complicates the rate of implant resorption and simultaneous bone growth (Huang et al., 2006). However, the conversion of silica-based bioactive glasses to apatite *in vivo* is three times faster than

recorded *in vitro*. Unlike *in vitro* results, almost full conversion of bioactive glass to apatite was observed after 24 weeks post-implantation (X. Liu et al., 2013).

Table 2.1: Composition of selected bioglasses and the common method of synthesis.

Glass name	SiO ₂	P ₂ O ₅	B ₂ O ₃	CaO	Na ₂ O	K ₂ O	MgO	mol% or wt%	Method of synthesis
45S5	46.1	2.6		26.9	24.4			mol%	MQ ^a
45S5B1	30.7	2.6	15.4	26.9	24.4			mol%	MQ
45S5B2	15.4	2.6	30.7	26.9	24.4			mol%	MQ
45S5B3		2.6	46.1	26.9	24.4			mol%	MQ
13-93	53	4		20	6	12	5	wt%	MQ
13-93B3		4	53	20	6	12	5	wt%	MQ
58S	60	4		36				mol%	SG ^b
77S	80	4		16				mol%	SG
S53P4	53	4		20	23			mol%	MQ
Phosphate glass		50		30	20			mol%	MQ

^a Melting-quench technique

^b Sol-gel technique

The bioactivity of materials is defined as the ability of a material to bond with living tissues and occurs in 12 stages for silicate bioactive materials (Figure 2.1). The physico-chemical mechanisms (the first 5 stages) involve the formation of HA-like apatite on the surface of bioactive glasses due to the (1) rapid ion-exchange of alkali ions with hydrogen ions of body fluids (2) network dissolution and formation of silanol (3) silica gel polymerization (4, 5) adsorption and crystallization of HCA layer. The next 7 stages involve formation of bioactive bond to tissues and the cellular events including (6) adsorption of biological moieties (growth factors) and (7-12) attachment, differentiation and proliferation of cells (Larry L. Hench, 1998; Larry L Hench, 1998).

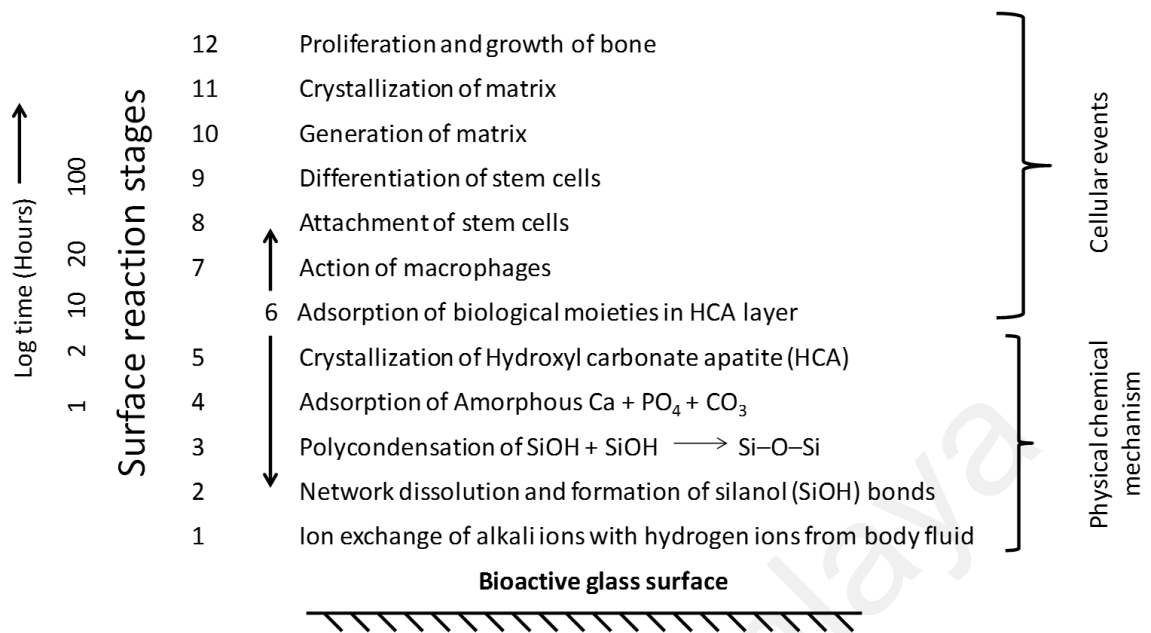


Figure 2.1: Sequence of interfacial reactions involved in forming a bond between tissue and bioactive ceramics [Reproduced with permission from (Larry L Hench, 1998)].

Bioglasses can bond to both hard and soft tissues to promote cell migration and differentiation and release ions which further stimulate the healing process at the site of injury (Jung, 2012). There are some advantages of using bioglasses over other bioactive ceramics such as sintered HA. For example, the ionic product of bioglasses stimulates the expression of genes of osteoblastic cells which in turn modulate osteogenesis and promote bone formation (Gerhardt & Boccaccini, 2010; Xynos et al., 2001). In general, bioactive glasses are considered as a promising material for osteoconduction and osteoproduction (Anselme, 2000).

2.3 Cellular response to bioglass materials

Apart from the processing of biomaterials, which requires close control over chemistry and morphology, the cellular response to biomaterials is possibly the most important characteristic that must be established prior to further development of clinical applications. There are many different cell culture tests reported in literature. In this study, we will outline only the most important examples in order to present the advantages of bioglass materials. For example, the evaluation of biological response to silicate bioactive glasses such as 45S5 and 13-93 (Table 2.1) demonstrated their ability to support proliferation and differentiation of osteoblastic cells and mesenchymal stem cells either *in vitro* or *in vivo* (Figure 2.2) (Brown et al., 2008; X. Liu et al., 2013). It is also reported that the control of borosilicate bioactive glasses crystallization might produce glass-ceramics with less cytotoxic effect on mouse lung fibroblast-like cells (L929) (Fernandes et al., 2016). A relatively high proliferation rate and multipotent differentiation of mesenchymal stem cells makes these cells promising for tissue engineering (Detsch et al., 2014). In addition, the osteogenic differentiation of umbilical cord and adipose derived stem cells by bioactive glasses has been reported in several studies (Detsch et al., 2014; Silva et al., 2014). The indirect and direct contact of relevant cells with particles of 45S5 bioglass confirmed the ability of this material to effectively stimulate the secretion of angiogenic growth factors such as vascular endothelial growth factor (VEGF) and basic fibroblast growth factor (bFGF) *in vitro*. Furthermore, the examined bioglass material (45S5) demonstrated its ability to promote angiogenesis both *in vitro* and *in vivo* (Day, 2005; Gorustovich et al., 2009; Hoppe et al., 2011).

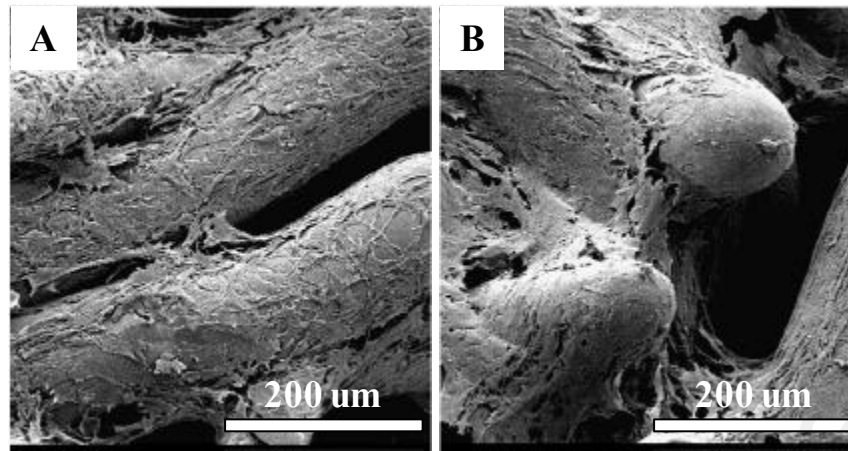


Figure 2.2: SEM micrographs of MC3T3-E1 cells cultured on 13–93 glass fiber scaffolds for: (A) 4 days; and (B) 6 days. The micrographs show increased cell density during the 6 day incubation and well-attached morphology [Reprinted with permission from (Brown et al., 2008)].

Primary osteoblast cell culture on 45S5 resulted in a significantly higher osteocalcin synthesis and alkaline phosphatase activity (ALP) at day 6, indicating bioglass augmented osteoblast commitment and selection of a mature osteoblastic phenotype (I. Xynos et al., 2000). Regardless of the promising results obtained from mesenchymal stem cells (MSCs) which have proliferated and differentiated on bioactive glass, no augmented production of the bone differentiation marker ALP was observed for the glass in comparison to culture plastics used as control (Reilly et al., 2007). The osteogenic differentiation of rat marrow stromal cells was investigated by Ohgushi et al (Ohgushi et al., 1996). The study revealed that an apatite layer formed on the surface of materials which in turn stimulates osteoblastic differentiation and facilitates the attachment of undifferentiated stem cells. In addition, implantation of 13-93 glass in Fisher 344 rats confirmed the biocompatibility of material and the ability to support tissue infiltration and osteoid deposition when seeded with MSCs (Q. Fu et al., 2010). To improve the biological response and facilitation of healing, bioactive glasses can be doped with trace elements and other therapeutic oxides. Depending on the

application, some ions can be incorporated into the glass composition in order to enhance bioactivity, biodegradability or to induce therapeutic effects in, for example, osteoporotic or cancer patients (Pan et al., 2010). For instance, Ca^+ , Mg^{2+} , Sr^{2+} , Na^+ and K^+ can be incorporated into bioglass composition to tune bioactivity. Al^{3+} and Ga^{3+} can improve glass strength, and Ag^+ , Zn^{2+} , Cu^{2+} and Ti^{3+} when dosed in controlled concentrations can give antibacterial properties to bioactive glasses (Hoppe et al., 2011; Kaur et al., 2014).

2.4 Antibacterial activity of bioglass materials

Durable, smart materials that can be utilized as a medium for controlled release of bioactive agents present a significant interest for contemporary biomaterials research (Valappil et al., 2008). For bioglass materials the ions are incorporated into the glass structure and those ions are not a separate phase in the material, and so the overall rate of ion release is assessed by the rate of glass degradation (A. Ahmed et al., 2011). The dissolution rate of a glass network is dependent on the glass chemical composition and surrounding medium conditions (Leppäranta et al., 2008). For this reason, many therapeutic ions such as Ag^+ , Cu^{2+} , Ti^{3+} , Sr^{2+} , Zn^{2+} , Mg^{2+} , Al^{3+} , Fe^{3+} , and BO_3^{3-} have been added to the structure of bioactive glasses to tailor their properties for a particular application. The accepted fact is that doping of those elements into glasses can modify the dissolution rate as well as inducing a therapeutic effect through ion release. Of particular interest is the antibacterial effect which should be considered in designing a material for bone tissue engineering. An ideal implant should support the adhesion of the desired cells while at the same time preventing bacterial adhesion and the formation of bacterial “biofilm”. Biomaterial-associated infections can cause serious complications in orthopedic implant surgery. Once the biofilm is formed it is virtually impossible to break it with antibiotics (Belt et al., 2001). Often, the only remedy is

a revision surgery and implant replacement because biofilm growth protects the organisms from the host immune system and antibiotic therapies (Belt et al., 2001). One strategy to prevent biofilm formation on the implant surface is by using antimicrobial components (Bruellhoff et al., 2010). A suitable antibacterial agent should be effective against a broad range of Gram positive and Gram negative bacteria (A. Ahmed et al., 2011). Implant-associated bactericide should also have long lasting antibacterial action and low bacterial resistance along with implant safety to surrounding tissue (A. Ahmed et al., 2011). The exact mechanisms of the antibacterial action of bioactive glasses are not fully understood. It has been suggested that bacterial depletion happens due to an increasing pH and the subsequent osmotic effect as a result of ion release from glasses (Stoor et al., 1998). Ions such as Ag^+ , Zn^{2+} , Cu^{2+} and Ga^{3+} are known for their bactericidal properties. These ions can be released when abio-glass is in contact with aqueous medium, thus retarding bacterial adhesion and biofilm formation. Silica-based glasses containing bactericidal metal ions are considered to be promising candidates for such antibacterial materials (Catauro et al., 2004).

2.5 Silicon and calcium functions in human body

Silicon (Si) is an essential trace element in human body and whole body contains around 1-2 g Si (Jugdaohsingh, 2007). It plays an important role in connective tissues, particularly bone and cartilage (Carlisle, 1986; Sripanyakorn et al., 2005). Si is involved in bone formation by promoting extracellular matrix formation (e.g. collagen synthesis) and matrix mineralization while Si deficiency can result in depressed growth by reduced bone mass or slow healing of fractures. It has been found that Si supplementation with monomethyl trisilanol increased bone mass in osteoporotic patients (Jugdaohsingh, 2007; Sripanyakorn et al., 2005). It has been reported that average circulating Si in human body is in the range of

50-200 $\mu\text{g/l}$ and the majority of absorbed silica excreted in urine (Sripanyakorn et al., 2005). The test conducted by Lai et al. for 7 months revealed that the resorbed silica from implanted Bioglass® 45S5 in the tibiae of rabbits was safely extracted through urine. Furthermore, the detectable Si extraction was lasted until 24 weeks and the maximum rate of silicon extraction was 12.8 mg/day (Lai et al., 2002). Thus, due to beneficial effect of Si on bone health, Si-containing materials have gained increased attention over the past few decades.

Calcium is the fifth most abundant element in the human body after oxygen, carbon, hydrogen, and nitrogen and it makes up 2 % of the body by weight (Nordin, 1997). Nearly all the body calcium (99%) is in the skeleton. The remainder is in the teeth, the soft tissues, the plasma, and the extravascular fluid. The body needs calcium every day not just to keep the bones and teeth strong over life time but to ensure proper functioning of muscles and nerves (Pravina et al., 2013). Calcium deficiency disease, also known as hypocalcemia, rises the risk of developing diseases such as osteoporosis (Nordin, 1997). Osteoporosis is a systematic bone disorder in which the rate of bone resorption surpasses bone formation (Chitambar, 2010). It can be characterized by low bone density and micro-architectural deterioration of bony tissue which results in enhanced fracture risk (Elise Verron et al., 2010). Recently it is proved that gallium can increase the concentration of calcium and restrain the osteoclast activity (Chitambar, 2010).

2.6 Gallium-doped bioactive glasses

Ga ions can increase the concentration of calcium and retard osteoclast activity. The biological function of Ga *in vivo* and its low toxicity effect on osteoblasts and osteoclasts led to it being approved by the Food and Drug Administration (FDA) (Chitambar, 2010).

However it is dose-dependent and at levels over 14 ppm induces apoptosis (Bernstein, 1998; Franchini et al., 2012). It has been reported that Ga^{3+} ions reduce resorption and differentiation of osteoclasts without negatively affecting osteoblast viability or activity when used in doses ranging from 0-100 μM (Hall & Chambers, 1990; Elise Verron et al., 2010). The anti-resorptive properties of Ga^{3+} could be effective for treatment of diseases that are associated with the accelerated loss of bone mass such as multiple bone metastases, osteoporosis and Paget's disease. Gallium compounds such as gallium nitrate and gallium maltolate have attracted attention due to their reported therapeutic effects on certain bone cancers *i.e.* hypercalcemia, osteosarcoma, myeloma and Paget's diseases of the bone (E Verron et al., 2012; Warrell, 1997). Bone cancer is one of the few cancers that may still be cured even if it has spread. However, sometimes complete removal of cancerous cells is difficult and can increase the risk of cancer recurring after surgery (Wren et al., 2013). Gallium can inhibit bone cancer through various mechanisms such as modification of DNA structure, changing DNA and protein synthesis, enzyme inhibition. and prevention of microtubule assembly (Collery et al., 2002). Gallium gained a significant role in the treatment of bone cancer due to the following reasons: 1) it restricts osteoclast activity without changing viability 2) its ability to decrease crystal solubility 3) it increases bone calcium content. The anti-inflammatory and immunosuppressive gallium compounds have also been proved in animal models (Bernstein, 1998; Chitambar, 2010; Wren et al., 2012).

Although gallium does not have any specific role in human physiology, its special relationship with proteins and iron can improve biological response. Since only one-third of circulating transferrin is occupied by iron, it has free sites for more reactions (Chitambar, 2010). Gallium (redox inactive) due to same ionic radius, coordination number and electronegativity has selected as a good candidate to substitute with Fe^{3+} (redox active)

whereas in same condition gallium can sustain being reduced (Franchini et al., 2012; Pickup et al., 2009). Therefore, Ga^{3+} can react with the remaining sites and form transferring-gallium complexes and diminish the bacterial uptake of Fe^{3+} as well as enhancement of microorganism vulnerability (Malavasi et al., 2013; Valappil et al., 2009). Furthermore, Ga can be replaced with Fe^{3+} in proteins and act as antibacterial (Chitambar, 2010). Thus, researchers have attempted to dope Ga into commercial bone substitute materials such as hydroxylapatite (Melnikov et al., 2009), tricalcium phosphate (Mellier et al., 2011) and 45S5 bioactive glass (Franchini et al., 2012; Lusvardi et al., 2013).

The effect of Ga on apatite formation has been investigated (R. Bockman et al., 1986) and it has been reported that Ga has an inhibitory effect on HA deposition and growth (Blumenthal et al., 1989; Y. Okamoto & Hidaka, 1994). The Ga-doped Brushite showed reduced rate of HA formation in a solution containing calcium. This phenomenon was as a result of Ga adsorption on the apatite surface which further prevents the growth of hydroxyapatite (Korbas et al., 2004). In addition, to observe the impact of Ga on bioactivity, Franchini *et al.* (Franchini et al., 2012) examined a series of 45S5 containing Ga up to 3.4 mole %. The bioactivity test in SBF revealed that there is a competition between Ca and Ga for phosphate and as a result the phosphates consume rapidly and concentration of calcium was sufficient for calcite formation. It is hypothesized that this replacement can block crystallite growth. When the amount of Ga was at its lowest (1 mol%) as compared to silicon, calcium and sodium, it did not modify the structure of glass and thus had no effect on either the leaching properties nor on degradation (Franchini et al., 2012).

Doping Ga in glasses offers both benefits and drawbacks. Ga can act as both a network former and modifier, depending upon composition and quantity (Figure 2.3) (Aina et al., 2011). Ga can both retard apatite formation and slow down degradation rate; however, it has

a beneficial influence on the secretion and synthesis of type I collagen while it decreases osteocalcin gene expression. Although Ga compounds have demonstrated good results in the treatment of cancer-associated bone disease and osteoporosis, there are not enough studies which have investigated the cellular response of Ga-containing bioactive glasses. Thus, further experiments are required to assess the biological response of bioactive glasses doped with Ga. The effect of Ga on cell performance is further discussed in chapter 4.

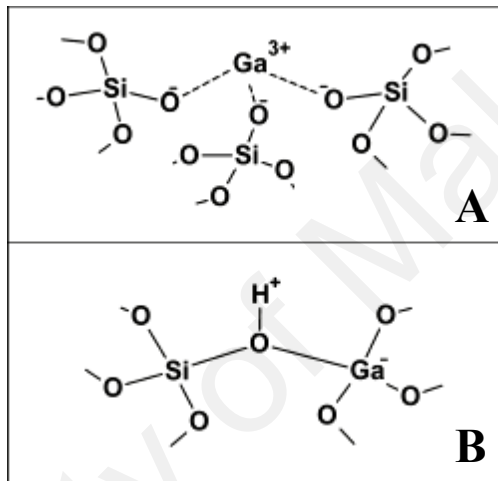


Figure 2.3: Possible structure of surface Ga sites; (A) Ga act as network modifier, and (B) Ga acts as network former [Reproduced with permission from (Aina et al., 2011)].

2.7 Zinc-doped bioactive glasses

Zinc is one the most important nutritional trace elements in the human body and plays a vital role in the activation of bone cells (Yamaguchi, 1998). Indeed, zinc has a stimulatory influence on bone formation and mineralization, and an inhibitory influence on bone resorption (Yamaguchi, 1998; Yamaguchi & Yamaguchi, 1986). About 85 % of the body's zinc (1.4-2.3 g) is contained in bone and muscle, and the remaining 15 % has been found in other soft tissues (e.g. liver and skin). Zinc concentration in the adult human skeleton is about

100 $\mu\text{g g}^{-1}$ (Clayton, 1979; Tapiero & Tew, 2003). Zinc deficiency is a common reason for bone growth retardation due to reduction in osteoblastic activity, in collagen content, in proteoglycan synthesis, and in alkaline phosphatase (ALP) activity (Calhoun et al., 1974). Low Zn bioavailability can also lead to inadequate immunoresistance to infections in elderly (Mocchegiani et al., 2001; Ripa & Ripa, 1994). Furthermore, it has been found that osteoporotic patients have lower skeletal Zn content than normal (Reginster et al., 1988). The oral administration of Zn compounds such as Zn-chelating dipeptide and Zn sulfate in rats has been shown to be effective in the treatment of osteoporosis. By using them, bone formation was stimulated as a result of increased DNA, calcium, and protein content, as well as ALP activity. The stimulatory effect of Zn on protein and RNA synthesis results in increasing ALP activity (Reginster et al., 1988).

Not only do Zn compounds indicate a stimulatory effect on the proliferation of mouse marrow cells but also they show an inhibitory effect on osteoclast-like cell formation (Kishi & Yamaguchi, 1994). On the other hand, excessive supplementation of Zn compounds can also result in some human disorders such as growth retardation, anaemia, and immunosuppression (Ripa & Ripa, 1994). Thus, the beneficial effect of Zn is greatly reliant on the dose and duration of treatment (Mocchegiani et al., 2001). It is reported that Zn concentration of 5.89 mg/l can inhibit the normal growth of osteoblasts (Yamamoto et al., 1998). Despite a discrepancy in the results associated with the biological response to Zn doped bioactive glasses, the majority of them, regardless of synthesis method, are in agreement with a decrease in dissolution of glasses by addition of Zn (Goel et al., 2013; Kamitakahara et al., 2006; Oudadesse et al., 2011). Although Zn is known to be a potent inhibitor of apatite crystal growth, it was found that Zn^{+2} release, at nontoxic levels, does not completely inhibit initial apatite deposition (Ito et al., 2002). Zinc initially retards HA

nucleation however it does not prevent the growth of HA at longer immersion times in SBF. Although Zn-containing bioglasses contained a lower number of HA nuclei on their surface, the nuclei were larger than that on the Zn-free control. In addition, the number of nuclei decreased with increasing Zn concentration (Figure 2.4). Furthermore, it is understood that retarded HA formation of zinc-doped bioactive glasses can further facilitate slower HA crystallization and thus a higher efficiency of bone bonding *in vivo* (Courthéoux et al., 2008).

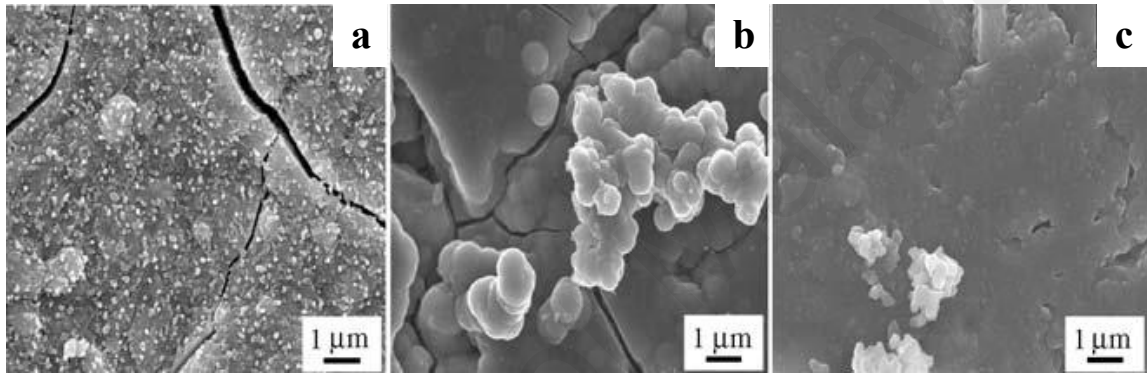


Figure 2.4: SEM images of apatite growth on the surface of (a) 58S (b) 58S-0.5% Zn (c) 58S-4% Zn after 1 day soaking in SBF [Reprinted with permission from (R. L. Du et al., 2006)].

Zinc addition to bioactive glasses has contradictory effects on cell response, with some studies mentioning a stimulatory effect of Zn on bone formation at up to 5 mol% and others reporting the optimal amount of Zn being less than 1 mol% (Balamurugan et al., 2007; Haimi et al., 2009). This effect can be highlighted by the glass formulation as it affects dissolution properties. The impact of Zn incorporation into the bioactive glass on the antibacterial properties and cell responses is further discussed in chapter 4.

In summary, Zn-containing bioactive glass acts in a dose-dependent way and its influence on living tissue is based on its concentration, bioavailability, and cell type. Therefore, more

work is required to optimize the Zn content and understand its release kinetics when incorporated into the glasses to hinder its adverse reactions without affecting HA formation.

2.8 Scaffold-guided tissue engineering and scaffold materials

2.8.1 Polymers: general requirements for bone regeneration

A polymer should have specific characteristics for its use as a scaffold in tissue engineering, including biodegradability, biocompatibility, lack of immunogenicity, ease of processability, strength and biological functionality (Puppi et al., 2010). Polymeric scaffolds have attracted a great deal of attention in the field of tissue engineering due to their properties such as high surface-to-volume ratio, controlled porosity, biodegradation, and mechanical integrity (Dhandayuthapani et al., 2011). The properties of polymers depend on the composition, structure, and arrangement of their constituent macro-molecules (Dhandayuthapani et al., 2011; Tian et al., 2012). The polymer may be used as such for scaffold fabrication or may be modified before or after scaffold fabrication on demand (Verma et al., 2011). Scaffold materials can be synthetic or natural, degradable or non-degradable, depending on their application (Verma et al., 2011).

The geometry and anisotropic properties of natural bone makes the designing of an 'ideal bone scaffold' difficult (Bose et al., 2012; Olszta et al., 2007). The material must be chosen and designed with compatible resorption and degradation rate. Sufficient mechanical properties are also necessary in order to retain adequate structural integrity of the scaffold until the newly grown tissue is capable to maintain mechanical load and complex biological functions (Puppi et al., 2010). A scaffold for tissue engineering must provide sufficient

mechanical support since it is responsible for tissue volume preservation. The mechanical properties of a scaffold must be matched with those of natural bone particularly stiffness and strength (Alvarez & Nakajima, 2009). The cortical bone Young's modulus is between 15 and 20 GPa and that of cancellous bone is between 0.1 and 2 GPa. For cortical bone, the compressive strength varies between 100 and 200 MPa, and for cancellous bone is between 2 and 20 MPa (Bose et al., 2012; Olszta et al., 2007). Stress shielding would occur when the transplanted bone stiffness is not matched to natural bone (Allo et al., 2012). Implants with a higher stiffness can lead to stress concentration in the surrounding area and ultimately increase the likelihood of failure. Uneven load sharing between bone and scaffold caused by stiffness inequality is known as stress shielding. The effect of this phenomenon appears in the bone remodeling process.

The mechanical properties of scaffolds are highly dependent on the type of polymer, fabrication technique, and porosity. Increasing porosity negatively influences scaffold strength and thus the void volume should be greatly controlled to allow both the accommodation of the large number of cells and the maintenance of the structural strength required for scaffold in load-bearing tissues (Bose et al., 2012; Puppi et al., 2010). An ideal scaffold should also degrade at a rate comparable with the rate of bone growth, physically creating open space for new bone formation, until full regeneration is achieved. Bioabsorbable scaffolds as surgical devices can reduce the number of surgeries since there is no need to perform a second operation to remove the implant (Akmaz et al., 2004; Guarino et al., 2008). The degradation of polymeric materials are influenced by their structure and properties such as molecular weight and distribution, glass transition temperature and crystallinity as well as environmental conditions such as medium, temperature and pH (L. Wu & Ding, 2004).

Polymeric materials can degrade by either surface or bulk erosion with chain scission caused by water or enzymatic attack (Chen et al., 2013). The surface erodible polymers degrade from the surface and the original shape of the sample always remains but becomes thinner during the degradation process (Langer & Peppas, 2003; Q. Liu et al., 2012). In addition, there is a linear relationship between mechanical properties and degradation time. In bulk-degradable polymers weight loss occurs throughout the sample which can result in a loss of strength with time. However the initial sample size could remain for a longer time (Q. Liu et al., 2012; Shi et al., 2009). It should be noted that the degradation rate of a scaffold is slower than solid block polymer for the bulk-degradable polyesters. The release of acidic degradation products from a solid block polymer is more difficult and could consequently lead to autocatalytic effect (S. Li et al., 1990; L. Wu & Ding, 2004). In case of porous scaffolds, the degradation is dependent on porosity and the pore size. Wu and Ding observed that scaffolds with lower porosities and larger pore sizes degraded faster than those with higher porosity and smaller pore sizes (L. Wu & Ding, 2004). This has been attributed to the effect of wall thickness and surface area so that both large wall thickness and smaller surface area can lead to a slow diffusion rate and high concentration of degradation product which can cause faster acid-catalyzed degradation. Nonetheless, the influence of material composition was more significant on degradation rate than pore morphology (L. Wu & Ding, 2005). High porosity (75-90 %) and pore interconnectivity are required to allow secure and fast bone growth (Alvarez & Nakajima, 2009). The porous network of scaffolds simulates the ECM architecture allowing cells to interact effectively with their environment (Dhandayuthapani et al., 2011). According to previous research, pore sizes between 200 and 400 μm facilitate cell adhesion, ingrowth and reorganization *in vitro* and neovascularization *in vivo*. Moreover, pore interconnectivity is important as it can facilitate nutrient diffusion to cells and removal of metabolic waste from cells (Puppi et al., 2010). In addition, bone tissue

engineering scaffold should be bioactive and osteoconductive in order to make a strong bond with the host tissue (M. Wang, 2003).

2.7.2 Elastomers as biomimetic scaffold materials

A general definition in polymer science states that elastomeric materials have glass transition temperatures (T_g) below room temperature thus enabling high molecular mobility. In case of biomaterial applications, it is important that the T_g of elastomers is lower than body temperature in order to retain a high degree of elasticity. Such materials can withstand elongation up to several hundred percent at relatively very low stress. Since the deformation is elastic, once the force is removed the elastomer will return to its original shape (Y. Li et al., 2012). The elastic properties are always influenced by the crosslinking density (Cordier et al., 2008). For that reason, elastomers can be processed in many different ways and the processing method can be used to control mechanical properties.

Elastomers have found a broad range of applications in tissue engineering not only because of reversible properties but also due to their ability to mimic the ECM of most tissues. Their application is not limited to soft tissues such as blood vessels, heart muscles, and nerves; their composites have also found applications in hard tissues such as bone and cartilage due to their high filler loading capacity (Serrano et al., 2010). Elastomers can be divided into two categories: natural and synthetic. There are some benefits and concerns associated to the both groups of elastomers which should be precisely considered in materials design for biomedical applications. Of particular interest are natural products/polymers because of their inherent biocompatibility and benign nature. However, due to a lack of sufficient mechanical properties and tedious purification techniques, synthetic elastomer

offer more possibilities in terms of tailored material properties (Chen et al., 2013). The synthesized elastomers can be adjusted for a particular application by controlling the synthesis reaction conditions. Predictable and reproducible physical, chemical and degradation properties of synthetic polymers can be modified to meet the specific requirements of different applications. Moreover, they are processable into desired shapes and sizes (Puppi et al., 2010). A variety of properties can be obtained and further modifications are possible without altering bulk properties by designing synthetic polymers (Tian et al., 2012). There are also two types of synthetic elastomers: 1) thermoplastic elastomers (physically crosslinked) such as polyurethane (PU), poly (hydroxyalkanoate) (PHA) and poly(caprolactone) (PCL)-based elastomers; and 2) thermoset elastomers (chemically crosslinked) such as poly (polyolsebacate) (PPS) and poly (diol citrate) (PDC). Figure 2.5 provides the basic classification of elastomeric materials used for biomedical applications.

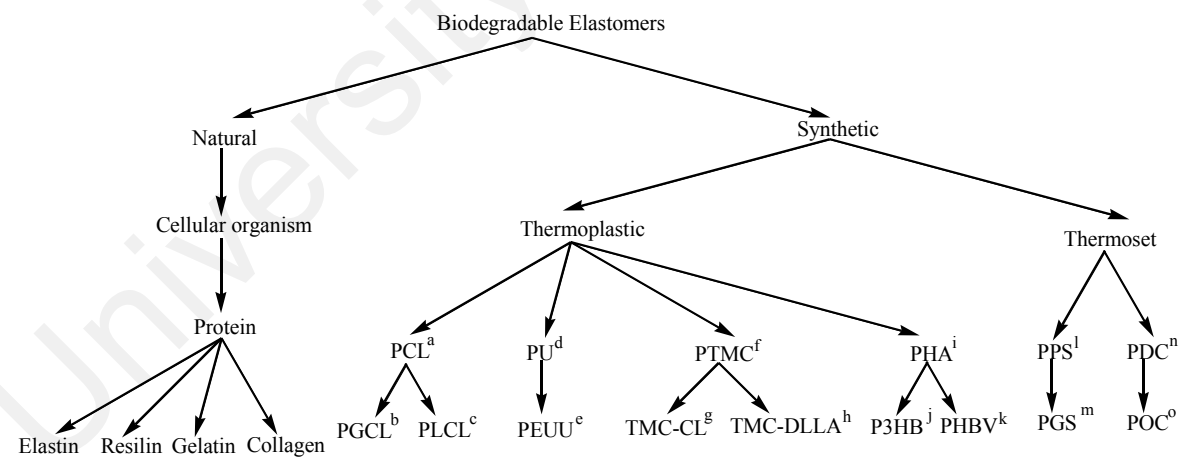


Figure 2.5: Classification of elastomers accompanied by examples of each group (Y. Li et al., 2012; Shi et al., 2009; You & Wang, 2011): ^aPoly (ϵ -caprolactone/glycolide); ^bPoly (ϵ -caprolactone/lactide); ^cpolyester urethane urea; ^dPoly(1,3-trimethylene carbonate); ^ePoly(1,3-trimethylene carbonate/caprolactone); ^fPoly(1,3-trimethylene carbonate/D,L-lactide); ^gPoly (3-hydroxybutyrate); ^hPoly (3-hydroxybutyrate-co-3-hydroxyvalerate); ⁱPoly(glycerol sebacate); ^jPoly (1,8-octanediol) citrate.

Thermoplastic elastomers (TPEs) are physically crosslinked which render them with both benefits and disadvantages. Physical crosslinking in TPEs mainly derives from hydrogen bonding or van der Waals forces and are therefore reversible under action of heat and solvents (Chen et al., 2013; Q. Liu et al., 2012). These elastomers can be synthesized by using the monomers containing two or more hydroxyl (-OH) or carboxyl (-COOH) functional groups in polyesterification reaction. Other TPEs can be synthesized by ring opening polymerization or double bond reactivity (Q. Liu et al., 2012). Significant feature of TPEs is that they can be easily recycled because of the thermoreversible nature of polymer networks. The physical crosslinks in TPEs disappear at elevated temperatures and the materials show flow behavior typical of a low molecular weight polymer whereas they behave as irreversible crosslinks at service temperature (Van der Mee et al., 2008). Furthermore, the degradation of TPEs can be controlled by changing constituent segments (Y. Li et al., 2012). However, thermoplastic materials undergo heterogeneous degradation due to crystalline regions which further can cause nonlinear loss of mechanical properties (Rezwan et al., 2006). In addition, the weak physical crosslinks can creep in long term or under cyclic mechanical deformation (You & Wang, 2011). In contrast, thermoset elastomers (TSEs) are chemically crosslinked or covalently crosslinked which is usually irreversible and stronger than physical crosslinks (Q. Liu et al., 2012). Thermoset biodegradable elastomers synthesized through polycondensation of multifunctional monomers, ring opening polymerization and microbial polymerization can crosslink mainly through thermo-curing or photo-curing. Curing locks the elastomer in final shape and reheating cannot cause TSEs to flow like TPEs. Thermoset elastomers can be synthesized in completely amorphous form. This can lead to homogenous weight loss through combination of bulk and surface erosion degradation which is the main reason for maintaining the 3D structure of scaffolds prepared from thermoset elastomers (Amsden, 2007; Y. Li et al., 2012). However, curing may lead to some limitations since it may cause

difficulties with materials processing. An example of this harsh curing condition is the high temperature (more than 100 °C) along with vacuum for days in curing of PGS (Y. Wang et al., 2002).

2.8 Elastomer/bioglass composite scaffolds

The original concept of using bioceramics as reinforcing phase in polymeric composites was introduced by Bonfield *et al.* in 1980s (Bonfield et al., 1981). Composites of polymers and bioactive glasses have been made with the aim to improve both mechanical properties and the biological response to materials. As previously discussed, polymers suffer from insufficient strength and poor bioactivity whereas bioactive glasses suffer from low fracture toughness, brittleness and low flexibility when used alone (Hacker & Mikos, 2009; Lü et al., 2009; Rezwan et al., 2006; Woodruff & Huttmacher, 2010). To engineer composites for hard tissue replacement, materials should have mechanical properties suitable for the purpose. In order to achieve this goal, bioactive glasses can be sintered or combined with polymers (as fillers or coatings), resulting in composite materials with improved bone repair ability (Chen & Boccaccini, 2006; Roether et al., 2002). To date, several studies have been conducted into the development of bioactive and biodegradable composites. This has been achieved by either dense or porous systems using bioactive glasses in the form of particles or fibers (Kim et al., 2008; Lu et al., 2005). A composite can profit from the advantages of both polymeric and bioglass phases e.g. high toughness and processability of polymers and the bioactivity and adequate strength of bioglasses (Boccaccini et al., 2010; Rich et al., 2002). Due to the elastomeric properties of tissues, elastomers and their composites have drawn continuing interest for tissue engineering applications. Table 2.2 provides an overview of

elastomer/bioactive glass composites and their physical properties. Detailed descriptions and an overview of the most relevant findings in the field of elastomeric polymer/bioglass composites are outlined in following sections.

University of Malaya

Table 2.2: Elastomer/bioglass composite materials.

Polymer		Bioglass	Percentage of Bioglass	Glass particle size	Compression (C), Tensile(T), Flexural (F) strength (MPa)	Modulus (MPa)	Porosity (%)	Contact angle (°)	Fabrication technique	Cell type	Reference
scaffold	membrane										
Natural polymers											
Gelatin		SiO ₂ -P ₂ O ₅ -CaO	10, 20, 30, 40, 50	10-80 nm	2.8-5.6 (C)	51-78	72-86		Direct foaming/ Freeze-drying	SaOS-2 cells	(Mozafari et al., 2010)
Gelatin		SiO ₂ -CaO	10	6 µm					Direct foaming/ Freeze-drying	Human dental pulp cells	(Nadeem et al., 2013)
Gelatin/Chitosan		SiO ₂ -P ₂ O ₅ -CaO	1	<100 nm					Freeze-drying	MG-63 osteoblast cells	(Peter et al., 2010)
Synthetic elastomers											
PCL		45S5	10, 50, 75	<45µm, <75µm					Salt-leaching		(Cannillo et al., 2010)
PCL		45S5	5, 10, 20	20 µm	0.04-0.12 (C)	0.45-1.15	~86		Particle leaching/ freeze extraction		(Ródenas-Rochina et al., 2013)
		HA		200 nm	0.07-0.10 (C)	0.68-1.11					
PCL		45S5	25, 50	<45µm	92-214 (KPa) (C)	132-251 (KPa)	88-92		Solid-liquid phase separation	MC3T3-E1	(Fabbri et al., 2010)
PCL		45S5	10	≤38 µm		48.35	~75		Melt extrusion based additive	MC3T3	(Poh et al., 2013)
		SrBG (46.46 SiO ₂ -1.07 P ₂ O ₅ -26.38 Na ₂ O-23.08 (3SrO:1CaO)				59.18					
PCL		SiO ₂ -CaO (75S25C)	10, 20, 30, 40	70 nm	19-21.5 (T)	198-851		81-56	Melt blending and thermal injection moulding		(Ji et al., 2015)

Table 2.2: Continued.

Polymer		Bioglass	Percentage of Bioglass	Glass particle size	Compression (C), Tensile (T), Flexural (F) strength (MPa)	Modulus (MPa)	Porosity (%)	Contact angle (°)	Fabrication technique	Cell type	Reference
scaffold	membrane										
	PCL	SiO ₂ -P ₂ O ₅ -CaO	10, 20, 30	4 μm (Particle) 450 nm (Fiber)	150 (T) 180 (T)	9 8			Solvent casting	MC3T3-E1	(Jo et al., 2009)
	PCL	SiO ₂ -P ₂ O ₅ -CaO	20	240 nm (Fiber)					Solvent casting	MC3T3-E1	(H.-H. Lee et al., 2008)
	PCL	P ₂ O ₅ -CaO	18, 38, 39	20-25 μm (Fiber)	25-30 (F)	0.5-2.4 (GPa)			Compression molding		(I. Ahmed et al., 2008)
P(CL/DL-LA)		S53P4 (53SiO ₂ , 23Na ₂ O-20CaO-4P ₂ O ₅)	5, 10	<45 μm, 90-315 μm		190-900 (KPa)	60-75		Solvent casting/ particulate leaching	Rat bone marrow stromal cells	(Jaakkola et al., 2004; V. Meretoja et al., 2006; V. V. Meretoja et al., 2014; Pamula et al., 2011)
	P(3HB)	45S5	5, 20	<5 μm		0.8-1.1 (GPa)			Solvent casting		(Misra et al., 2007)
	P(3HB)	45S5	10, 20	29 nm					Solvent casting	MG-63 human osteosarcoma	(Misra et al., 2009)
	P(3HB)	45S5	10, 20, 30	<5 μm 29 nm		1.1-0.8 (GPa) 1.1-1.6 (GPa)		87-55 87-61	Solvent casting	MG-63 osteoblast cells	(Misra et al., 2008)

Table 2.2: Continued.

Polymer		Bioglass	Percentage of Bioglass	Glass particle size	Compression (C), Tensile (T), Flexural (F) strength (MPa)	Modulus (MPa)	Porosity (%)	Contact angle (°)	Fabrication technique	Cell type	Reference
scaffold	membrane										
P(3HB)		CaO–SiO ₂ –P ₂ O ₅	10, 20, 30	~33 nm			84		Salt-leaching		(Hajiali et al., 2010)
P(3HB) (coated)		45S5		<5 μm					Slurry-dipping coating		(Olsen-Claire et al., 2006)
PU		45S5	5,10,20	<10 μm		0.12-0.81			Polymer coagulation/salt leaching		(Ryszkowska et al., 2010)
PU/PVA		SiO ₂ –CaO–P ₂ O ₅	10, 25	87 nm				38-81	Freeze-drying	Rat primary osteoblasts cells	(de Oliveira et al., 2012)
PU (coated)		SiO ₂ –P ₂ O ₅ –CaO–MgO–Na ₂ O–K ₂ O		<32 μm	0.12-0.1 (T)	0.12-1.35		95-87	Slurry-dipping coating		(Baino et al., 2009)
PU/PDLLA (coated)		45S5		<5 μm					Slurry-dipping coating		(Bil et al., 2007)
	PGS	45S5	5, 10, 15	~5 μm	0.42-1.53 (T)	0.38-1.62			Solvent casting	SNL mouse fibroblasts	(S.-L. Liang et al., 2010)
	PGS	45S5	2, 5, 10	20–50 nm		0.22-2.5			Solvent casting	SNL mouse fibroblasts	(Chen et al., 2010)

2.9.1 Composite scaffolds: fabrication techniques

Different methods have been used for fabricating porous composite scaffolds with tuneable pore sizes and interconnectivity as schematically illustrated in Figure 2.6. Table 2.3 also outlines those methods that have been previously reported in literature along with their advantages and disadvantages. More detailed descriptions can be found elsewhere (Kramschuster & Turng, 2012; M. Okamoto & John, 2013; Rezwan et al., 2006). Possibly the oldest and the most popular technique for scaffold fabrication is solvent casting/particulate leaching (SC/PL). In terms of polymer/bioglass composite materials there is a limitation to the level of bioglass inclusion into the polymer matrix. High amounts of bioglass can cause a precipitation phenomenon and the quality of mixing can vary with the manual ability of the operator. Further, the leaching step in water can cause development of calcite which can deteriorate the bioactivity of glass (Cannillo et al., 2010). The effect of various solvents (Fabbri et al., 2010) and porogens (Cannillo et al., 2010) were investigated on composite scaffolds made from PCL/bioglass using a porogen-leaching technique in order to evaluate physical, structural, and mechanical properties. Using dioxane instead of dimethylcarbonate as the solvent and a mixture of NaCl–NaHCO₃ as the porogen led to the attainment of larger pores with more homogenous distribution.

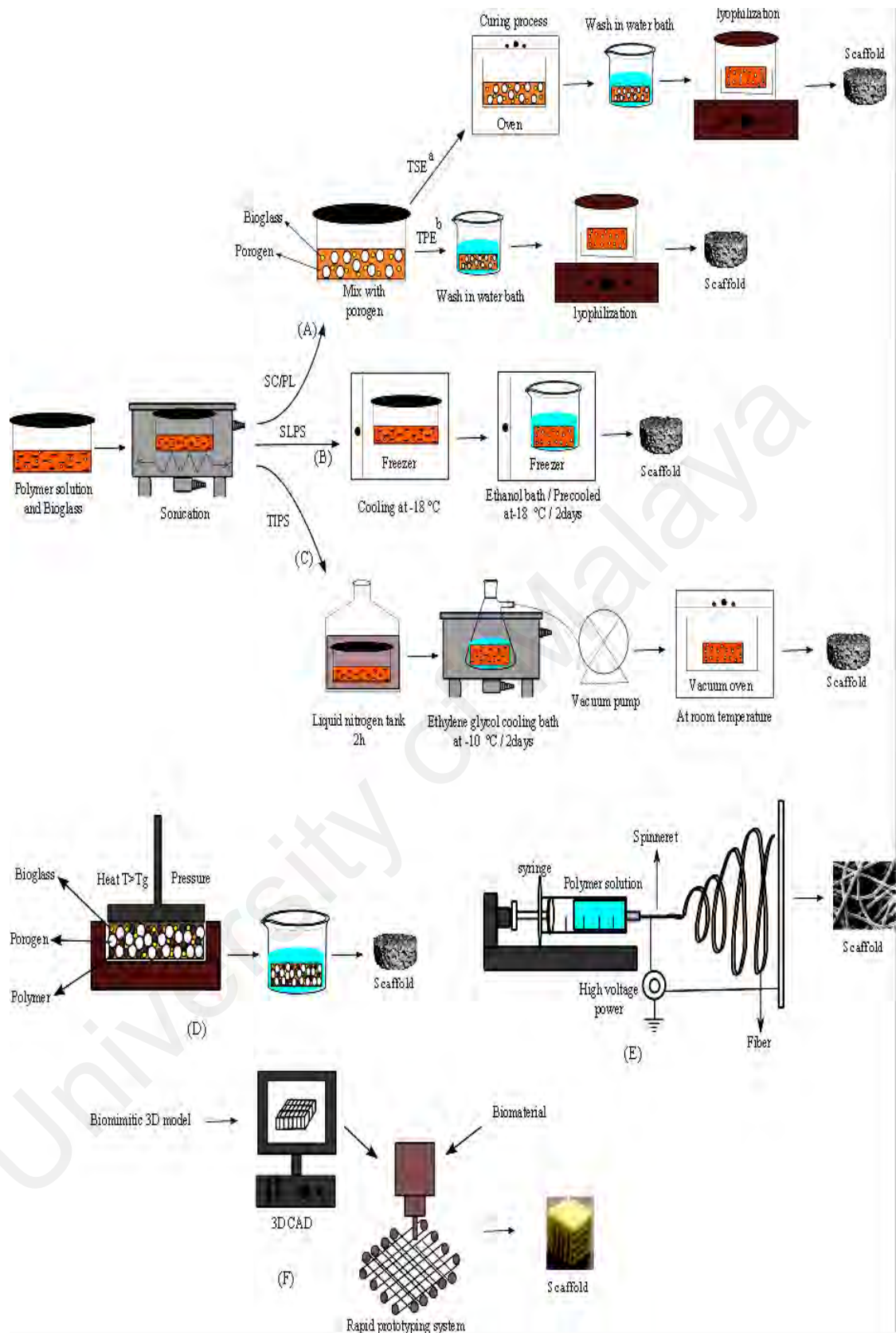


Figure 2.6: Schematic diagram of some common methods for fabrication of composite scaffolds including standard synthesis conditions; A) Solvent casting-particulate leaching (SC/PL) B) Solid-liquid phase separation (SLPS) C) Thermally induced phase separation (TIPS) D) Melt-molding E) Electrospinning F) Rapid prototyping techniques. ^a Thermoset elastomer; ^b Thermoplastic elastomer

Table 2.3: Benefits and drawbacks of common techniques for composite scaffolds fabrication (Boccaccini et al., 2003; Cannillo et al., 2010; Cao et al., 2006; Fabbri et al., 2010; W.-J. Li & Cooper Jr, 2011; Liebschner et al., 2003; Mano et al., 2007; Narayan, 2009; Peltola et al., 2008; Puppi et al., 2010; Subia et al., 2010).

Technique	Benefits	Drawbacks
Solvent casting/ particulate leaching (SC/PL)	-very simple -Control over porosity and pore size	-Residual solvents and porogen material -Difficult to accurately design the interconnectivity of the pores -precipitation phenomenon
Thermally induced phase separation (TIPS)	-Highly porous structure -Uniform porous scaffold -Highly interconnected structure -Highly anisotropic scaffold	-Small pore size -Long processing time -Technique sensitive
Solid-liquid phase separation (SLPS)	-Proper pore size distribution -Highly interconnected structure -High levels of porosity -Homogenous distribution of particles	-Residual solvent in thick constructs
Rapid prototyping or Solid freeform (SFF)	-Customization of the products to meet the individual needs -Ability to create complex geometries and high accuracy features -Possibility to control pore size and distribution of pores within the scaffold	-Limited polymer type -Highly expensive equipment
Slurry-dipping coating of scaffold	-Simple and quick -High bioactivity	-Pore clotting - residual solvent - Peeling-off of particles -Macrodelamination of the coating

It was found that the pores in scaffolds prepared by SC/PL were poorly interconnected to each other and the structure of the resultant scaffold collapsed following 6 weeks soaking in SBF (Figure 2.7) (Cao et al., 2006). It was attributed to thicker walls of SCPL scaffold which further can cause the autocatalytic hydrolysis effect. Thus, the SCPL scaffold showed a significant reduction of strength after 2 weeks immersion in SBF.

However the high interconnectivity of TIPS scaffold was the main reason for releasing the degradation product and thus the scaffold maintained its structure and mechanical integrity for longer (Cao et al., 2006). Nonetheless, SCPL is the most common method used for scaffold fabrication from thermoset bioelastomers due to the need to curing process (Kang et al., 2006).

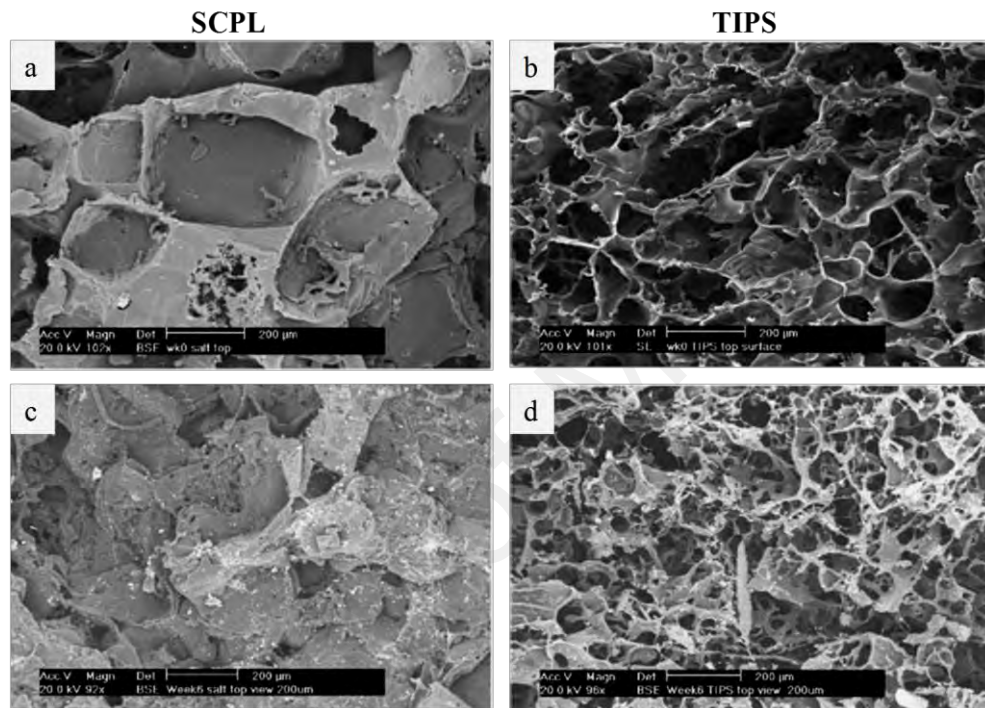


Figure 2.7: SEM images of the radial cross-sections of PLGA disks (13×6 mm) during the 6 weeks' degradation *in vitro*. (a and c) Salt-leached scaffolds; (b and d) TIPS scaffolds [Reprinted with permission from (Cao et al., 2006)].

Fabbri *et al.* believed that SLPS technique has advantages over TIPS and SCPL (Fabbri et al., 2010). Based on their opinion using a miscible solvent such as ethanol to remove the frozen solvent instead of vacuum sublimation in TIPS can lead to complete and effective solvent removal. Furthermore, the rapid solvent solidification and subsequent phase separation avoid the precipitation phenomenon which is observed for SCPL. In a study by Boccaccini *et al.* composite scaffolds prepared by two different methods of TIPS and slurry-dipping coating were compared in terms of bioactivity (Boccaccini et al.,

2003). It was clearly seen that coated scaffolds induced higher bioactivity in respect to filled scaffolds. HA particles were formed on the coated sample after 7 days of immersion in SBF and a thick and uniform layer of HA was formed after 28 days.

SFF was originally developed for the manufacturing industry enabling the fabrication of objects with unique materials, combinations and complex geometries which could not be achieved by conventional techniques (C. Liu et al., 2007). SFF is widely used in fabrication of the porous scaffolds due to efficiency and rapid fabrication. This particular technique provides highly reproducible scaffolds with following properties: optimal control over porosity, controlled pore size distribution and interconnectivity (Kramschuster & Turng, 2012; K. Leong et al., 2003). To our knowledge, there are no available published reports for the fabrication of elastomer/bioglass composites by using SFF technique.

2.9.2 Thermoplastic elastomer/bioglass composites

2.9.2.1 Poly (α -caprolactone) based thermoplastic elastomers

Poly (α -hydroxyl esters) such as poly (lactic acid) (PLA), poly (glycolic acid) (PGA), and their copolymers poly(lactic-co-glycolic acid) (PLGA) have been used in tissue engineering and drug delivery due to their excellent biocompatibility (Rezwan et al., 2006). However, the stiffness mismatches with ECM and their plastic deformation under cyclic loading limits applicability (Chen et al., 2012; Serrano et al., 2010). The alternative to polylactides/glycolides is poly (α -caprolactone) (PCL), a thermoplastic polyester elastomer approved by the FDA (Rezwan et al., 2006). However, due to its hydrophobicity, PCL degrades slowly (El-Kady et al., 2010; You & Wang, 2011). Copolymers of PCL with PLA, PGA and PLGA have been fabricated with the aim of

overcoming the problems of single polymer systems. Most of these copolymers have been synthesized by ring opening polymerization using $\text{Sn}(\text{Oct})_2$ as the catalyst (S. H. Lee et al., 2003). The mechanical and thermal properties as well as degradation rate of these copolymers can be tuned by controlling the composition and molecular weight of the copolymer phase (Rich et al., 2002). Copolymers show faster degradation than homopolymers and the properties of copolymers can vary from crystalline to amorphous depending on the co-monomer ratio. In addition, due to possessing ester moiety, their degradation proceeds by hydrolysis through di-esterification. The degradation products can be easily removed during the metabolic process (Chen et al., 2013). However, there are concerns about the acidic nature of degradation products, which can cause inflammation (Selling, 2010).

Bioglass particle size, composition and method of fabrication have a significant influence on the mechanical properties of PCL-based scaffolds (Cannillo et al., 2010). In general, both modulus and bioactivity are dependent on bioglass content (Fabbri et al., 2010). Rodenas-Rochina *et al.* compared scaffolds of PCL, PCL-nano-HA and PCL-micro-Bioglass composites prepared by particle leaching/freeze extraction using polyethylmethacrylate beads as porogen (Ródenas-Rochina et al., 2013). All scaffolds showed good mechanical properties (modulus= 0.12-6.8 MPa and yield strength= 0.02-1 MPa) and high interconnected porosity (about 86%), but elastic modulus decreased with increased filler content, likely caused by an agglomeration phenomenon. The study showed that addition of 5% inorganic filler promoted osteoblastic cell adhesion but did not stimulate cell differentiation in comparison to pure PCL. Additionally, differentiation was inhibited by HA, while cell adhesion was improved with HA as a result of enhanced protein adsorption (Ródenas-Rochina et al., 2013).

The properties of composite materials are highly dependent on the shape, size and size distribution of the reinforcing phase (M. Wang, 2003). For example, Jo *et al.* fabricated composite of PCL with sol-gel derived bioactive glass nano-fibers ($60\text{SiO}_2\text{-}36\text{CaO-}4\text{P}_2\text{O}_5$ mol %) and compared with a composite fabricated by bioactive glass micro-particles (Jo *et al.*, 2009). The results showed more evenly distributed nano-fibers due to their uniform shape and size in comparison to the micro-particulates. The incorporation of nano-fibers into the matrix effectively increased stiffness and elastic modulus of PCL, while micro-particulates had no significant influence on mechanical integrity. Ahmed *et al.* also fabricated composites of PCL and phosphate-based bioglass fibers ($\text{P}_2\text{O}_5\text{-CaO}$; 20-25 μm) using compression molding technique. Notably, the modulus increased from 0.5 GPa for pure PCL to approximately 2.5 GPa for composite film containing 18% volume fraction bioactive glass fiber (I. Ahmed *et al.*, 2008). The degradation rate of the composites was increased by increasing glass fiber content, which leached out into solution and was replaced by water residue in the structure (Figure 2.8).

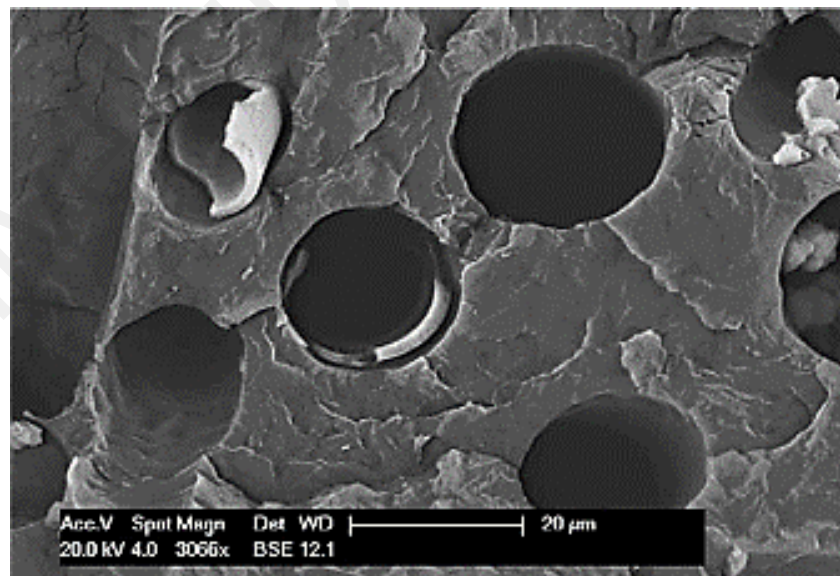


Figure 2.8: SEM images of PCL/glass fiber composite after 5 weeks immersion in deionized water [Reprinted with permission from (I. Ahmed *et al.*, 2008)].

The *in vitro* biological properties of materials were examined using MC3T3-E1 osteoblastic cells (Jo et al., 2009; H.-H. Lee et al., 2008). Cell attachment, differentiation and proliferation were significantly improved for the nanocomposites. Furthermore, *in vivo* testing using Sprague–Dawley albino rats showed prominent biocompatibility and bone formation (Figure 2.9) around nanocomposites compared to the microcomposites and pure PCL (Jo et al., 2009). These results indicate that there was no inflammatory response of the tissue samples to the nanocomposite at the defect sites.

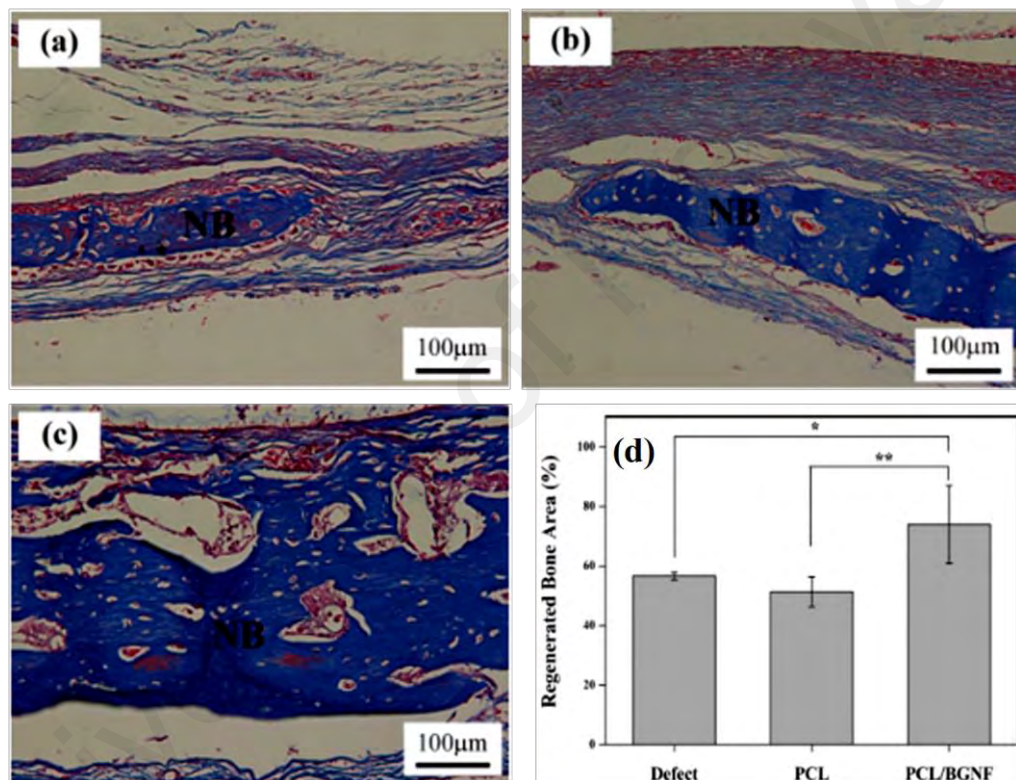


Figure 2.9: Optical micrographs of the newly formed bone (NB) in the vicinity of the defect center with a higher magnification: (a) empty defect; (b) pure PCL membrane; and (c) PCL/nanofiber bioglass composite membrane [Reprinted with permission from (Jo et al., 2009)].

Copolymers of PCL with PLA (PLACL) and PGA (PGACL) were synthesized with the aim of improving biodegradation and mechanical properties (Gan et al., 1999; Holmbom et al., 2005; Rich et al., 2002). Rich *et al.* synthesized composites of poly (CL/DLLA)/bioactive glass (S53P4) by applying various bioglass particle sizes and

contents. The composites with higher bioglass contents and smaller particle sizes resulted in faster HA deposition, weight loss and stiffness. T_g values were almost equal for all the samples, as a result of weak physical interactions between the bioglass and matrix (Rich et al., 2002). In a similar study, Meretoja *et al.* prepared copolymers of poly (CL/DLLA) with two different concentrations of precursors, namely PDLLA-rich, and PCL-rich polymers filled with glass (S53P4) (V. Meretoja et al., 2006). The results indicated that both copolymer composites had similar porosity and mass loss, while the compressive strength was higher for PCL-rich samples which also exhibited lower water absorption as a consequence of higher crosslinking density. Overall, the composites showed enhanced osteoblast adhesion and mineralization and when implanted into Sprague-Dawley rats, a random distribution of bone within the implants demonstrated that the scaffolds supported angiogenesis and osteoconductivity. The unfilled scaffold supported tissue ingrowth, but the composite showed improved ectopic bone formation (V. V. Meretoja et al., 2014).

In general, with the composite scaffolds composed of bioactive glasses and PCL-based materials (regardless of method of fabrication and glass size), porosity slightly decreased with glass content and pore shapes were irregular (Cannillo et al., 2010). However, in most cases 1-5 % reduction in porosity was observed (Ródenas-Rochina et al., 2013). Although higher water uptake was observed for the composites in comparison to the unfilled matrix, there was a threshold after which water uptake decreased (El-Kady et al., 2010; Rich et al., 2002). The higher weight loss for composites relative to the unfilled polymer was attributed to the role of glasses in fluid ingress into the bulk of the sample as well as bioglass dissolution. As a result, voids appeared within the scaffold and subsequently the surface was exposed to increased hydrolytic attack (Blaker et al., 2005; Rich et al., 2002).

2.9.2.2 Poly (hydroxyalkanoates) (PHA) based composites

PHAs are a class of thermoplastic aliphatic polyesters with applications in tissue engineering, due to their occurrence in nature, their nontoxic degradation products, and optimal compatibility with human cells (Misra et al., 2006). So far, many types of PHAs (more than 100) have been reported, each with different structures and stiffnesses, from elastomeric to hard materials (Steinbüchel, 2001). However, the use of PHAs is mainly confined to two polymers: poly (3-hydroxybutyrate) (P(3HB)) and poly (3-hydroxybutyrate-co-3-hydroxyvalerate) (PHBV). The main drawback associated with this group of polymers is their bioinertness. As a solution, bioglasses can be added to improve bioactivity and strength (Misra et al., 2007).

2.9.2.2.1 Poly (3-hydroxybutyrate)

P(3HB) is a member of the PHA group and has nontoxic degradation products and mechanical properties comparable to synthetic biodegradable polyesters such as polylactide (Engelberg & Kohn, 1991). The brittleness of crystalline P(3HB) limits clinical applications, but the addition of bioactive fillers can address this. Composite films of P(3HB) and bioglass (45S5) have been prepared by Misra *et al.* using a solvent-casting technique (Misra et al., 2008; Misra et al., 2007). Surprisingly, the addition of bioglass micro-particles had an adverse effect on the Young's modulus of P(3HB) in comparison to the unfilled material but this reduction was more manifest for the composites with lower bioglass concentration, presumed to be as a result of low interfacial strength between the polymer chains and bioglass. The addition of bioglass to P(3HB) causes an increase of T_g and a reduction in crystallinity. *In vitro*, the addition of nano-bioglass to P(3HB) made the composites highly bioactive, such that HA crystals were formed on

their surfaces after 5 days immersion in SBF (Misra et al., 2009; Misra et al., 2007). Glass particles were also coated on the surface of polymer scaffolds to enhance bioactivity (Boccaccini et al., 2003). Olsen-Claire *et al.* reported the fabrication of slurry coated P(3HB) meshes and fibers with bioglasses of mean particle size $< 5 \mu\text{m}$. The *in vitro* bioactivity of these samples revealed that HA crystals formed on the composite surface 3 days after immersion in SBF (Olsen-Claire et al., 2006).

In vitro evaluation of P(3HB)/nano-bioglass revealed that MG-63 human osteosarcoma cell proliferation decreased with bioglass quantity, and cell proliferation significantly reduced for the composite containing 20% bioglass compared to a tissue culture plastic control (Misra et al., 2009).

2.9.2.2.2 Poly (3-hydroxybutyrate-co-3-hydroxyvalerate)

PHBV is a copolymer of P(3HB) with a different percentage of 3-hydroxyvalerate (3HV). Incorporation of 3HV into the P(3HB) structure increases flexibility but decreases strength. Scaffolds of PHBV and bioglass (58S) were fabricated using compression molding, thermal processing, and salt particulate leaching techniques (H. Li et al., 2005). First, PHBV, bioglass and salt particulates were mixed and compression molded in a stainless-steel mold. After heating in a furnace at $180 \text{ }^\circ\text{C}$, the disk was immersed in water to leach the salt particulates. The compressive yield strength of the composites increased from 0.16 to 0.41 MPa with the addition of 20% bioglass. 3 days immersion in SBF revealed HA deposition on the surface (Figure 2.10) (H. Li et al., 2005). The water-contact angle noticeably decreased with increasing bioglass inclusion, inferring improved hydrophilicity.

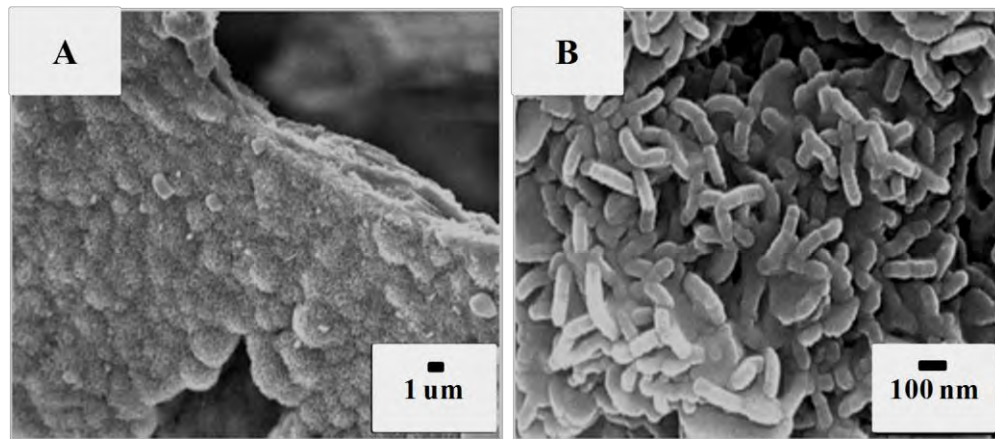


Figure 2.10: SEM images of composite with 20 % bioglass after immersion in SBF for 3 days [Reprinted with permission from (H. Li et al., 2005)].

2.9.2.3 Composite of polyurethane/bioglass

Polyurethane (PU) is the generic name for a class of synthetic polymers synthesized from polyisocyanates, polyalcohols and a chain extender (Bayer et al., 1937; Gunatillake et al., 2003; Howard, 2002; Rodríguez-Galán et al., 2011). The degradation and biocompatibility of PUs can be controlled by manipulating their macromolecular composition (Asefnejad et al., 2011). Generally, polyurethane elastomers (PUEs) have a linear segmented copolymer chemistry composed of a macrodiol, an isocyanate chain extender. PUEs and their composites have been used in artificial skin (Gogolewski & Pennings, 1983), cardiac tissues (Alperin et al., 2005), knee joint meniscus (Spaans et al., 2000), and drug delivery systems (Sivak et al., 2008).

Bioglasses have been added to PUs to improve their bioactivity and mechanical properties (de Oliveira et al., 2012). Ryszkowska *et al.* synthesized polyurethanes from 4,4-dicyclohexylemethane diisocyanates, poly(caprolactonediol), and ethylene glycol with different molar ratios, namely 2:1:1, 2:3:1 and 5:1:4. Scaffolds containing bioglass had a more uneven structure compared to pure PU (Figure 2.11). Due to the use of PCL in PU synthesis, it is assumed that the scaffolds undergo bulk degradation through

hydrolysis of ester bonds, indicating that polyurethane soft segments (ester bonds) are more susceptible to degradation than urethane bonds. DMA results revealed that composites have both a higher storage modulus before immersion in SBF, and also a modulus increase with increasing bioglass content after 8 weeks immersion (Ryszkowska et al., 2010).

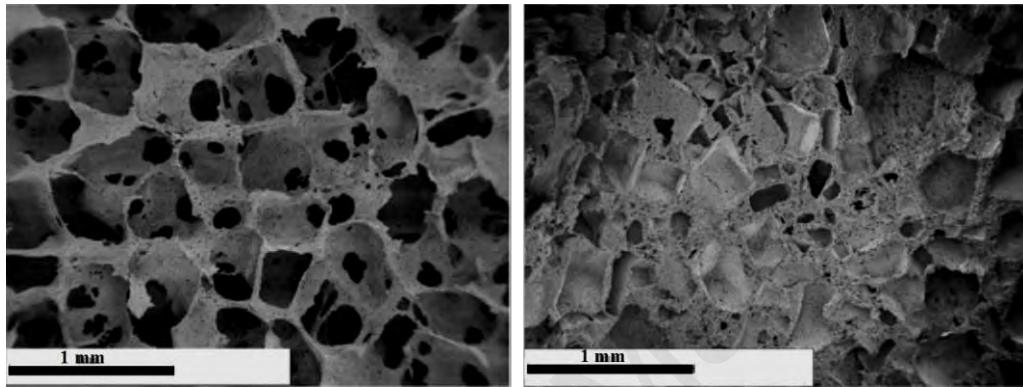


Figure 2.11: SEM images of porous samples of (a) pure polyurethane and (b) composite containing 20 % bioglass [Reprinted with permission from (Ryszkowska et al., 2010)].

The study by de Oliveira *et al.* suggested that there is a threshold for filler additions to result in improvements. In this study, nanocomposites of a degradable polyurethane/polyvinyl alcohol blend and bioglass nanoparticles ($\text{SiO}_2\text{--CaO--P}_2\text{O}_5$) were fabricated by freeze-drying (de Oliveira et al., 2012). The composite scaffold with 10% bioglass had higher compressive strength than the unfilled polymer, but both scaffolds recovered to about 95 %. The tensile modulus increased for composite containing 10 % bioglass as the glass particles react with polyvinyl alcohol (Figure 2.12). These composites also exhibited good bioactivity *in vitro* with improved cell growth and proliferation (de Oliveira et al., 2012).

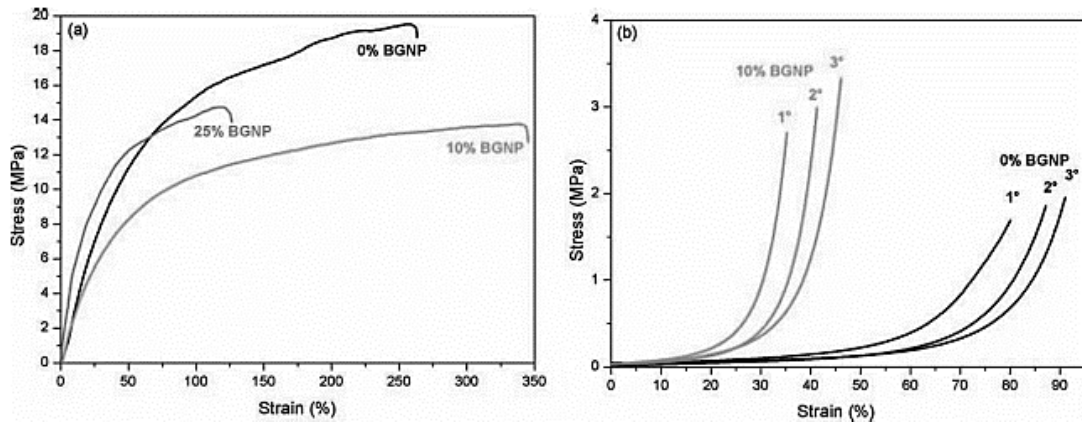


Figure 2.12: (a) Tensile stress–strain curves of PU/PVA blend, composites PU/PVA with 10 and 25 % of BGNP; and (b) Compressive stress–strain curves of foams PU/PVA and PU/PVA with 10% of BGNP, essayed successive referred as 1, 2, and 3 tests, respectively [Reprinted with permission from (de Oliveira et al., 2012)].

Other studies have investigated the influence of bioactive glass coats on the mechanical, degradative and bioactive properties of PU foams. The scaffold made of PU was coated by $\text{SiO}_2\text{--P}_2\text{O}_5\text{--CaO--MgO--Na}_2\text{O--K}_2\text{O}$ bioactive glass using a slurry coating technique (Figure 2.13). The stiffness and strength of the scaffold was higher than that of the uncoated polymer when the porosity was 8% less than the uncoated scaffold.

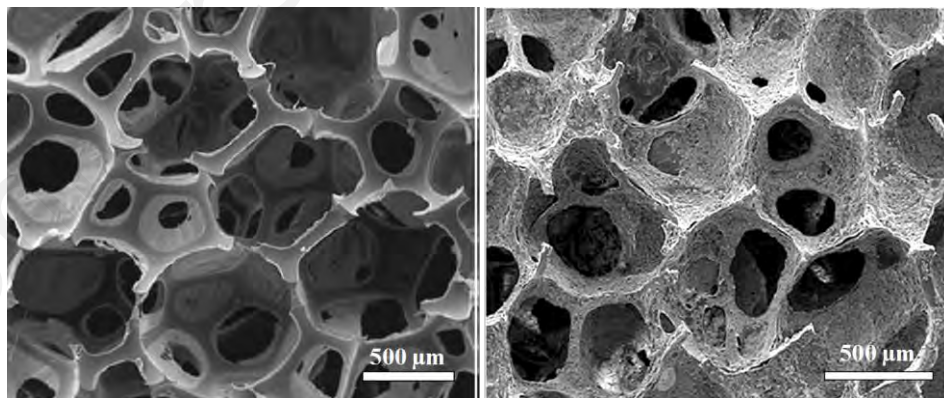


Figure 2.13: SEM images shows the morphology of: a) neat PU scaffold; b) composite scaffold [Reprinted with permission from (Baino et al., 2009)].

However, strength and stiffness were low in comparison to human bone (Baino et al., 2009). There was a higher weight loss from composites than from pure polymers (Figure 2.14) (Bil et al., 2007).

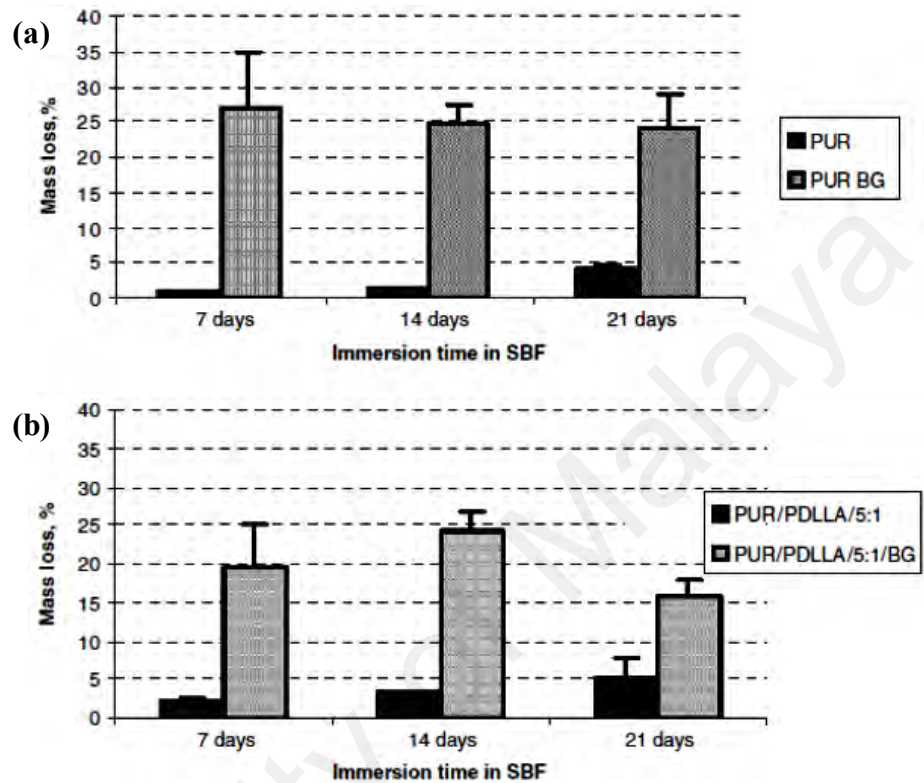


Figure 2.14: Comparison of mass loss of: (a) Bioglass-coated and uncoated PUR; and (b) PUR/PDLLA scaffolds during immersion in SBF for up to 21 days [Reprinted with permission from (Bil et al., 2007)].

2.9.3 Thermoset polyester/bioglass elastomer composites

2.9.3.1 Poly (diol citrate)

Two members of this group of elastomers are poly (polyolsebacate) (PPS) and poly (diol citrate) (PDC). PDCs (Figure 2.15) were first synthesized through a simple polycondensation reaction of non-toxic monomers such as citric acid and various aliphatic linear diols (1,6-hexanediol, 1,8-octanediol, 1,10-decanediol, or 1,12-dodecanediol) under mild conditions (Yang et al., 2004; X.-Q. Zhang et al., 2009). The pre-polymer is soluble in various solvents such as ethanol, dioxane and acetone that

facilitate its use in the production of scaffolds of different shapes and sizes. Furthermore, PDCs can be crosslinked at body temperature (Yang et al., 2004). Yang and coworkers observed that mechanical properties, degradation profile and surface characteristics of PDCs can be influenced by modifying curing conditions (time and temperature) and by the initial monomer molar ratio of monomers (Yang et al., 2004). Increasing the time and temperature of curing led to enhanced crosslinking density, which subsequently improved mechanical properties and decreased degradation (Yang et al., 2006). Among the PDCs, poly (octanediol citrate) (POC) attracts most interest because of its mechanical properties (ultimate tensile strength of 6.1 MPa, Young's modulus of 0.92– 16.4 MPa, and elongation at break of 117–265%) (Barrett & Yousaf, 2009; Serrano et al., 2010; Yang et al., 2004). In addition, 1,8-octanediol is the largest aliphatic diol that is water soluble and without any toxicity report (Yang et al., 2004). POC has free carboxylic groups derived from citric acid which eliminates the need for surface pre-treatment and consequently facilitates the conjugation of proteins such as fibronectin (Xu et al., 2012; Yang et al., 2006). Another major benefit of POC is good cell adhesion and confluence without requiring any treatment. Yang *et al.* (Yang et al., 2006) observed a better growth and cell viability of smooth muscle and human aortic endothelial cells on POC films compared to PLLA. The *in vivo* test in rats illustrated that fibrous capsule thickness in POC (approximately 50 μm) was as same as PGS and smaller than PLGA and did not change after one month of implantation. A thinner fibrous capsule is beneficial for mass transfer between a cell-based implant and surrounding tissues (Yang et al., 2004; Yang et al., 2006).

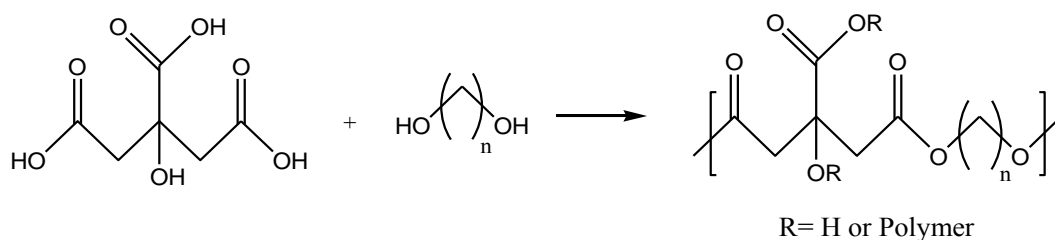


Figure 2.15: General structure of PDC

Several studies have developed composites of POC and bioceramics (e.g. HA) for load bearing applications (Chung, Qiu, et al., 2011; Qiu et al., 2006). Qui *et al.* (Qiu et al., 2006) investigated the mineralization of POC composites loaded with HA. Mineral nodules started to form after 3 days immersion of the composite surface and the surface was almost covered with calcium phosphate nodules at day 15 (Figure 2.16). Shirazi *et al.* also observed that the crystalline mineral nodules were deposited on the POC/ β -calcium silicate composite surface after 7 days incubation in SBF. The authors observed that the apatite formation ability increased in line with increasing calcium silicate content (Shirazi et al., 2014).

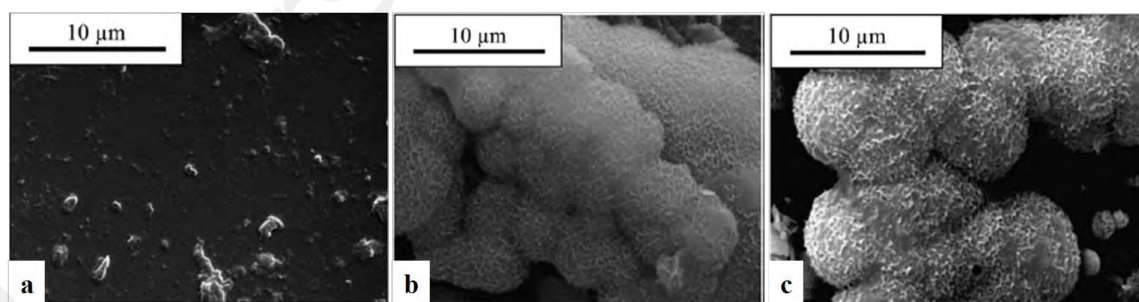


Figure 2.16: Apatite mineralization in SBF after 15 days of incubation at 37 °C for A) POC B) POC-HA composite with 40 wt% HA and C) POC-HA composite with 65 wt% HA [Reprinted with permission from (Qiu et al., 2006)].

26 weeks implantation of POC-HA and PLL revealed that leukocytes were in close proximity to PLL implants. The results proved that POC-HA composite had a higher average of osteoblast and trabecular bone surface area whereas PLL capability on osteoid

surface area was higher. By 52 weeks, tissue ingrowth into POC-HA was increased in comparison to PLL, which highlights an additional benefit of these novel biomaterials. Furthermore, a composite containing 60% HA showed a better compatibility, less fibrous capsule thickness, and higher rate of bone regeneration (Chung, Kodali, et al., 2011).

In another study by Chung *et al.* the effect of micro and nanoparticles of HA on the POC composite was investigated (Chung, Kodali, et al., 2011). Qualitative observations suggested that with increasing HA content, a decrease in the interparticle and interaggregate distance occurred, giving the appearance of a homogenous particle phase with increased packing (Figure 2.17). The microparticles within the microcomposites were less uniformly distributed, and increasing HA content increased the heterogeneity of the surface topography. Nanocomposites had significantly higher stiffness and strength relative to their corresponding microcomposite counterparts. Notably, there were no significant differences between high and low content (60 and 40 wt %) within composites of equally sized HA, whether nano or microparticles, for the above discussed characteristics, suggesting that particle size may be more important than HA content during bone formation.

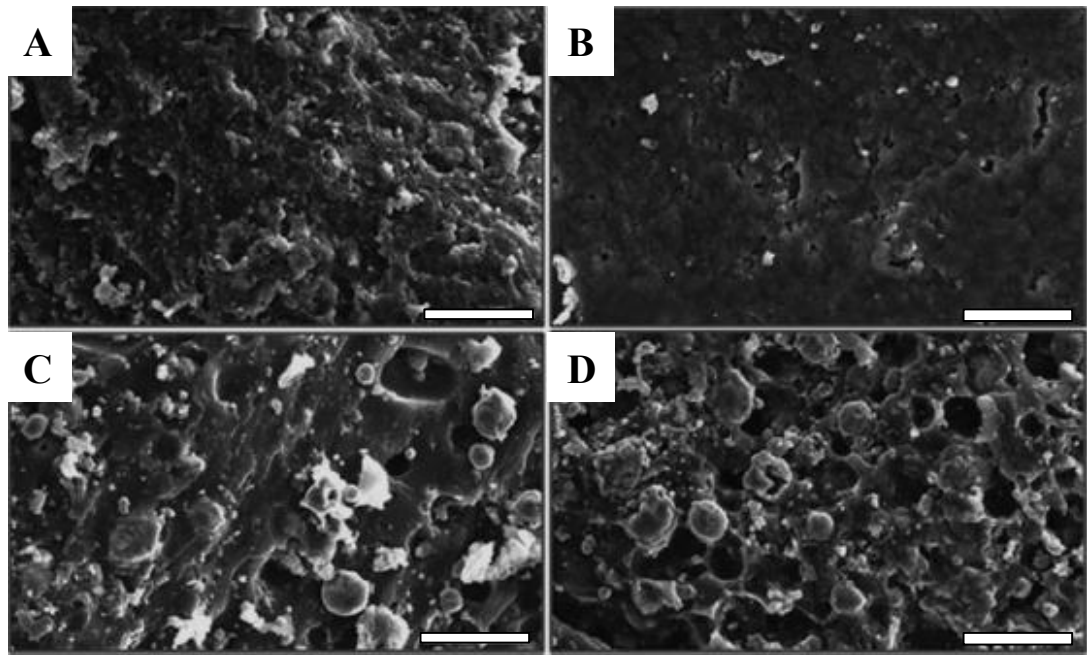


Figure 2.17: SEM images of POC–HA composites. (A) 40nano, (B) 60nano, (C) 40micro, and (D) 60micro. An increase in nanoparticle content enhanced surface homogeneity, whereas an increase in microparticle content enhanced heterogeneity. SB for all POC–HA composites (A,B,C,D) = 50 μm [Reprinted with permission from (Chung, Kodali, et al., 2011)].

It was found that surface roughness was increased for the microcomposite whereas higher trabecular bone formation at the interface of bone-implant was observed for the nanocomposite (Chung, Kodali, et al., 2011). After 6 weeks implantation in New Zealand rabbit knees, a thin layer of cartilage covered the surfaces of the implants (Figure 2.18) and the complete recovery of surrounding articular cartilage was observed. However, so far, no attempt has been made to produce therapeutic ion-releasing bioglass composites with biocompatible POC elastomers.

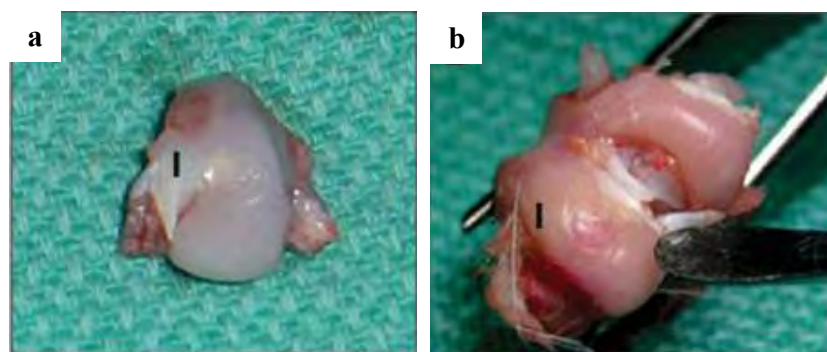


Figure 2.18: Digital images showed new cartilage layer formed over POC-HA (a) nanocomposite; (b) microcomposite; implanted 6 weeks in New Zealand rabbit knee [Reprinted with permission from (Chung, Kodali, et al., 2011)].

2.9.3.2 Poly (glycerol sebacate)

Poly (glycerol sebacate) (PGS) is a synthetic biodegradable thermoset elastomer composed of glycerol and sebacic acid (S.-L. Liang et al., 2010). Depending on the extent of crosslinking, Young's modulus can fall in the range of 0.05-1.5 MPa (Chen et al., 2010). PGS degrades by approximately 17% in 60 days in PBS, whereas implantation in Sprague–Dawley rats reports full degradation over the same period of time (Chen et al., 2010). Stuckey *et al.* observed complete PGS resorption over almost 6 weeks *in vivo* (Stuckey et al., 2010). Therefore, fast degradation of PGS can cause an increase in the acidity of the environment, and consequently increase cellular toxicity (Chen et al., 2010; S.-L. Liang et al., 2011; S. Liang et al., 2012). To address the above issues, alkaline fillers such as bioglass have been mixed with PGS. Liang *et al.* studied the biodegradation of PGS/45S5 composite and PGS/PLA copolymer under both static and cyclic mechanical loading in buffered solution and culture medium (S.-L. Liang et al., 2011). Increasing bioglass content led to faster degradation and increased swelling; the ester-type crosslinking competed with ionic linkages, and since ionic bonds were unstable in aqueous media, the rate of degradation was enhanced. Second, bioglass neutralized pH and thus hydrolysis rate decreased (S.-L. Liang et al., 2011). The authors also investigated

the mechanical properties of pure PGS and its composites containing micro-bioglass (5, 10, 15 %) (S.-L. Liang et al., 2010); the addition of which significantly increased elongation at break and Young's modulus in dry conditions. However, the modulus showed a dramatic decrease for composites in aqueous culture medium. Additionally, the composites with the highest bioglass content (15%) exhibited the biggest decrease in modulus from 1.62 to 0.59 MPa after one day incubation relative to composites with 10 and 5 %. This was attributed to the decline in ester bond formation since this type of bonding is more robust compared to ionic metal carboxylate bonds (S. Liang et al., 2012). In a related study, Chen et al. prepared composite films of PGS and nano-bioglass (Chen et al., 2010) which exhibited higher modulus in comparison to the microcomposites even though less bioglass was used (S.-L. Liang et al., 2010).

In vitro indirect cytotoxicity testing using SNL mouse fibroblasts revealed that the cytotoxicity of composites with low bioglass content was comparable with culture dish and PDLLA used as controls (Chen et al., 2010; S.-L. Liang et al., 2010). A high bioglass concentration resulted in high cytotoxicity attributed to high pH, which could be a result of the release of Ca^{2+} and Na^+ ions. However, the addition of up to 5% nano-bioglass significantly increased biocompatibility so that the percentage of dead cells for nanocomposites was approximately similar to when using a culture plastic dish or PDLLA (Chen et al., 2010). Significant cell proliferation was observed for all the composites after 2 days culture (Chen et al., 2010; S.-L. Liang et al., 2010).

2.10 Composite materials from natural elastomers and bioglass

Natural polymers have low toxicity, low disposal costs, and renewability (Shogren & Bagley, 1999). Those commonly used in bone tissue engineering include collagen, elastin, alginate, silk, chitosan and hyaluronic acid (Dhandayuthapani et al., 2011; S.-H.

Lee & Shin, 2007). Natural elastomers have benefits for tissue engineering applications in terms of cell adhesion, cell responsive degradation and re-modeling (Puppi et al., 2010; Varghese & Elisseeff, 2006). For example, collagen and elastin play a vital role in many extracellular structural tissues due to their wide range of elastic properties, including complete recovery after deformation (Urry et al., 2002). Nonetheless, they suffer from inadequate physical properties in terms of solubility and rapid degradability (Puppi et al., 2010; Sionkowska, 2011). Therefore, it is required to hydrolyze the natural macromolecules into shorter chains, which are usually soluble in water. For example, the soluble derivatives of elastin (i.e. elastin peptides, digested elastins and tropoelastin) and collagen (i.e. gelatin) have a wide range of medical applications (Wise et al., 2009). However, the high degradation rate of these derivatives, which causes a rapid loss of mechanical properties, limits their application. It is possible to blend them with synthetic polymers or inorganic materials to produce composites (Cascone et al., 1997; Perez et al., 2013; Sionkowska, 2011). In many cases, various crosslinking techniques can yield natural materials with high mechanical integrity (Bigi et al., 2001; Vieth et al., 2007). For example, Mozafari *et al.* fabricated nanocomposite scaffolds of gelatin and bioglass using a direct foaming technique followed by freeze-drying and lamination (Mozafari et al., 2010). Crosslinking was carried out using glutaraldehyde. The compressive modulus and strength of the resultant scaffolds were increased by the presence of the bioglass when the porosity and pore size were comparable to cancellous bone (in the range of 72-86 % and 200-500 μm respectively) (Mozafari et al., 2010). Nadeem *et al.* also employed a direct foaming technique for the production of scaffolds from gelatin and sol-gel derived calcium silicate bioglass (Nadeem et al., 2013). Crosslinking was carried out using dehydrothermal treatments over a range of temperatures and exposure periods in the sequence with genipin. The period of dehydrothermal crosslinking had a significant influence on the final properties, especially the degradation profile. The weight loss

reached its lowest percentage when gelatin was treated for 48 hr, suggesting an optimal degree of crosslinking and aqueous stability (Haugh et al., 2009). It is important to note that the scaffold demonstrated cellular bioactivity almost equal to neat bioglass (Figure 2.19).

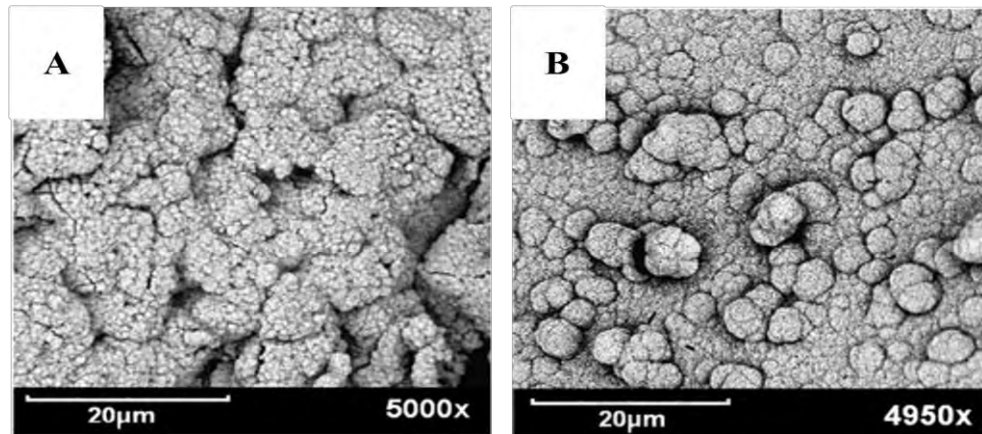


Figure 2.19: SEM images of: (A) gelatin/bioglass scaffold; and (B) bioglass particles with apatite on the surface after immersion of 3 days in SBF [Reprinted with permission from (Nadeem et al., 2013)].

Peter *et al.* prepared composite scaffolds composed of a blend of chitosan and gelatin with sol-gel derived nano-bioglass ($\text{SiO}_2\text{-CaO-P}_2\text{O}_5$) by a freeze-drying technique (Peter et al., 2010). It was reported that the swelling and degradation ratios were significantly reduced for scaffolds containing bioglass which was assumed to be due to the formation of strong bonding between hydrophilic groups of gelatin and bioglass. In addition, lower degradation of scaffolds was attributed to neutralization of the acidic degradation products of chitosan, as a result of bioglass leaching into the aqueous solution. Evaluation of cellular response *in vitro* showed the gelatin/bioglass scaffolds had appropriate biocompatibility when seeded with SaOS-2 cells (osteoblastic cell model) and human dental pulp stems cells (HDPSCs) (Mozafari et al., 2010; Nadeem et al., 2013). Observation of composite scaffolds by SEM after 3 days in culture revealed ECM secreted onto the surface of scaffolds, indicating the effective cellular migration and

osteoconductivity of scaffolds. Higher levels of cell attachment were observed for the untreated samples within the first 3 hrs, which was attributed to a higher density of free amino acid groups on untreated samples, in comparison with the cross-linked ones. More amino acid groups result in a higher cumulative surface charge, which facilitates cell attachment (Nadeem et al., 2013). The composite scaffolds supported hPDLF growth and maintained their osteogenic differentiation capacity as observed from alkaline phosphatase staining (Figure 2.20). Incorporation of nanoparticles further increased the concentration of binding sites at the surface of the material (Peter et al., 2010). Osteoblastic cells (MG-63) were well attached and spread on the scaffolds.

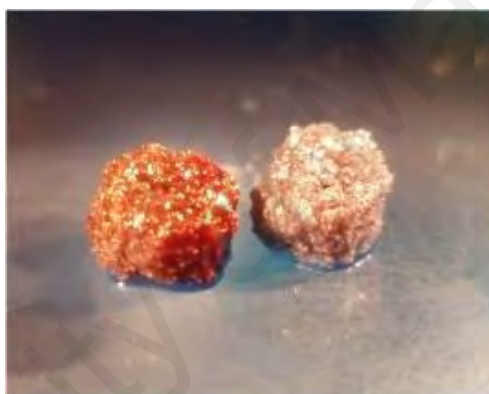


Figure 2.20: Alkaline phosphatase staining image obtained from microscope for: left-Composite and right-control [Reprinted with permission from (Nadeem et al., 2013)].

Srinivasan *et al.* reported the fabrication of a new nanocomposite scaffold from alginate and bioactive glass ($\text{SiO}_2\text{-CaO-P}_2\text{O}_5$) (Srinivasan et al., 2012). The results showed improved protein adsorption and MG-63 with hPDLF cell attachment and proliferation on nanocomposites in respect to pure alginate scaffold. The authors observed that there was no significant difference in cell viability of either hPDLF or MG-63 cells between all scaffolds. Furthermore, ALP activity showed a significant increase for hPDLF cells as compared to MG-63 cells. Very recently composites of carboxymethyl cellulose–dextran and bioactive glass ($\text{SiO}_2\text{-Na}_2\text{O-CaO-ZnO-Ga}_2\text{O}_3$) containing various amount of Ga were fabricated. The results indicated that all the composite materials have

antimicrobial efficiency against *E. coli*, *C. albicans* and *S. aureus* (Keenan, Placek, Hall, et al., 2016). It was found that composite extracts did not decrease neither fibroblast nor osteoblast viability while composites with the highest amount of Ga significantly decreased MG-63 osteosarcoma viability after 30 days (Keenan, Placek, Coughlan, et al., 2016; Keenan, Placek, Keenan, et al., 2016). The result revealed that the composites have potential as bone void-filling materials and for anti-cancerous applications.

2.11 The effect of filler size: polymer / bioglass nano- and micro- composites

It is established that filler size can affect strength, bioactivity and cell proliferation (Vollenweider et al., 2007). Misra *et al.* compared the influence of micro (<5 μm) and nano (29 nm) bioglass particles when mixed into a P(3HB) polymer matrix (Misra et al., 2008). The authors observed that addition of nano-size bioglass has a greater impact on mechanical and structural properties of composite films than micro-size fillers (Figure 2.21). Young's modulus for the unfilled polymer was between that of the micro and nanocomposites while the nanocomposites with 10 % bioglass demonstrated the highest modulus. The higher modulus of nanocomposites was attributed to the higher interfacial surface area which results from an increase in load transfer between polymer and filler. On the other hand, agglomeration of micro-particles is the main reason for lower strength. The obtained data for mechanical properties by Caridade *et al.* for composite films of chitosan/45S5 bioglass are comparable with the results from Misra *et al.* (Caridade et al., 2013). Results from both groups indicated an increase in Young's modulus with decrease in filler size (from nano to micro) (Misra et al., 2008). Contrary to those results, nanocomposite scaffolds produced from PDLA filled with nano-size 45S5 bioglass had lower strength than either pure PDLA or microcomposite scaffolds (Gerhardt et al.,

2011). On the other hand, porosity was increased, by the addition of nano-bioglass, to about 93.4 %, compromising mechanical properties.

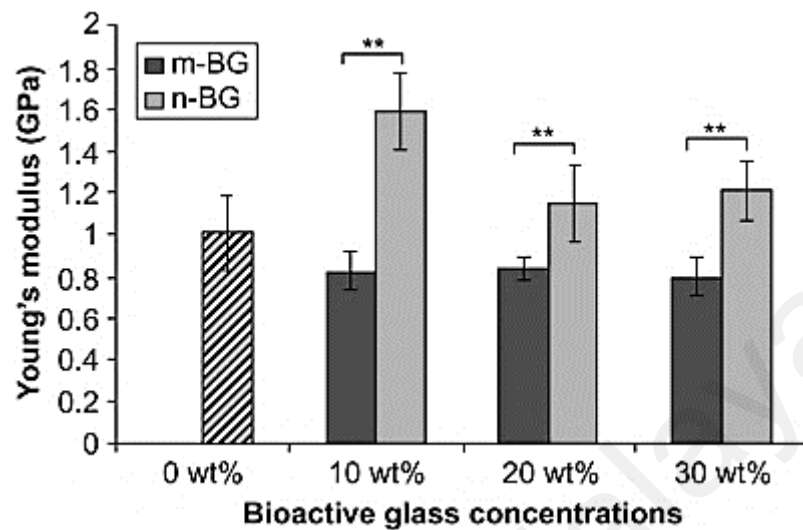


Figure 2.21: Modulus comparison for various concentrations of m-BG and n-BG particles in P(3HB)/bioactive glass composites [Reprinted with permission from (Misra et al., 2008)].

In vitro assessment of P(3HB)/bioglass composites demonstrated that both weight loss and water uptake percentage increased with immersion time (Misra et al., 2008). As expected, the increase in degradation and swelling was more obvious for nanocomposites than microcomposites. The *in vitro* cellular response of composites containing nano and micro bioglass were compared in some studies (Gerhardt et al., 2011; Misra et al., 2008). In general, the composites indicated higher protein adsorption in comparison to unfilled polymers. Nanocomposites had higher protein adsorption relative to microcomposites (Misra et al., 2008). This can be explained by the higher roughness resulting from nano-size particles. In contrast, cell proliferation was impaired by the increased concentration of bioglass. The inverse relationship between protein adsorption and cell proliferation was elucidated by the changes in protein conformational for the thicker layers (Misra et al., 2008). Similar results were obtained by Gerhardt *et al.* where the cell viability showed a decrease with an increase in the amount of bioglass added to PDLA (Gerhardt et al.,

2011). The destructive influence on cell viability was more significant with nano-bioglasses and was attributed to the increase in pH of the culture medium, as a result of accelerated ion release by highly reactive nano-bioglasses which could possibly compromise the beneficial influence of nano-roughness.

University of Malaya

CHAPTER 3: EXPERIMENTAL

3.1 Introduction

The initial sections (3-2, 3.3, 3-4, and 3-5) detail the procedure for synthesizing bioactive glass and POC and the fabrication methods for composite scaffolds and films. This is followed by a description of the techniques used to characterize the structural, thermal and mechanical properties of the scaffolds (3.6.1-3.6.6). The methods used for testing degradation, swelling, ion release, acellular mineralization, and ion penetration into the surrounding bone are described in detail (3.6.7 and 3.6.10-3.6.13). The chapter then describes the methods used to evaluate the biological features of the scaffolds *in vitro*. Antibacterial activity of the samples was evaluated by the two popular techniques, namely i) turbidity measurement, and ii) plate counting technique (3.6.15). After that, the interaction between scaffolds and human osteoblasts and mesenchymal stem cells was assessed. The cytotoxicity and the osteogenic differentiation of the scaffolds were examined and the techniques used are explained in detail (3.6.16 and 3.6.17).

3.2 Synthesis of bioactive glass

A bioactive glass with the formulation $0.48\text{SiO}_2\text{-}0.12\text{CaO}\text{-}0.32\text{ZnO}\text{-}0.08\text{Ga}_2\text{O}_3$ was synthesized through a conventional melt-quench method (Figure 3.1). The proper amounts of silica, calcium oxide, zinc oxide and gallium oxide (Sigma-Aldrich, $\geq 98\%$) were weighed out and ball milled for 1 h. The mixture was dried and fired at $1500\text{ }^\circ\text{C}$ for 1 h in a platinum crucible and then quenched into water. The obtained frit was then ground using a ball mill, sieved to a particle size below $45\text{ }\mu\text{m}$.

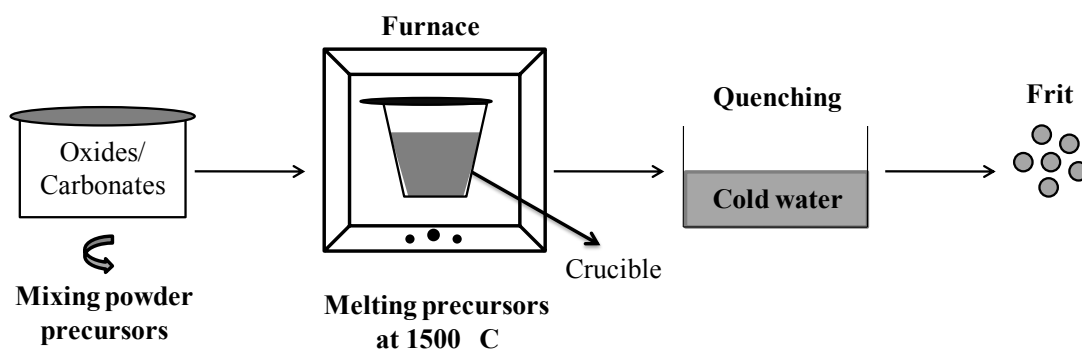


Figure 3.1: Schematic diagram of melt-quench technique for synthesizing bioglass.

3.3 Synthesis of POC

POC pre-polymer was synthesized by a polycondensation reaction as schematically illustrated in Figure 3.2 (Djordjevic et al., 2009; Yang et al., 2006). An equimolar amount of citric acid (11.84 g) and 1, 8-octanediol (9 g) (Sigma-Aldrich, $\geq 98\%$) was weighed out and poured into a 250 ml three neck round bottom flask. The flask was transferred to a silicone oil bath and heated up to 160-165 °C under constant nitrogen flow and vigorously stirred. Once the mixture was melted and transparent, the temperature was reduced to 140-145 °C and kept constant for 1 h. The resultant pre-polymer was stored in a refrigerator (5 °C) for further characterization.

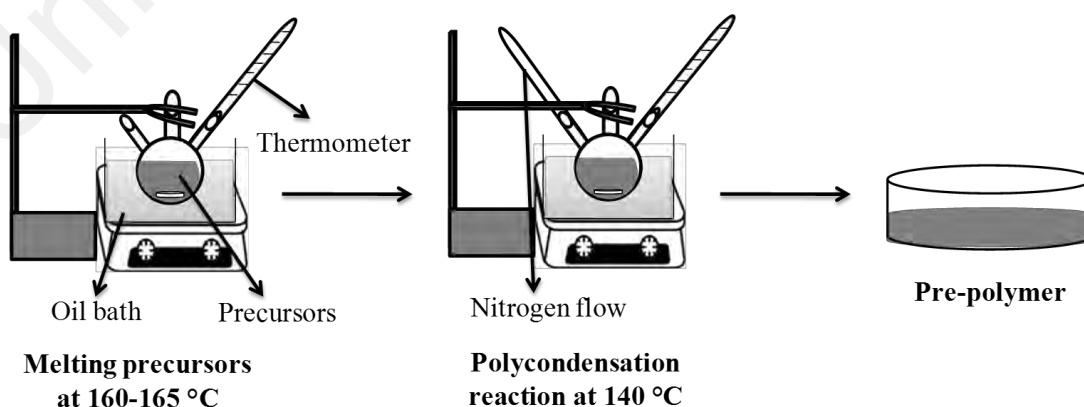


Figure 3.2: Schematic diagram of the method of synthesizing POC pre-polymer.

3.4 Fabrication of POC/bioglass film

The POC/bioglass composite films were prepared through a solvent-casting technique. Predetermined amounts of POC pre-polymer were dissolved in 1,4-dioxane to obtain a 20 wt% solution. Three different concentrations of bioglass (*i.e.* 10 %, 20 % and 30 % ~ w/w to pure POC pre-polymer) were added to the solution and sonicated (Ultrasonic, ST-UB5200LT, SASTEC) for 30 min. The composites were named POC-BG-10% (10 % bioglass), POC-BG-20% (20 % bioglass) and POC-BG-30% (30 % bioglass). The mixtures were then transferred into a TeflonTM molds with 7 mm diameter and left in oven at 80 °C for 7 days. The resultant films with approximately 1 mm thickness were taken out from the mold and cut to the cylindrical shape for characterization.

3.5 Fabrication of POC/Bioglass scaffolds

Composite scaffolds were prepared by employing a salt-leaching method as schematically illustrated in Figure 3.3. First, the POC pre-polymer was dissolved in 1,4-dioxane in a polyethylene container to obtain a 20 wt% solution. Then different concentrations of bioglass (10, 20 and 30 wt%) were added to the solution and sonicated for 30 min. After that, 90 wt% of sieved salt (NaCl) was added to the mixture (w/w to solvent-free POC-BG mixture) and left in the oven at 80°C for one week. After curing and solvent evaporation, the NaCl-POC-BG blocks were removed from the container and NaCl was washed for 4 days in distilled water. The water was replenished every 12 h. Once the washing was completed, the resultant scaffolds were frozen at -80 °C and cut to the cylindrical shape (6 mm diameter and 5 mm height). Finally, the scaffolds were lyophilized using a freeze-dryer (FreeZone 2.5, LABCONCO, 7670531).

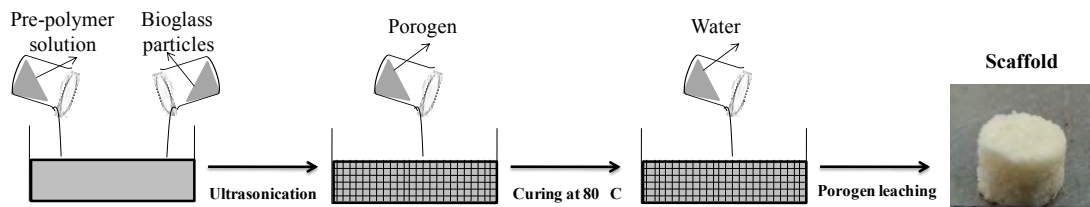


Figure 3.3: Schematic diagram of composite scaffold fabrication.

3.6 Characterization

3.6.1 Morphological and structural characterization of the bioglass

The microstructures and morphology of the bioactive glass were observed by field emission scanning electron microscopy (FESEM: Quanta™ 250 FEG—FEI, USA). Elemental analysis was performed by energy dispersive spectroscopy (EDS: 20 mm X-Max, Oxford Instruments, Oxford, UK) attached to the FESEM. X-ray diffraction (XRD) patterns were obtained using an X-ray diffractometer (PANalytical Empyrean) with Cu K_{α} radiation (40 kV, 40 mA).

3.6.2 Field emission scanning electron microscopy (FESEM)

Scaffold morphology was investigated by Field Emission Scanning Electron Microscopy (FESEM; Zeiss-Auriga laser, Germany). The samples were placed on aluminum stubs with 8 mm diameter and the images were taken in various magnifications and accelerated voltage of 15 kV.

3.6.3 Fourier transform infrared spectroscopy (FTIR)

Infra-red spectra of scaffolds and films were recorded in attenuated total reflectance mode (ATR-FTIR400, Perkin Elmer instruments, USA) within the wavelength range of 400-4000 cm^{-1} in room temperature.

3.6.4 Thermal analysis

The glass transition temperature (T_g) of scaffolds was measured by *differential scanning calorimetry* (DSC8000, Perkin Elmer instruments, USA). The samples of 5-10 mg were encapsulated in standard aluminum pans and all tests performed under a nitrogen atmosphere. The samples were analyzed at a rate of 10 $^{\circ}\text{C}/\text{min}$ between -50 $^{\circ}\text{C}$ to 150 $^{\circ}\text{C}$. First heated to 150 $^{\circ}\text{C}$ (first heating cycle) then it was to -50 $^{\circ}\text{C}$ and finally heated up again to 150 $^{\circ}\text{C}$ (second heating cycle). T_g was measured from the DSC endothermic curves in the second heating cycle. The effect of temperature on the composite scaffolds was evaluated by thermogravimetric analysis (TGA4000, Perkin Elmer instruments, USA). 5 mg samples were heated in air atmosphere from 35 $^{\circ}\text{C}$ to 900 $^{\circ}\text{C}$ at a heating rate of 10 $^{\circ}\text{C}/\text{min}$ using aluminum crucible. The real glass content was calculated as follows:

$$\text{Glass content (wt \%)} = \left[\frac{W_g}{W_g + W_p} \right] \times 100 \quad 3.1$$

Where W_g is weight of the glass and W_p is weight of the polymer

3.6.5 Mechanical tests

Dynamic mechanical analysis (DMA) was performed on prepared scaffolds. Rectangular samples with dimension of 35 \times 13 \times 2 mm (length \times width \times thickness) were analyzed using a DMA 8000 (Perkin Elmer instruments, USA). Data were collected

at temperature scan with dual cantilever bending geometry. The samples were scanned in the temperature range of -60 °C to 40 °C at a heating rate of 2 °C/min, oscillation frequency of 1 Hz and maximum strain level of 0.05 mm. Mechanical compression tests were conducted to determine compressive modulus. The cylindrical scaffolds (6 mm diameter and height of 5 mm) were tested using an Instron5544 (USA) mechanical tester fitted with a 2 KN load cell at a crosshead speed of 1 mm/min (n=6). The specimens were compressed to 50 % of initial volume. The average compressive modulus (E_c) and standard deviation was calculated by slope of initial linear region of strain-stress curve. The recovery ratio of the specimens was measured after 1 min unloading the pressure.

3.6.6 Porosity estimation

The porosity of the scaffolds was measured by the Archimedes principle (Ródenas-Rochina et al., 2013). Five replicates from each design were weighed before and after immersion in n-Hexane. The estimated porosity was calculated from dividing the volume of pores by the total volume of samples:

$$\text{Porosity} = \frac{V_{\text{pores}}}{V_{\text{poc}} + V_{\text{pores}}} \quad 3-2$$

V_{pores} was calculated by dividing the weight difference between W_{dry} and W_{wet} scaffolds with density of n-Hexane (ρ_{hexane}).

$$V_{\text{pores}} = \frac{W_{\text{wet}} - W_{\text{dry}}}{\rho_{\text{hexane}}} \quad 3-3$$

V_{poc} was measured from quotient of W_{dry} of scaffolds by density of POC (ρ_{poc}). Density of POC (1.2429 g/cm^3) was already reported by Yang *et al.* (Yang et al., 2006).

$$V_{poc} = \frac{W_{dry}}{\rho_{poc}} \quad 3-4$$

3.6.8 *In vitro* degradation test

The weight loss of samples was determined by soaking scaffold cylinders (6 mm diameter and 3 mm height) into phosphate buffered saline (PBS, pH 7.4) for 7, 14, 21, 28 days. Samples were immersed in 10 ml PBS in 15 ml centrifuge tube. The tubes were kept diagonal and moderately shaken at 37 °C using orbital shaker incubator (Benchtop, Ind. & Vac. Instrument). The PBS was refreshed every week. The scaffolds were removed from PBS at the set time intervals, washed three times with distilled water and oven dried to a constant weight. The weight loss was recorded (%) and plotted against time intervals (n=5). The weight loss of scaffolds was calculated using the following equation:

$$\text{Weight loss \%} = \frac{W_i - W_1}{W_i} \times 100 \quad 3-5$$

Where, W_i is the initial weight of scaffold and W_1 is the weight of scaffold after immersion in PBS.

3.6.8 Acidity measurement

The pH study was performed on the scaffold cylinders (6 mm diameter and 3 mm height) within one week of soaking in PBS. The scaffolds were immersed in 10 ml PBS and shaken moderately in an orbital shaker incubator at 37 °C. The pH was measured everyday using a pH meter (Accumet^(R), AB15 Basic) with an attached glass combination

pH electrode. The electrode was calibrated by the calibration standard solution at every time point.

3.6.9 Contact angle measurements

Static contact angle was carried out on films to measure the hydrophilicity of the samples. The measurement was carried out at room temperature by a sessile drop method using a high-performance image processing system from Dataphysics Instruments (OCA 15EC, Germany). Samples were tested by adding equal volume of water (20 μ L) using a motor driven syringe. Photos were recorded after 2 min and water contact angles were measured by analyzing the drop images (n=5).

3.6.10 Swelling studies

The swelling-in-water and in-PBS experiments were performed on composite films (6 mm diameter and 1 mm thickness). The dry weight of the sample was noted as M_0 . The films were swollen in distilled water and PBS at room temperature for 6 h. After the predetermined time, the water was removed from the sample surface by gently dabbing onto a tissue paper and the new weight (M_w) was recorded (n=5). The ratio of swelling was calculated using the following equation:

$$\text{Swelling ratio} = \frac{M_w - M_0}{M_0} \times 100 \quad \mathbf{3-6}$$

3.6.11 Ion release studies

The analysis of ion release was carried out by soaking 11-14 mg cylindrical composite scaffolds in 10 ml phosphate buffered saline (PBS, pH 7.4) in a conical flask. Samples

were placed in an orbital shaker incubator for periods of 1, 7, 14 and 28 days. The scaffolds were taken out from PBS at timed intervals and the extracts were refrigerated (5 °C) prior to being analyzed by a plasma-atomic emission spectrometer (MP-AES) Agilent 4100 (Agilent Technologies, Inc., Santa Clara, CA, USA) for Si, Ca, Zn and Ga concentration measurement in the solutions.

3.6.12 Acellular *in vitro* tests in SBF

In vitro bioactivity was evaluated in an acellular simulated body fluid (SBF) prepared according to the method reported by Kokubo and Takadama. (Kokubo & Takadama, 2006) Three replicates for each sample of the cylindrical scaffolds (11-14 mg) were immersed separately in 20 ml SBF and incubated at 37 °C. At pre-determined time intervals (1, 7, 14 and 28 days) the samples were removed from the solutions and gently washed with distilled water and dried at 37 °C. Further, all the samples were analyzed by SEM-EDS for elemental composition and morphology. The ionic concentrations of extract solutions from the scaffolds were analyzed by Inductively Coupled Plasma Mass Spectrometry (ICP-MS, Agilent 7500, USA).

3.6.13 *In vitro* tests to evaluate ion penetration into bone tissue matrix

The test was carried out according to a method described by Wren et al. (Wren et al., 2009). Bovine bone specimens (2 cm × 2 cm × 1 cm) were sourced from a local butcher, cleaned by detaching any soft tissues using a cutter and a 5mm hole was drilled through the centre. The specimens were washed thoroughly with ultrapure water and then soaked in highly saturated NaCl solution (Sigma-Aldrich) for 1 day. The as-prepared sterilized scaffolds (6 mm diameter × 6 mm height) were used to fill the voids of the bones. The

specimens were immersed into PBS and incubated for 7 days at 37 °C. At day 7, specimens were removed from PBS and dried in a vacuum oven at 37 °C. A piece of bone was used for each scaffold, an unfilled sample of bone (without scaffold implantation) was used as a positive control and a sample of bone without incubation in PBS was used as a negative control. Further, energy disperse spectrometric analysis (EDS) of the bone surface was performed to quantitatively characterize the concentration of ions taken up by the bone.

3.6.14 Scanning electron microscopy and energy disperse spectrometric analysis

Microanalysis was obtained using an energy dispersive spectrometer (EDS: 20 mm X-Max, Oxford Instruments, Oxford, UK) and the INCA software connected to a scanning electron microscope (SEM: Quanta™ 250 FEG—FEI, USA) at 20 KV. All scaffolds were gold-coated using a 150 rotary-pumped sputter coater (Quorum Technologies). All samples were analyzed in triplicate under the same microscopy conditions. Analysis was performed from the scaffold-bone interface onto the edge of bone specimen.

3.6.15 Antibacterial tests

Antibacterial tests were performed using turbidimetric and plate counting techniques (Hild et al., 2013; Z.-C. Xing et al., 2010). Turbidimetric method was performed as a qualitative measure of bacteria growth. The growth of a gram-negative (*Escherichia coli*, ATCC 15597) and a gram-positive bacterium (*Staphylococcus aureus*, NCTC 6571) in LB broth in the presence of rectangular composite scaffolds (1 cm wide × 3 cm length) was investigated following 10 h incubation and the results compared with a pure LB broth culture as control. Before performing the test, the scaffolds were autoclaved at 126 °C

and the monomer residues in scaffolds were washed in PBS followed by rinsing with distilled water in order to adjust the pH to physiological level. 50 µl of bacteria culture with the final cell density of approximately 10^5 - 10^6 colony forming unit per millimeter (CFU/ml) were inoculated in 10 ml solution of autoclaved LB broth and constructs in 15 ml conical tube. The tubes were incubated at 37 °C and shaken at 100 rpm using an orbital shaker incubator (Benchtop, Ind. & Vac. Instrument). The optical densities of the cultures were serially monitored every 2 h up to 10 h at 595 nm (OD 595) using a microplate reader (BMG LABTECH, Offenburg, Germany). In order to determine the viable bacteria, cultures (after 10 h) were diluted to 10^{-6} and placed on LB agar plates and incubated at 37 °C overnight. After incubation, the colonies were quantified and digital images of the plates were captured.

3.6.16 Osteoblast responses to the scaffolds

3.6.16.1 Cell culture, attachment, morphology and viability of osteoblasts

Human osteoblast cells were purchased from Lonza (Lonza, USA, cat. #CC-2538) and expanded in growth medium consisting of Dulbecco's modified Eagle's medium (DMEM; Gibco-Invitrogen, USA) supplemented with 20 % fetal bovine serum (FBS; Gibco -Invitrogen, USA), 100 µM 2-mercaptoethanol (Sigma-Aldrich, USA), 100 U/ ml penicillin and 100 µg/ml streptomycin (Gibco-Invitrogen, USA) and incubated at standard conditions (humidified atmosphere, 5 % CO₂, 37 °C) for enough expansion.

Before seeding the cells into the scaffolds, the samples were placed in 24-well plates, washed three times with PBS, left to dry at room temperature and placed under UV for overnight. The sterilized scaffolds were soaked with FBS free DMEM for 3 h, the media were removed and the scaffold was left for another 3 h in the incubator.

In order to determine the human osteocytes cells viability, MTT (3-(4,5 dimethylthiazol-2-yl)-2,5-diphenyltetrazolium bromide) assay was performed. Human osteocytes were seeded at 5×10^5 cells per scaffold at optimal conditions (37 °C, 5 % CO₂ in humidified incubator). The cell-seeded scaffolds and cell-free scaffold (control) were placed in 96-well plates and incubated for 1, 7, 14 and 28 days. Following the incubation periods, the scaffolds were removed, 10 µL solution of freshly prepared 5 mg/ml MTT in PBS was added to each well and allowed to incubate for an additional 3 h. Plates were then swirled gently to facilitate formazan crystal solubilisation. The absorbance was measured at 570 nm using a microplate reader (Tecan Infinite M200 Pro). Percentage of cytotoxicity was calculated as follows:

$$\text{Cytotoxicity \%} = (\text{Absorbance of cell-seeded scaffold} / \text{Absorbance of cells-free scaffold}) \times 100 \quad \text{3-7}$$

In order to observe the cell attachment and morphology, cells were cultured for 7 days into the scaffolds (1×10^5 /scaffold) and then fixed with 3 % glutaraldehyde in PBS for 24 h at 4 °C. After thorough washing with PBS, samples were dehydrated sequentially in 50, 70, 95, and 100 % ethanol. Then the fixed samples were freeze-dried, sputter coated with gold, and observed under SEM (HitachiS-530).

3.6.16.2 RNA isolation and cDNA synthesis and qPCR microarrays

Total RNA was isolated from osteocytes-seeded scaffolds using Trizol™ reagent, according to the manufacture's procedure (Invitrogen, Netherlands). All required equipment was treated with DEPC-dH₂O overnight and autoclaved on liquid cycle at 15 lbs/sq.in., 121 °C for 45min. One ml of Trizol™ solution was added to each containing

the harvested cells and shaken vigorously. Next, 200 μ l chloroform was added to each tube and the tubes were vigorously shaken for 15s and incubated for 3min at room temperature. The mixture was centrifuged for 15 min at 4 °C and 12000 g. The colourless upper aqueous phase that contained RNA was carefully removed (avoiding the interface) and placed into a new 1.5 ml microcentrifuge tube. At this step 600 μ l of aqueous phase was recovered. Then, 0.5 ml of isopropanol was added, mixed and incubated at room temperature for 15 min. The mixture was centrifuged for 15 min at 4 °C and 12000 g. The supernatant was discarded and 1ml of 75 % ethanol was added, vortex and centrifuged again for 3 min, at 4 °C and 7500 g. This step was repeated as washing step and the white pellet was left to dry for 10min at room temperature. The pellet was resuspended with 50 μ l DEPC-dH₂O, vortex, placed on ice for 10min, heated at 65 °C for 10 min and placed on ice again before storage at -80 °C.

After reading total RNA concentration at A_{260}/A_{280} , DNase treatment was performed to remove any contaminating genomic DNA. The RNase-free reaction components were mixed into 0.5 ml microcentrifuge tube on ice as follows:

- 1 μ g RNA sample
- 1 μ l 10X DNase I reaction buffer (Invitrogen, Netherlands)
- 1 μ l DNase I, Amp Grade, 1U/ μ l (Invitrogen, Netherlands)
- DEPC-treated water to 10 μ l

The reaction mixture was incubated at room temperature for 15 min. Then, DNase I was inactivated by adding 1 μ l of 25 mM EDTA and incubating for 10 min at 65 °C. The RNA samples were converted to cDNA using High Capacity cDNA Reverse Transcription Kit (Applied Biosystems, USA). The first step was preparation of 2X RT master mixtures (Table 3.1).

Table 3.1: Components and the required volumes of each component for preparation of 2X RT master mixtures.

Component	Volume (μ l)
10X buffer	2.0
25X dNTP Mix (100mM)	0.8
10 X RT random primers	2.0
MultiScribe™ Reverse transcriptase	1.0
RNase inhibitor	1.0
Nuclease – free water	3.2
Total per reaction	10.0

The second step was adding 10 μ l of RNA sample into each tube containing same amount of master mix and mixed by pipetting. The tubes were briefly centrifuged to spin down the contents and to eliminate any air bubbles. The tubes were placed in the PCR machine and thermal cycle conditions were applied (Table 3.2).

Table 3.2: Thermal cycling conditions used for RT-PCR experiment.

	Step 1	Step 2	Step 3	Step 4
Temperature	25 °C	37 °C	85 °C	4 °C
Time	10 min.	120 min.	5 min.	--

Real-Time PCR (RT-PCR) was performed by ABI 7500 instrument using Syber green™ fluorescence dye (Applied Biosystems, USA.) to assess the expression of genes of interest. The relative gene expression was quantified using β - *actin* as an endogenous gene control. The primers were designed using ABI 7500 instrument software, SDS2.1. The total volume of RT-PCR reaction was 12.5 μ l and the reaction components are reported in Table 3.3.

Table 3.3: The reaction components, required volumes of each component and their final concentrations used in RT-PCR experiment.

Reaction component	$\mu\text{l}/\text{sample}$	Final concentration
2X syber mix.	6.5	1X
Primers mix.	1.25	50 to 900 nM
cDNA	3.0	50 to 100 ng
Nuclease free water	2.0	--
Total	12.5	--

All replicates were given in the same thermal cycling conditions of RT- PCR (Table 3.4). There were three replicates for each sample of target gene or endogenous gene (Table 3.5).

Table 3.4: thermal cycling conditions used for RT-PCR experiment.

PCR stages	Enzyme activation	Melt temperature	Anneal/extend
Stage 1	10 sec. at 95°C	-----	-----
Stage 2	-----	3 sec. at 95°C	20 sec. at 60°C

Table 3.5: Primer sequences of Collagen type I and III genes used for RT-qPCR.

Gene name	Primer sequence
Collage I	Forward COLI-F-5-CCTGGATGCCATCAAAGTCT-3 Reverse COLI-R-5- GAATCCATCGGTTCATGCTCT-3
Collage III	Forward COLIII-F-5-CTAAAGGCGAAGATGGCAAG-3 Reverse COLIII-R-5-TTTCCCATCACTTCCTGGTC-3

3.6.16.3 Indirect Immunostaining

Cells were grown into the scaffolds ($5 \times 10^5/\text{scaffold}$) for 7 days. Then, cells were trypsinized and reseeded on cover slides fixed in 6-well plates and for 24 h. Next, the cells were washed three times with PBS and fixed with ice-cold methanol for 15 min at

-20 °C. After the washing steps, the cells were incubated with a coating buffer for 1 h at room temperature. A mouse antibody specific to collagen I (abcam, USA, cat. # ab90395) or collagen III (abcam, USA, cat. # ab3610) were added separately and the cells were incubated for overnight at 4°C. The cells were washed three times with PBS and incubated for 30 min with an anti-mouse IgG labeled with FITC fluorescent dye (Invitrogen, USA, cat. # 62-6511).

3.6.17 hBMSC responses to the scaffolds

3.6.17.1 Cell culture and seeding

Using standard laboratory protocols, hBMSCs were isolated, Ethical approval for human bone marrow collection was obtained from the medical ethics committee of University of Malaya Medical Centre (MECID.NO: 201412-865). The cells were cultured in a medium (Invitrogen, Carlsbad, CA, USA) supplemented with 15 % fetal bovine serum (FBS; Invitrogen), 100 U/mL penicillin (Sigma–Aldrich, USA), and 100 mg/mL streptomycin (Sigma–Aldrich) in tissue culture flasks at 37 °C under a humidified atmosphere of 5 % CO₂. When the cells reached near confluence (80 %–90 %), they were detached by trypsin/EDTA (Cell Applications, San Diego, CA, USA) and then sub-cultured into the next passage.

Prior to cell culture experiments, the samples were sterilized by incubation in 70 % ethanol for 3 h and washed with sterile PBS (pH 7.4). After sterilization, samples were washed 3 times in serum-free cell culture medium for 48 h. Then, the desired amount of the cells (5×10^4) in the growth medium was dropped into the scaffold and left for 1 h in the incubator (37 °C and 5 % CO₂) for cell attachment and then topped up with 1 ml of media.

3.6.17.2 Cell adhesion and morphology

Cell attachment and morphology on the scaffolds were observed by a FESEM. Cells were cultured for a period of up to 14 days into the scaffolds, fixed with 4 % glutaraldehyde in PBS at 4 °C overnight and post-fixed in 2% osmium tetroxide. After thorough washing with PBS, the scaffolds were dehydrated in a serial ethanol. Then, the samples were immersed in hexamethyldisilazane (Sigma-Aldrich) twice for 10 min and air-dried at room temperature by keeping the samples in fume hood. The sample colours were changed to black after processing (Figure 3.4). The dried samples were sputter coated with gold and observed under FESEM.

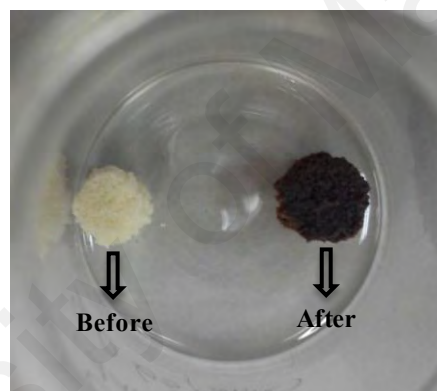


Figure 3.4: Digital photographs of representative cell-seeded scaffolds before and after fixation.

3.6.17.3 Cell distribution and density

To investigate cell distribution and density within the scaffolds, hBMSCs-laden scaffolds were stained with NucBlue® Live ReadyProbes™ Reagent (Hoechst 33342, Invitrogen, USA) solution; 1 drop of NucBlue per ml of medium (according to the manufacturer's description). After 20 min of incubation at room temperature the samples were analyzed using confocal laser scanning microscopy (CLSM; Leica TCS SP5 II,

Leica Microsystems CMS GmbH, Mannheim, Germany) at excitation /emission, 495 nm/515 nm.

3.6.17.4 Cell proliferation

Cell proliferation was assessed with AlamarBlue[®] (DAL1025, Invitrogen, Inc.) according to the standard protocol. Before adding the AlamarBlue[®] fresh media was replaced. AlamarBlue[®] was added to the samples (10 % v/v of medium) and incubated at 37 °C in an incubator (with 5 % CO₂) for 4 h. The supernatant samples were pipetted into a centrifuge tube and centrifuged at 10,000 rpm. 100 µl Aliquots from each sample were transferred to a 96-well plate, and the fluorescence of AlamarBlue[®] was measured using a fluorescence plate reader (BioTek epoch) at a wavelength of 570 nm and 600 nm.

3.6.17.5 ALP activity

The differentiation of the hBMSCs was evaluated by measuring the alkaline phosphatase (ALP) activity using an ALP Colorimetric Assay Kit (Abcam, ab83369) employing *p*-nitrophenol phosphate as substrate. After culturing for 3, 7 and 14 days, the cells were washed with PBS and trypsinized. The cell pellets were disrupted via a freezing/thawing process. Following that, 30 µl supernatant were added to 50 µl of *p*NPP ALP substrate solution and incubated at 37 °C for 60 min. Action was then stopped by adding 50 µl of stop solution (3N NaOH) into each well. The activity of ALP in cell lysates measured with a microplate reader at 405 nm.

3.6.17.6 RNA isolation and cDNA synthesis and qPCR microarrays

At 0, 7, and 14 days, the media was removed from the scaffolds by spinning at 1000g for 10s, followed by washing in sterile PBS and spinning again to remove excess liquid. This washing procedure was repeated three times. After the last spin, cultured scaffolds were incubated in Trizol at room temperature for 3 min to complete homogenization. The RNA-containing Trizol solutions were transferred to individual RNase-free vials and 200 μ l chloroform was added to each tube, followed by vortex-mixing. After 2 min incubation on the bench, the samples were centrifuged at 12,000 g, 4 °C for 15 min. The upper aqueous layer was collected and RNA was isolated using the AllPrep DNA/RNA Mini Kit (Qiagen; #80204), according to the manufacturers' instructions. RNA concentration was determined by measuring absorbance at 260 nm in a spectrophotometer ($A_{260} = 1$ equals 40 mg/ml) and the purity of RNA was estimated from the ratio of readings at 260 nm and 280 nm.

1 μ g total RNA for each sample was used as a template for cDNA synthesis using the QuantiTect Reverse Transcription kit (Qiagen), including a gDNA digestion step. The protocol was 2 min at 42 °C, 15 min at 42 °C, and 3 min at 95 °C. Real-time PCR was performed with 1 μ l aliquots of the diluted cDNA in a 25 μ l reaction volume using QuantiFast SYBR Green PCR kit (Qiagen) to determine the expression level of the osteogenic associated genes such as runt-related transcription factor 2 (Runx2), collagen type I (COL I), bone morphogenetic protein 2 (BMP2), osteonectin (SPARC), and osteocalcin (BGLAP) (Table 3.6). GAPDH was used as an internal control. Following Taq Polymerase activation step at 95 °C for 5 min, 40 amplification cycles were carried out by denaturing at 95 °C for 30 s and annealing and extension for 30 s at 60 °C. The reaction was monitored in real-time using a MiniOpticon (BioRad).

Table 3.6: Primer sequences of RUNX2, COL I, SPARC, BMP2, and BGLAP genes used for RT-qPCR.

Gene name	Primer Sequences
COL I	Forward 5'- CCC GCA GGC TCC TCC CAG -3' Reverse 5'- AAG CCC GGA TCT GCC CTA TTT AT -3'
RUNX2	Forward5'- CCG CCA TGC ACC ACC ACC T -3' Reverse5'- CTG GGC CAC TGC TGA GGA ATT T -3'
BMP2	Forward5'- TGG CCC ACT TGG AGG AGA AAC A -3' Reverse5'- CGC TGT TTG TGT TTG GCT TGA CG -3'
SPARC	Forward5'- TTG CAA TGG GCC ACA TAC CT - 3' Reverse5'- GGG CCA ATC TCT CCT ACT GC -3'
BGLAP	Forward5'- GGA GGG CAG CGA GGT AGT GAA -3' Reverse5'- GCC TCC TGA AAG CCG ATG TGG T -3'

3.6.17.7 Determination of calcium content

The calcium content in the supernatant was analysed using a calcium assay kit (Sigma-Aldrich) according to the manufacturer's protocol. Briefly, at 3, 7, and 14 days after culture, the culture medium was collected for direct measurement or stored at -20 °C. Calcium reagent working solution was then added to 50 µl of each sample, according to the manufacturer's instructions. The absorbance of the solution was measured at 575 nm using a UV-VIS spectrophotometer, and calcium content was expressed as µg calcium/flask (n = 3).

3.6.18 Statistical analysis

All data were expressed as mean \pm standard deviation and processed statistically by the software of IBM SPSS Statistics for Windows, Version 22. Differences between two independent samples were evaluated by using the nonparametric Mann-Whitney U test. The differences of the data were considered significant when $P < 0.05$.

University of Malaya

CHAPTER 4: RESULTS AND DISCUSSION

4.1 Introduction

In section 3, composite scaffolds comprising POC and a therapeutic ion-releasing bioactive glass were developed. The present chapter extends this investigation by testing the hypothesis that incorporation of bioactive glass into POC can modulate the overall performance of a scaffold. The study will investigate the physical and biological properties of prepared scaffolds and discuss the effect of therapeutic ions e.g. Ga^{3+} and Zn^{2+} on the biological characteristics.

4.2 Morphological and structural characterization of the bioglass

FESEM micrographs and EDS spectra of bioactive glass particles are shown in Figure 4.1. As can be seen in the FESEM image, the morphology of bioactive glass particles used to fabricate composite scaffolds were non-spherical, irregular and angular with at least one dimension less than $45\ \mu\text{m}$. Furthermore, the EDS spectrum confirmed that the chemical elements in the bioactive glass are Si, Ca, Zn, Ga and oxygen. The glassy nature of the bioactive glass particles was indicated by the broad halo depicted in Figure 4.1c, showing that the material was completely amorphous.

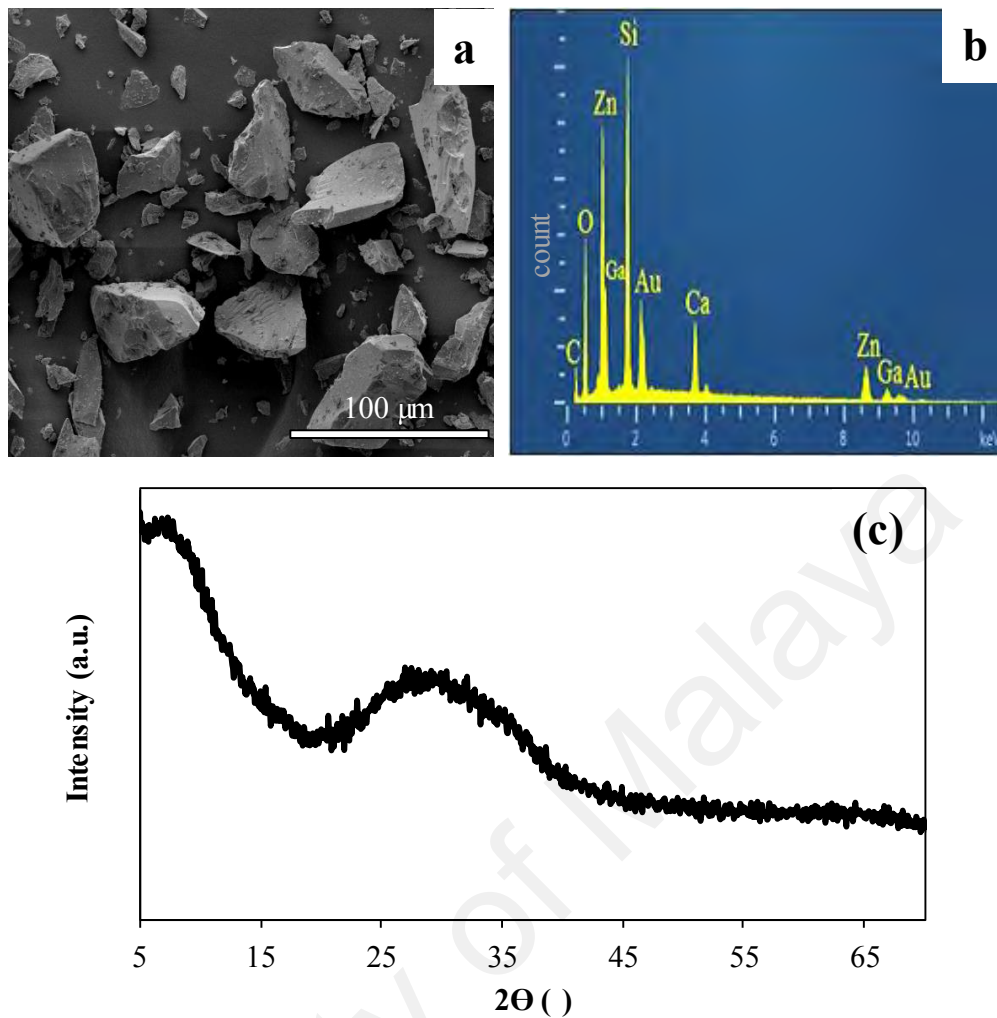


Figure 4.1: (a) FESEM micrograph showing the irregular shape of the glass particles; (b) EDS spectrum of bioactive glass showing the peaks of Si, Ca, Zn, Ga and O; and (c) XRD pattern of the bioactive glass particles showing the typical amorphous halo.

4.3 Surface morphology of scaffolds by FESEM

The porous structure of composite scaffolds was created through a solvent casting-porogen leaching technique. The obtained cylindrical scaffolds were cut into discs of 6 mm diameter and 3 mm thickness for further *in vitro* studies. Figure 4.2 (a and b) shows a macroscopic profile of representative POC/bioglass composite scaffolds and their elastic nature. The plan-view FESEM images of both the pure POC and the micro-composites in Figure 4.2 (c,d,e) illustrate the porous structure of the scaffolds with a uniform distribution of pores and a pore size recorded in the range of 200-300 μm (Figure

4.2-f). In addition, it can be seen that bioglass particles are well-dispersed and embedded into the polymer matrix (Figure 4.2-g) which in turn improve the load transferral across the filler-matrix interface and amend the composite stiffness (Misra et al., 2008). However, the larger particles were not fully incorporated into the matrix (Figure 4.2-h) and could easily be de-bonded from the matrix under loading. Therefore, the particles cannot transfer any loads which consequently lead to reducing composite strength (S.-Y. Fu et al., 2008).

University of Malaya

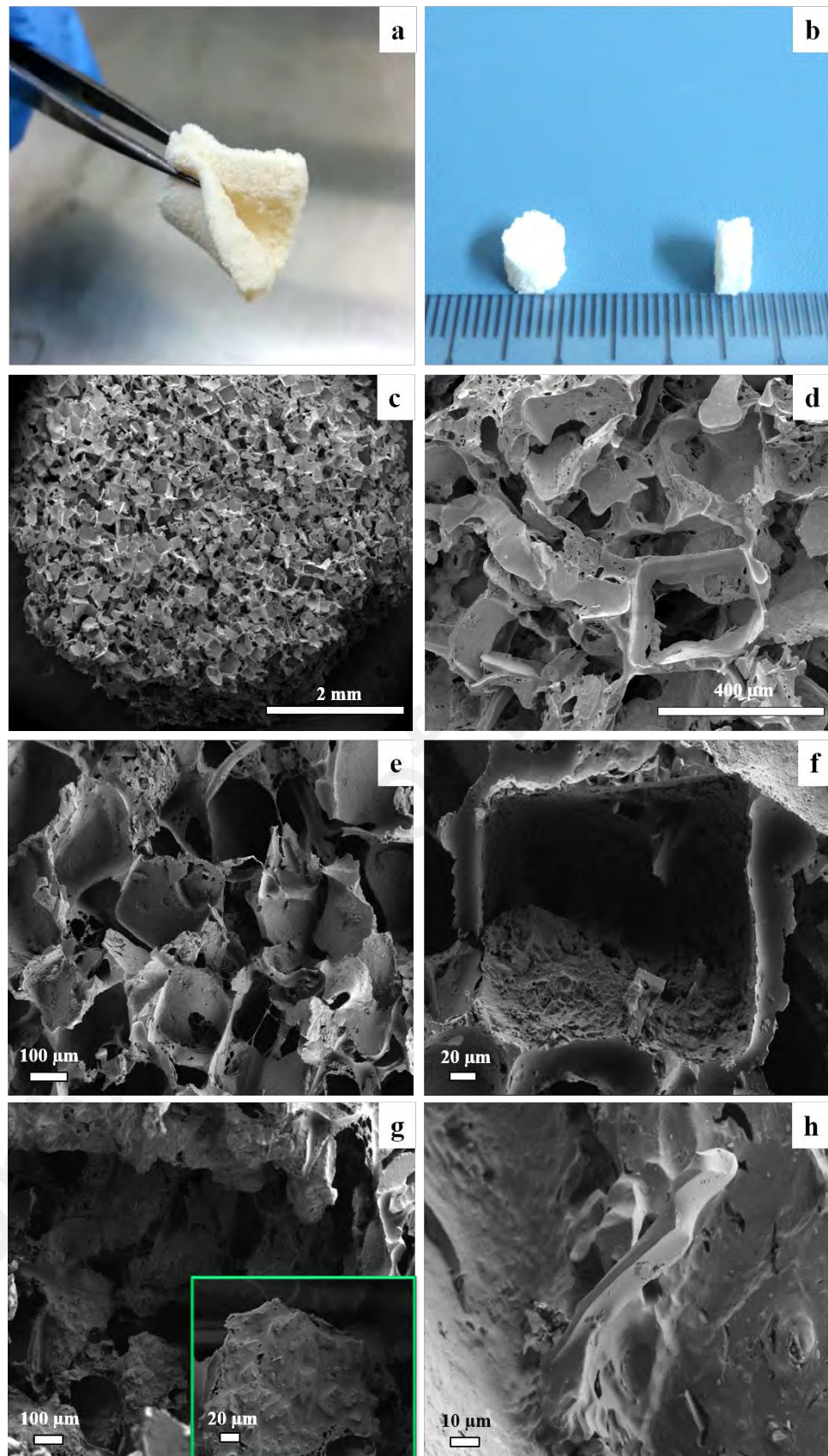


Figure 4.2: Digital photographs of representative POC-BG scaffolds: (a) demonstration of elastomeric nature of POC-BG-10% scaffold; (b) frontal and cross-sectional view of the POC-BG-30% scaffold prepared for cell culture. (c, d) Microstructure of scaffolds observed by FESEM: (c, d) POC-BG-20%; (e) POC; (f) POC-BG-30%; (g) POC-BG-20%; and (h) POC-BG-10%.

4.4 FTIR analysis

FTIR analysis was performed in order to characterize the type of interactions and crosslinking in both pure POC samples and the micro-composites. Figure 4.3 presents the FTIR spectra for composite scaffolds. The presence of ester bonds was confirmed by the two characteristic peaks at 1726 cm^{-1} and 1175 cm^{-1} ascribed to C=O and C-O stretching respectively which indicates successful polymerization of POC. The two peaks at 2856 cm^{-1} and 2932 cm^{-1} were attributed to symmetric and asymmetric methylene groups respectively which were found in all the spectra of the materials. The broad peaks centered at 3478 cm^{-1} were attributed to the unreacted hydroxyl (-OH) groups from citric acid (Yang et al., 2006). The results indicated that ester bands are more intensified for pure POC in respect to composites. It is inferred that calcium ions released from the bioglass interacted with free carboxylic acid groups in the POC resulting in a new carboxylate peak at 1621 cm^{-1} (S.-L. Liang et al., 2010). Thus, the reaction between the bioglass and POC led to a decrease in ester formation due to the ionic interaction of metallic carboxylate. The presence of this peak confirmed the hydrolysis of bioglass by the unreacted acid functionalities in the pre-polymer and consequently resulted in reduction of ester formation.

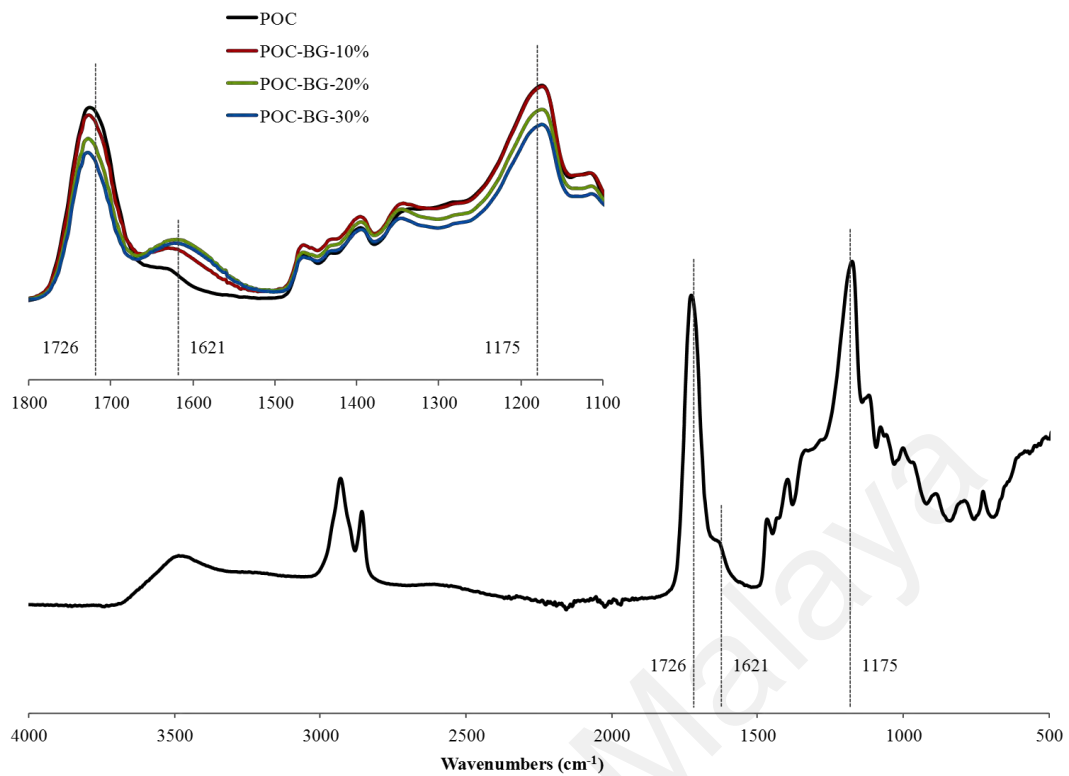


Figure 4.3: Representative ATR-FTIR spectrum of POC-BG composite; insert showing expanded spectral region for: pure POC (black); POC-BG-10% (red); POC-BG-20% (green); and POC-BG-30% (blue).

4.5 Thermal analysis

The thermogravimetric traces from pure POC and its microcomposites are shown in Figure 4.4. The analysis was carried out to investigate the bioglass content and dispersion in the composite scaffolds in respect to results obtained from equation 3.1 as shown in Table 4.1. The results show that, except for POC-BG-30%, thermal decomposition occurred through a two-step process. The almost complete weight loss (99.46 %) was observed for pure POC and thermal decomposition was detected at 650 °C. Similar degradations were observed for all composites between 220-600 °C. The thermograms indicated that thermal stability of the scaffolds was enhanced by increasing bioglass content. Analysis of thermal degradation on a randomly-selected sample from each composition indicated that POC-BG-10%, POC-BG-20%, and POC-BG-30% have total

weight loss of 88.5 %, 74 % and 71 % respectively. Accordingly, the pre-determined amount of bioglass in composites was 11 %, 26 % and 28.5 %. The comparison of results from experimental and theoretical revealed that there is a small discrepancy in glass content as a result of precipitation and agglomeration phenomena (Cannillo et al., 2010).

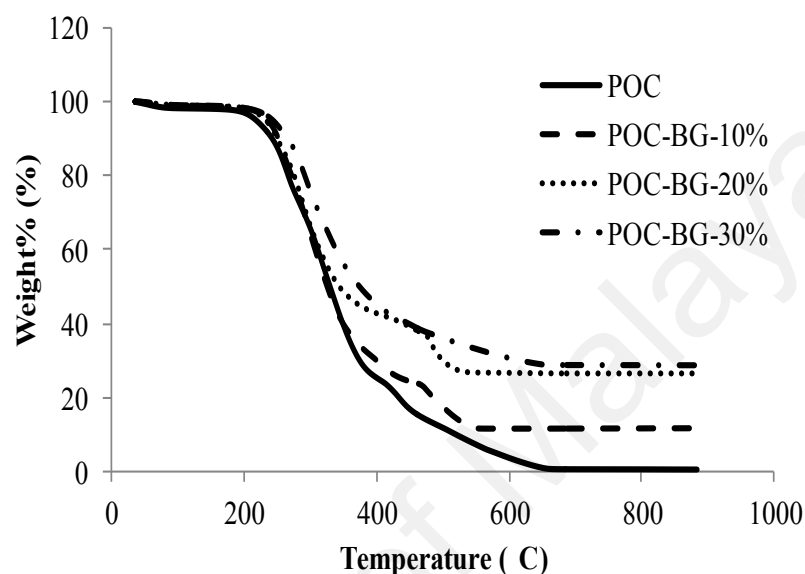


Figure 4.4: TGA curves measured for POC-BG composites in comparison to pure POC (Control).

Table 4.1: Comparison of theoretical and experimental bioglass content using total weight loss of the materials obtained by TGA.

Scaffold code	Total weight loss	Glass content calculated According TGA data	Glass content calculated According to Eq.
POC	99.469%	-	-
POC-BG-10%	88.456%	11.013%	10%
POC-BG-20%	73.458%	26.011%	20%
POC-BG-30%	71.072%	28.397%	30%

Data from the DSC thermograms of the pure POC and composites are shown in Table 4.2. All samples were found to be amorphous at body temperature with glass transition temperature (T_g) ranging from 2.5 to 25 °C. In addition, T_g values increased as the amount of bioglass increased. This can be ascribed to the higher rate of carboxylate formation in respect to ester bonds. As depicted by FTIR (Figure 4.3), ester peak intensity reduced

through the addition of bioglass and a new peak assigned to carboxylate was detected (S.-L. Liang et al., 2010; S. Liang et al., 2012). This is believed to be as a result of partial immobilization of polymer chains by increasing the crosslinking density while polymer adsorbed onto the bioglass surface and the physical crosslinks formed (Misra et al., 2007).

Table 4.2: The thermal and mechanical properties of POC-BG scaffolds.

Property	POC	POC-BG-10%	POC-BG-20%	POC-BG-30%
Storage modulus (kPa)	25.27	42.33	49.71	81.41
Loss modulus (kPa)	3.993	13.54	14.18	39.42
Tan δ at 37°C	0.15	0.26	0.28	0.48
T _g ^a at tan δ peak (°C)	0.5	4.1	9.4	12.5
T _g from DSC (°C)	2.76	16.11	22.56	24.58
E _c ^b (MPa)	0.31±0.10	2.60±0.69	4.00±1.00	6.78±1.62
Recovery (%)	95.99±0.72	82.92±4.65	73.83±1.60	53.65±2.58
Contact angle (°)	61.88±3.10	59.74 ± 4.90	60.20 ± 4.90	58.05 ± 1.60
Porosity (%)	83.00±1.87	84.89±0.68	86.00±1.01	86.23±1.73

Storage modulus, loss modulus and Tan δ measured for scaffolds at 37 °C. ^aT_g=Glass transition temperature. ^bE_c=Compression modulus

4.6 Mechanical properties and porosity

DMA analysis generally provides accurate data for evaluation of the viscoelastic properties of the as-prepared scaffolds. The storage modulus (E'), loss modulus (E'') and tan delta (tan δ) have been measured at body temperature (Table 4.2). T_g was determined as the peak of the tan δ curve (Figure 4.5). Tan δ represents the ratio of the dissipated energy to the energy stored per cycle (tan δ = E''/E') and is often known as damping. Tan δ

value was enhanced by increasing the bioglass content. The storage modulus increased by addition of bioglass in the temperature range, 20-40 °C; the highest storage modulus was observed for POC-BG-30% composite at 81.41 kPa. The storage modulus illustrated higher values as compared to loss modulus which confirms the elastic nature of scaffolds. It is believed that addition of bioglass enhances the stiffness since strand density increases due to formation of metallic carboxylate groups (S. Liang et al., 2012). Therefore, the physical interactions between POC and glass improve the storage modulus both below and above T_g . The addition of bioglass was seen to increase T_g from 0.5 °C for pure POC to 12.5 °C for POC-BG-30% composite. All the T_g values obtained by DMA were different from those acquired by DSC (between 2-13 °C). This may be as a result of partially increased degrees of crosslinking in the first heating step during DSC testing. Moreover, the increase in loss modulus by the addition of bioglass suggests that the composites possess remarkable dissipation capability relative to pure POC (Srinivasan et al., 2012). Thus, it can be concluded that addition of bioglass lead to the formation of ionic bonds which have significant impact on the partial immobilization of polymer chains.

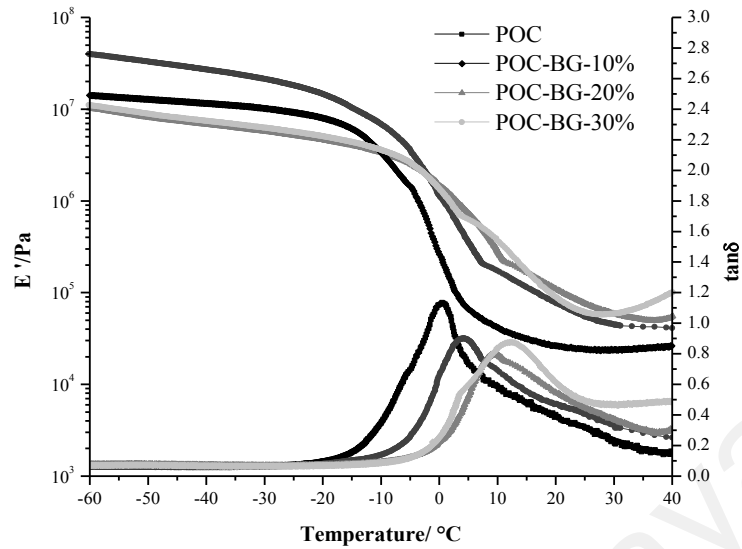


Figure 4.5: DMA analysis of composite scaffolds illustrating the typical plots of Tan delta ($\tan\delta$) and storage modulus (E') under bending mode.

An ideal material for hard tissue augmentation should have properties that match those of the host bone with suitable load transference across the interface to provide mechanical support during bone healing (Bose et al., 2012). The incorporation of bioglass particles into the polymer matrix can lead to increases in both strength and load transferral. For this purpose, the prepared scaffolds were tested from a standpoint of compression to investigate the effect of bioglass incorporation on recorded mechanical properties. Table 4.2 summarizes compressive modulus and recovery ratio of the porous scaffolds. The Young's modulus of the scaffolds increased in line with bioglass content and a significant difference was observed between POC-BG-30% (6.78 MPa) and pure POC (0.31 MPa). However, the recovery ratio has the opposite trend. This can be attributed to enhanced crosslinking density by addition of bioglass which increased the stiffness of the materials (S.-L. Liang et al., 2010).

Table 4.2 also shows measured porosity for composite scaffolds. A scaffold should possess an interconnected and uniformly distributed porosity with a highly porous surface

and microstructure (Bose et al., 2012). According to previous reported results, a pore size between 200-400 μm is suitable for cell adhesion and ingrowth *in vitro* and neovascularization *in vivo* (Puppi et al., 2010). When the pores are smaller than this, pore occlusion by cells could occur, inhibiting extracellular matrix production (Dhandayuthapani et al., 2011). Prepared scaffolds exhibited high porosities (>80%) as displayed in Table 4.2. Porosity increased with bioglass concentration; the pure POC scaffold showed the lowest porosity. It is postulated that the addition of bioglass improves structural stability. As a result, POC-BG-30% had the highest porosity of approximately 86 %. This is consistent with the previous study (Gerhardt et al., 2011) where 20% incorporation of bioglass into PDLLA led to an increase in porosity and it was more apparent for the nanocomposites in respect to microcomposites (Gerhardt et al., 2011). However, the work by Srinivasan *et al.* showed a decrease in porosity ratio by addition of more nano-bioglass (Srinivasan et al., 2012). Overall, the ideal porosity percentage can be defined by the final application and also when there is a compromise between mechanical and biological properties (Ryszkowska et al., 2010).

4.7 *In vitro* degradation study

The degradation of pure POC samples and the composite scaffolds were investigated using PBS. Figure 4.6 shows the weight loss of all prepared scaffolds. The data revealed that increasing the concentration of bioglass reduced the degradation rate as reported in terms of weight loss. Pure POC completely degrades after 6 months (Yang et al., 2004). In our case, the pure POC scaffold had the highest percentage of weight loss at about 16 % during 4 weeks of incubation and POC-BG-30% demonstrated the lowest weight loss which is probably due to the slow dissolution of bioglass. The low dissolution of bioglass is assessed by enhancing the acidic nature of the bioglass surface as a result of the

presence of Ga (Aina et al., 2011). However, Liang *et al.* ascribed the low degradation of composites from poly (glycerol sebacate) (PGS) and 45S5 bioglass to the variation in pH as bioglass has ability to release the alkaline ions and keep the buffer solution neutralized (S.-L. Liang et al., 2011). Composite scaffolds developed in the research contained herein showed similar behavior. Studies in PBS demonstrated the pH variation was not significantly influenced by the POC-BG-30% and it almost kept constant around 7.2. All the scaffolds illustrated a decrease in pH at day one from 7.4 (PBS) to 6.93, 7.04, 7.12, and 7.16 for pure POC, POC-BG-10%, POC-BG-20%, and POC-BG-30% respectively. After the initial drop the pH values remained almost constant over the course of 7 days.

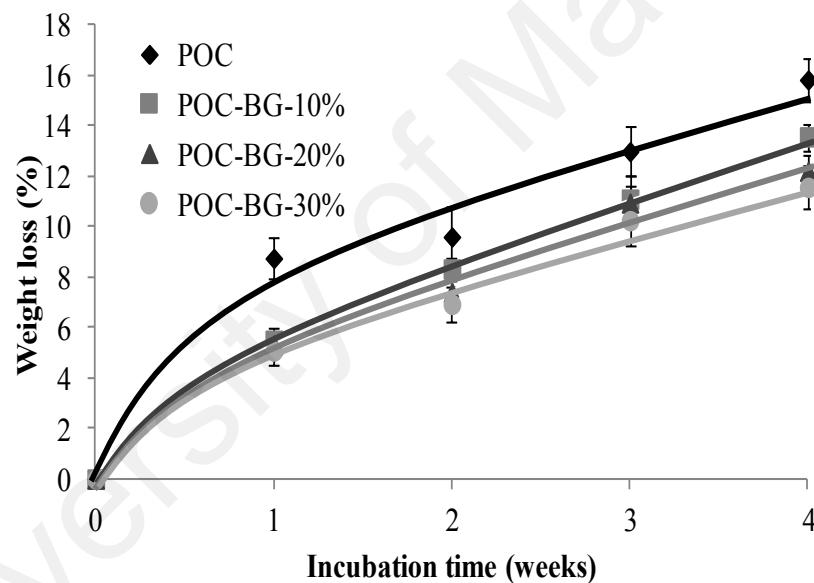


Figure 4.6: *In vitro* degradation profiles of composite scaffolds (PBS; 37 °C).

4.8 Water in air contact angle

Wettability plays a crucial role at the interface of a biomaterial with a biological system. Different biological events such as cell attachment, cell proliferation and protein adsorption can be considerably affected by wettability at the interface (Caridade et al., 2012). Static contact angle measurements were carried out to measure the hydrophilicity

of the prepared films. The data are displayed in Table 4.2. There were small differences between the wettability of all the compositions and the results were in the range of 58 to 62°. The composite films indicated lower contact angles (58-60°) compared with the pure polymer, presumably due to hydrophilic nature of bioglass. In this study the pure POC showed an average contact angle of about 62° which is in agreement with previously published results (Yang et al., 2006). The POC-BG-30% composite had the lowest contact angle around 58° which means more surface hydrophilicity in comparison to the pure POC films.

4.9 Swelling experiment

Swelling ratio is a standard method to characterize the hydrolytic stability of polymeric biomaterials in general (Peng et al., 2007). In order to assess the fundamental properties of the POC-BG composite we have chosen the sample films (Figure 4.7) over scaffolds, since the hydrophilic porous structure would contain significant amount of surface water trapped within the pores (Djordjevic et al., 2009). The swelling behavior of prepared films was investigated in water and PBS (Figure 4.7). The swelling ratio in water increased with bioglass content. The composite samples reached the equilibrium percentage swelling after 30 min incubation whereas pure POC reached the equilibrium after 1 h.

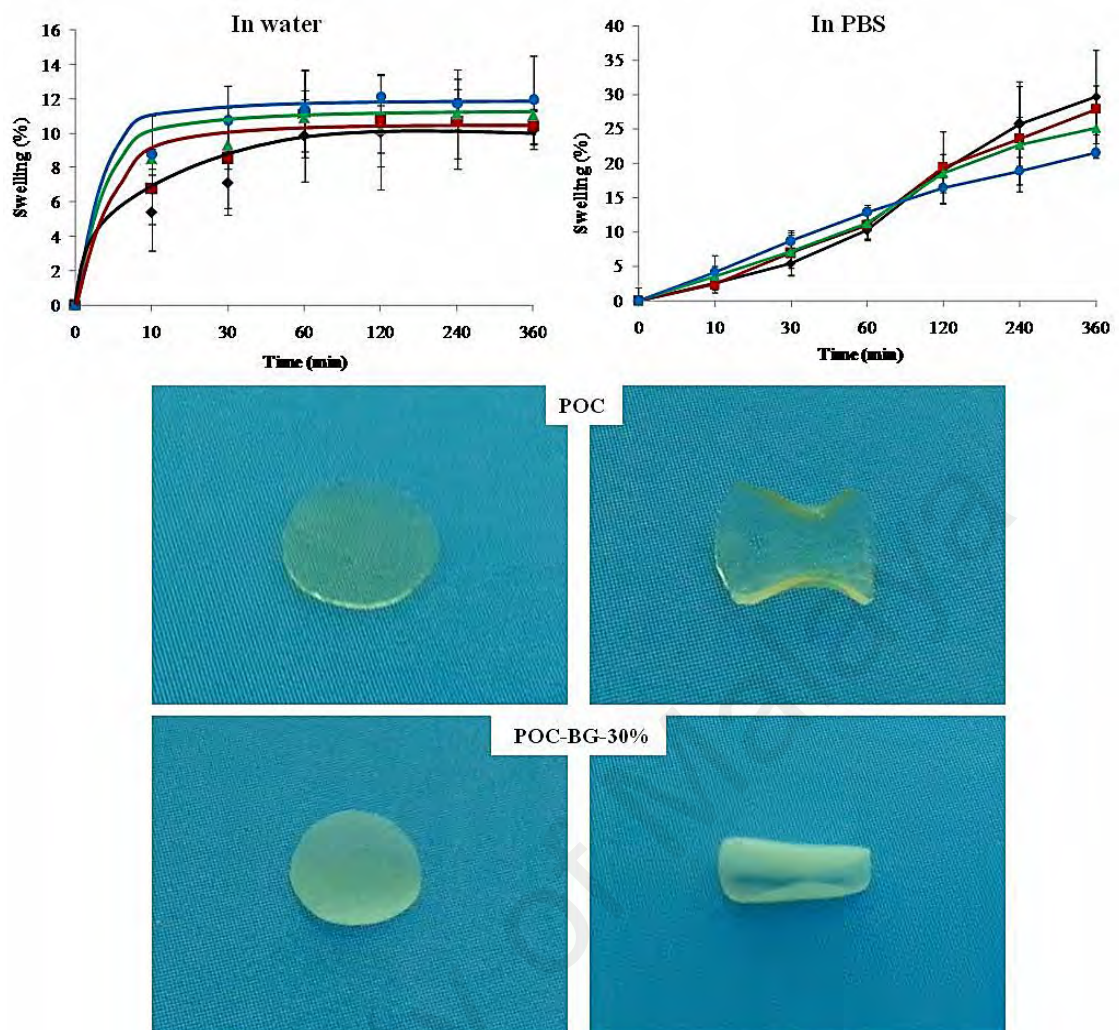


Figure 4.7: Swelling ratio in water and PBS of: pure POC (black-◆); POC-BG-10% (red-■); POC-BG-20% (green-▲); and POC-BG-30% (blue-●). The images show films of POC and POC-BG-30% after soaking in water (left) and PBS (right) for 6 h.

The composite with 30 % bioglass indicated maximum swelling of about 12 % and POC had the lowest (around 10%). This may be a result of higher hydrophilicity of composites as confirmed by water contact angle (Table 4.2). Likewise, the interaction of bioglass with polymer acid functionalities lead to formation of calcium carboxylate which further increase the polarity of the matrix (S.-L. Liang et al., 2010). Therefore, hydrophilic nature of bioglasses rendered the materials with improved hydrophilicity, favouring water absorption. Immersion in PBS showed almost 3 times higher percentage swelling for all tested films in comparison with the results obtained in water (Figure 4.7). However, a

different trend was observed in PBS: pure POC showed the highest swelling ratio (~30 %), while the highest content of BG in composite films resulted in the lowest swelling after 6 hr (POC-BG-30%; ~21 % percentage swelling). It should be noted that the ionic strength of PBS (0.16 M) is substantially higher than water (close to 0 M) which could have a significant influence on osmotic pressure within our elastomer composites (including pure POC) (Q. Xing et al., 2014). From macroscopic observation (Figure 4.7, bottom) PBS influences sample morphology possibly due to certain degree of crosslinks cleavage within polymer systems. The result is consistent with *in vitro* degradation experiment where pure POC showed the highest degradation rate in PBS (Figure 4.7).

4.10 Ion release study

The Si^{4+} , Ca^{2+} , Zn^{2+} and Ga^{3+} ions release profiles of POC-BG composite scaffolds in PBS are presented in Figure 4.8. Elemental concentration of all the components increased with time. As expected, all the composites showed a similar release trend with a statistically higher release of Si at every time point. The Ga^{3+} and Ca^{2+} ion release ratios were also found to increase over incubation time, with a maximum of 1.5 and 1.4 ppm, respectively. The increase in ionic concentration of Si^{4+} , Ca^{2+} and Ga^{3+} with incubation time revealed that POC is degrading alongside the glass phase. As composite scaffolds degraded over time, the medium was able to diffuse through the matrix thus causing more glass material to be released. Although a high Zn concentration is present in the glass series, very low concentrations of Zn^{2+} ions were recorded in the PBS solution over 1 to 28 days. The measured amounts (~ 0.03 ppm) were significantly lower than the reported average Zn^{2+} ion concentration of human plasma (0.95-1.30 ppm) and *in vitro* toxic levels (5.9 ppm and 6.1 ppm) for murine osteoblasts and L929 fibroblast respectively till 28 days of immersion in PBS (Lansdown, 1996; Yamamoto et al., 1998). It may reduce one

of the concerns about the release of high level of Zn^{2+} which may cause cytotoxicity to cells.

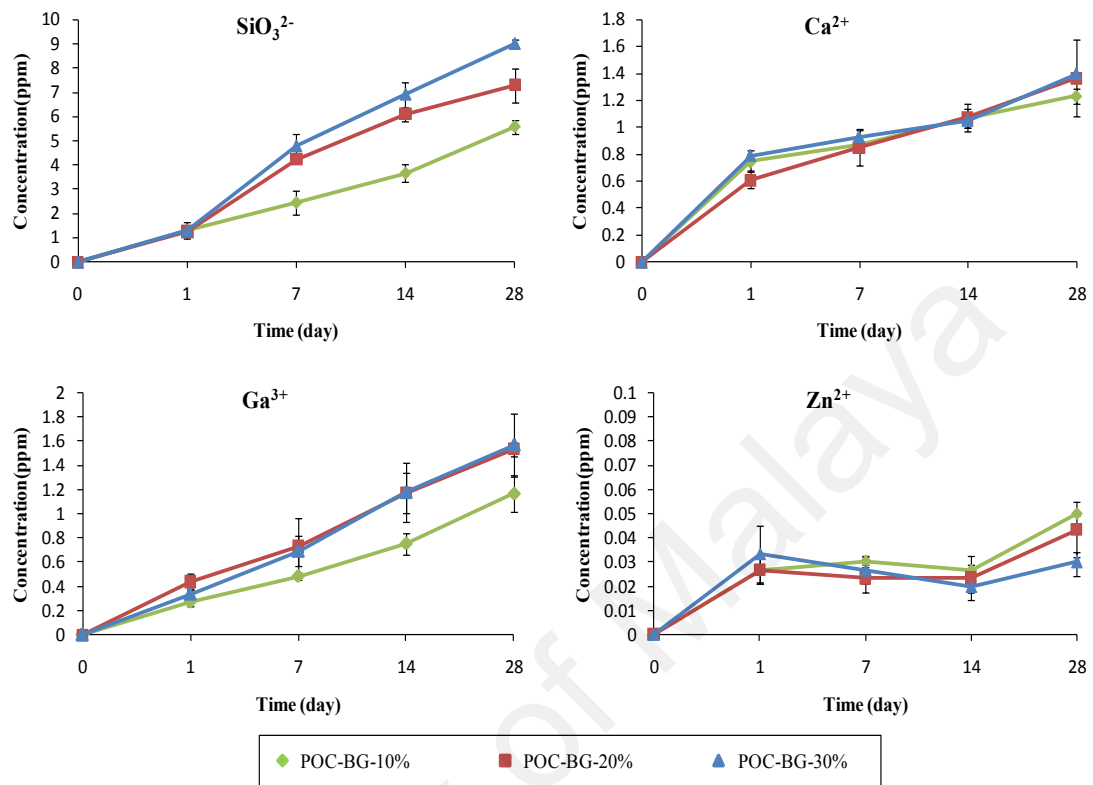


Figure 4.8: Ion release kinetics from composite scaffolds in PBS: AES plots of elemental concentrations of Si, Ca, Ga and Zn after 28 days of scaffolds immersion.

4.11 Acellular *in vitro* tests performed in SBF

Figure 4.9 shows the release of Ca^{2+} , PO_4^{3-} , Si^{4+} , Zn^{2+} and Ga^{3+} ions in SBF on day 1, 7, 14 and 28 days. The experiment was performed to assess *in vitro* behavior of POC-BG-10%, POC-BG-20% and POC-BG-30% in terms of chemical composition changes in the simulated body environment. The concentration of Ga^{3+} follows a steadily rising trend and POC-BG-30% showed the highest Ga^{3+} release at pre-determined time points. At the end of the experiment, Ga^{3+} concentration from POC-BG-30% extracts showed similar result observed for the ion release profile in PBS but not for POC-BG-10% and POC-BG-20%. However, the assessment of Zn^{2+} ion release revealed a higher concentration when

compared to the study in PBS (Figure 4.8), although the Zn^{2+} was still relatively low for the duration of the experiment, reaching a maximum of 0.24 ppm at day 28. There were no significant differences for Si^{4+} concentration measured in PBS and SBF at any time-points. The Ca^{2+} concentration in SBF across all groups increased at day 1 and it could be concluded that an increase in Ca^{2+} concentration is induced by the release of Ca^{2+} ions from composites. At day 7, Ca^{2+} concentrations reached the lowest level and then gradually increased until the end of the experiment (day 28). A small decrease in Ca^{2+} concentration in the later stages is most likely a consequence of the consumption of Ca^{2+} through the formation of calcium phosphate (CaP) on scaffold surfaces. The concentration of PO_4^{3-} decreased when composite scaffolds were soaked and was less than original SBF phosphorous concentration during the entire period of the experiment. The depletion of PO_4^{3-} from SBF confirms the formation of CaP layer on the scaffolds surfaces during incubation as presented in Figure 4.10. The formation of a CaP surface layer is considered essential for the biological success of the material as it may determine the suitability of material as a bone substitute by the ability to chemically bond to the adjacent living bone (Kokubo & Takadama, 2006). Thus, from the results, an interaction between the SBF and the composites has occurred. SEM-EDS analysis confirmed the presence of CaP layers on the surfaces of the composite specimens. However, the CaP formation ability was poor. The very low CaP-forming ability can be attributed to release of both Zn^{2+} and Ga^{3+} from the composite scaffolds.

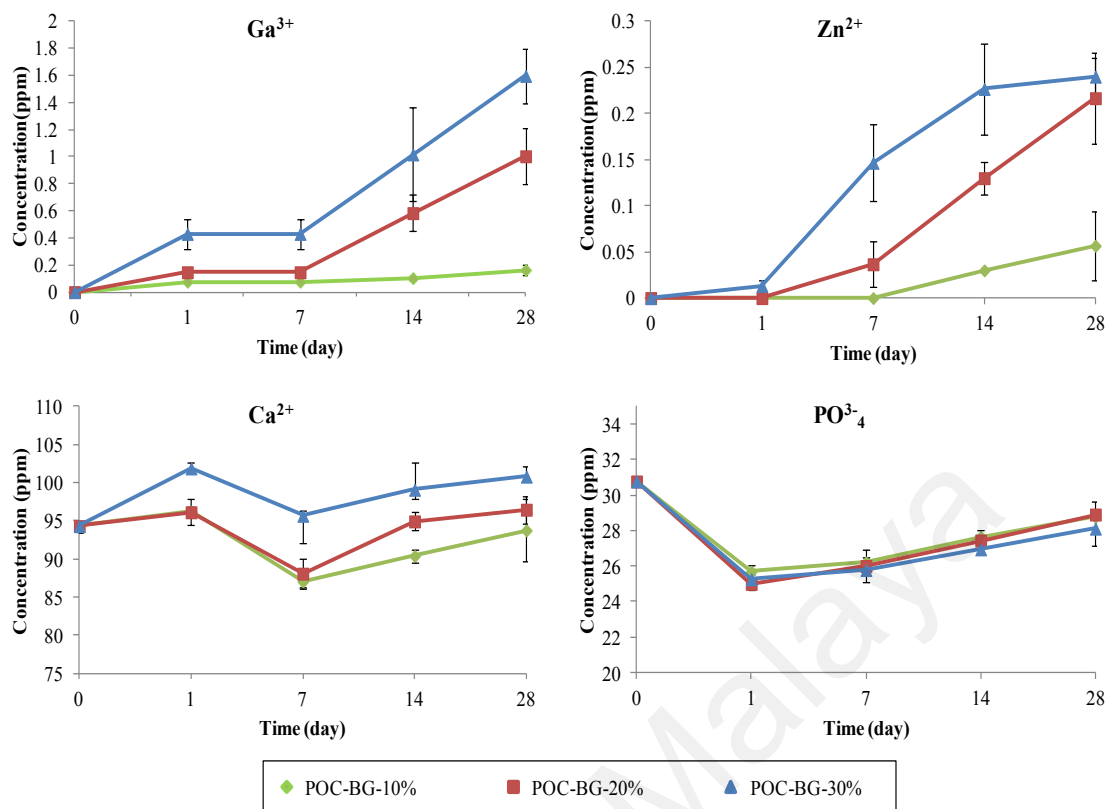


Figure 4.9: *In vitro* ion release kinetics for composite scaffolds in SBF: ICP plots of elemental concentration of Ca²⁺, PO₃⁻⁴, Ga³⁺ and Zn²⁺ vs. immersion time for the investigated composites.

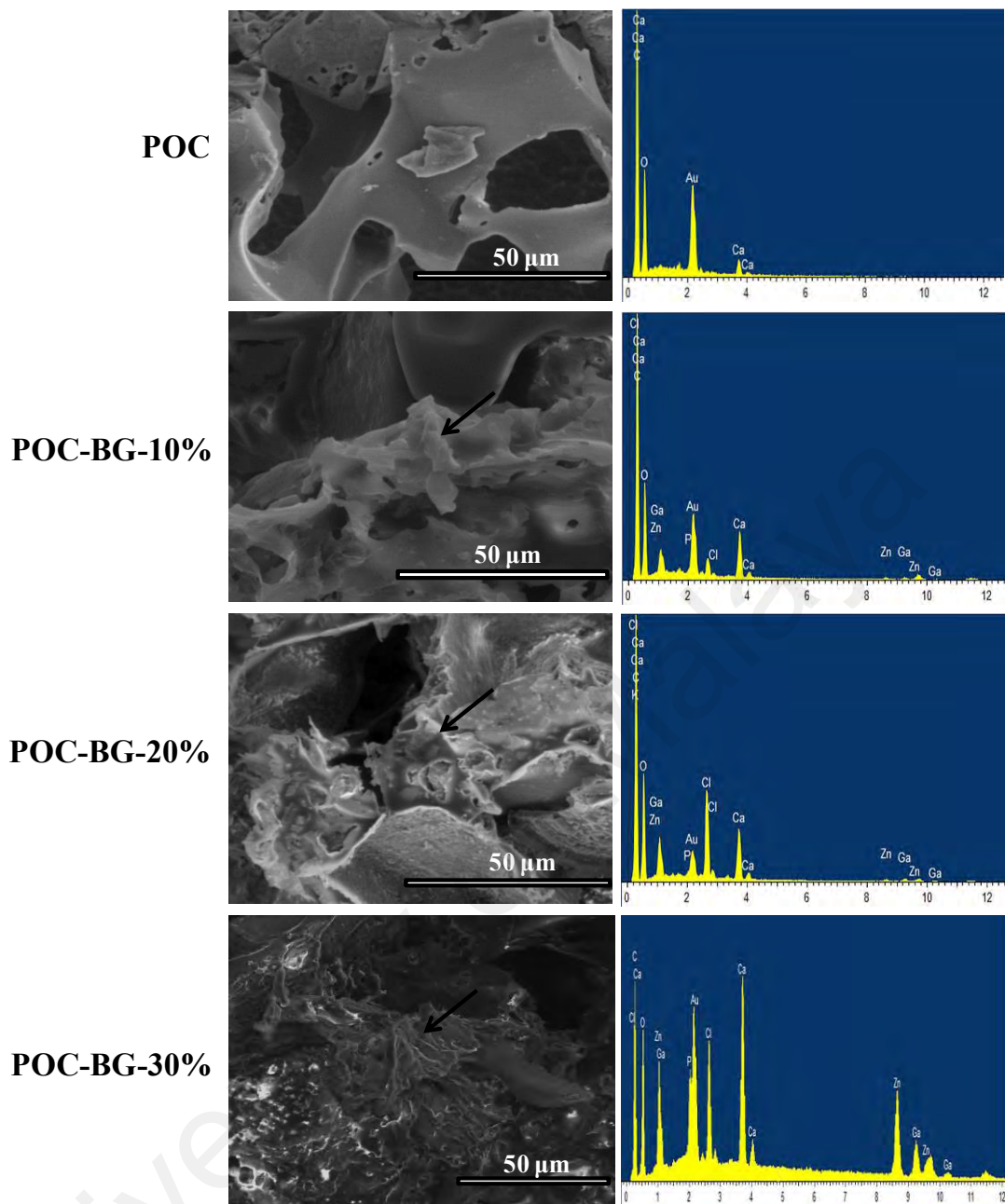


Figure 4.10: (left): SEM images confirm CaP layer deposition (arrows) on the composite scaffolds during immersion in SBF and (right): EDS profiles of the composite scaffolds after being soaked in SBF for 28 days.

Although Zn is known to be a potent inhibitor of apatite crystal growth, it was found that Zn^{2+} release at non-toxic levels does not completely inhibit initial apatite deposition (Ito et al., 2002). For example, Fuierer *et al.* reported that a low concentration of Zn^{2+} ions (0.25 ppm) was able to slow, but not stop, the rate of HA formation from supersaturated solutions by 78 % (Fuierer et al., 1994). They found that pre-adsorbed Zn

on the seed crystals was effective in retarding crystal growth as a result of formation of $\text{Zn}_2(\text{PO}_4)_3$ complexes. Zn initially retards HA nucleation and the number of nuclei decreases with the amount of Zn addition (R. L. Du et al., 2006). This phenomenon was explained by the ability of Zn to deactivate the HA nuclei. When nucleation sites are reduced, the chance for each HA nucleus to receive Ca^{2+} and PO_4^{3-} in SBF will increase. As a result, larger HA crystals could be produced. At longer soaking times, the available Zn on the surface is covered by the HA layer and, due to the higher bond energy of Zn-O (rather than Ca-O), the diffusion of Zn from the network into the solution is retarded and its influence on HA formation reduces (R. L. Du et al., 2006). Moreover, it is understood that retarded HA formation of Zn-doped bioactive glasses can further facilitate slower HA crystallization and thus provide a better bone bonding interface *in vivo* (Boyd et al., 2008). Indeed, the presence of Zn in the bioactive glass phase explains the lack of crystallinity associated with the formation of the apatite layers observed on composite scaffolds after immersion in SBF. Thus, the release of Zn^{2+} and its subsequent inclusion in the apatite layer favors the formation of amorphous apatite.

It has also been reported that Ga has an inhibitory effect on HA deposition and growth (Blumenthal et al., 1989). Ga-doped Brushite showed a reduced rate of HA formation in a solution containing Ca. This phenomenon is a result of Ga adsorption on the apatite surface which further prevents the growth of HA (Korbas et al., 2004). In addition, to observing the impact of Ga on bioactivity, Franchini *et al.* (Franchini et al., 2012) examined a series of glasses based on 45S5 that contained incrementally increasing amounts of Ga up to 3.4 mol%. The bioactivity test in SBF revealed that there is a competition between Ca^{2+} and Ga^{3+} for binding with phosphate ions. As a result, after a long period of soaking, the phosphate ions are not sufficient to precipitate with the continuously released Ca^{2+} from the glass to precipitate HA. Consequently, the Ca/P ratio of SBF and glass exceed the topical Ca/P ratio of HA (1.67) and carbonate ions from SBF

begin to form calcite. It is hypothesized that this replacement can inhibit crystallite growth (Franchini et al., 2012). Overall, the co-precipitation of Ga-phosphate might be partially responsible for delayed CaP precipitation (Aina et al., 2011). Ga may also act as a network former in the glass and consequently can reduce the solubility of the glass which will retard bioactivity (Aina et al., 2011). In addition, the increased acidity caused by Ga-containing bioactive glasses may be another reason for delayed apatite formation (Aina et al., 2011). The enhanced surface acidity of Ga-containing glass is expected to preliminarily inhibit the deposition of CaP, the essential prerequisite for HA crystallization. In the present study, the release of both Zn and Ga can extremely inhibit apatite formation and crystallization such that after 28 days of incubation in SBF it was still only partially covered by a CaP layer.

4.12 *In vitro* bone tests for ion penetration into bone tissue matrix

The digital image of a selected bovine bone implanted scaffold and the corresponding SEM image are shown in Figure 4.11. The specimens were examined by EDS at predetermined distances after 7 days soaking in PBS and the results are presented in Figure 4.12. Four points at various distances from the scaffold-bone interface (*i.e.* 0, 200, 1500 and 4500 μm) were investigated by EDS for the presence of all ionic species from the bioactive glass phase in the composite. Very low concentrations of Ga^{3+} (approximately 0.06 %) were absorbed into the bone from the specimens containing POC-BG-20% and POC-BG-30% scaffolds by up to 1500 μm from the implanted scaffolds. The highest Zn^{2+} concentration was detected at point 0 and it decreased with distance from the scaffold. The results demonstrate that Zn^{2+} ions were released from the scaffolds and taken up into the bone as far as 4.5 mm away from the implant. As expected, Zn^{2+} was not detected for the unfilled POC and control specimens.

The amounts of Ca^{2+} and phosphorous (P) ions, alongside the Ca/P ratio, were determined at all points (Figure 4.12). Significantly higher Ca^{2+} and PO_4^{3-} ionic concentrations to Zn^{2+} were detected at all points in the bone specimens and were attributed predominantly to the bone itself. P ionic concentration remained relatively constant in the observed area. The concentration of Ca^{2+} slightly decreased in the vicinity of the bone-scaffold interface as Zn^{2+} is incorporated into the bone. The observed patterns of Zn^{2+} and Ca^{2+} migration into bone specimens are consistent with a study by Wren *et al.* (Wren et al., 2009). However it is unclear whether the reduction in Ca^{2+} concentration was significant, since EDS is predominantly a qualitative tool and it cannot determine between low counts (Wren et al., 2009). Furthermore, higher Ca^{2+} was detected at the bone-scaffold interface for POC-BG-10% compared to POC-BG-20% and POC-BG-30% which can be attributed to the lower Zn^{2+} concentration recorded for the POC-BG-10% composite. As can be seen in Figure 4.12, no significant difference in Ca/P ratio was observed between any of the samples (calculated at approximately 1.3-1.5). This shows that incorporation of Zn^{2+} in bone does not influence the original Ca/P ratio of the mineral phase of bone. Although the theoretical fraction of Ca and P of bone should be 40.3% and 18.4% respectively, it can vary and is influenced by factors such as bone source, location and age as well as the presence of metabolic bone disease (Grynepas et al., 1987; Kuhn et al., 2008).

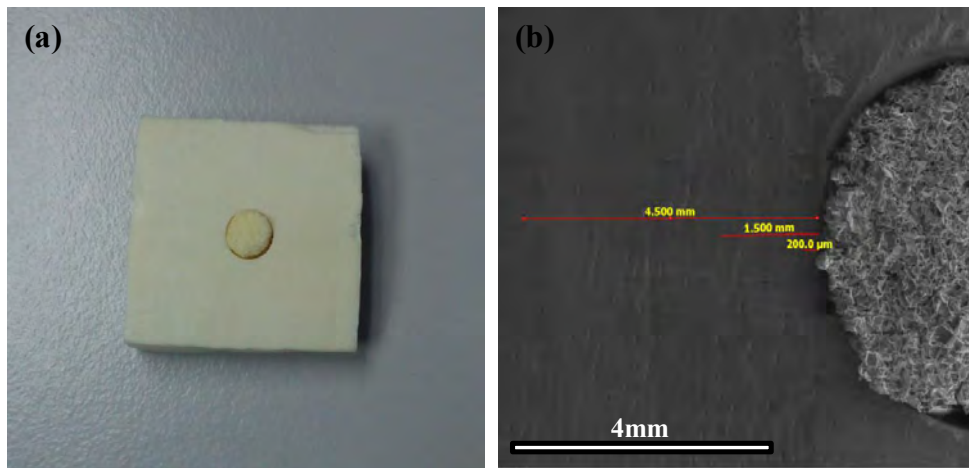


Figure 4.11: (a) Digital image and (b) SEM image of POC scaffold implanted into bone specimen.

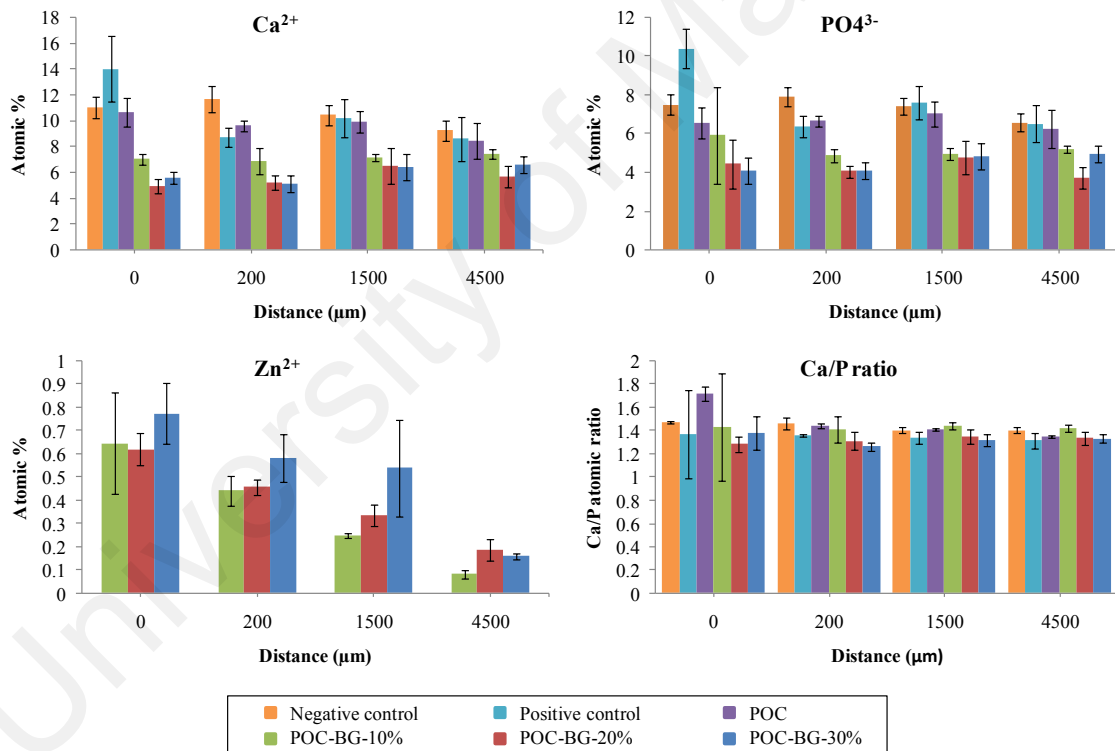


Figure 4.12: Normal atomic % EDS data for Ca, P and Zn content as well as Ca/P ratio at scaffold-bone interface at various distances 0, 200, 1500 and 4500 μm.

Comparison of results from the ion release study in PBS and scaffold implanted bones reveals that Zn²⁺ is released from composite scaffolds and quickly re-precipitated in bones while Ga³⁺ can be recorded in acceptable concentrations in buffer solutions. A possible

mechanism for this is the dissolution of Zn^{2+} and $ZnOH^+$ ions from the glass particles and precipitation of the hydroxide, $Zn(OH)_2$, onto the bone surface (Pasquet et al., 2014). It may also be the reason for the low levels of Zn^{2+} that observed in the extracts from the ion release experiments. Foley and Blackwell also observed the highest rate of Zn release from zinc phosphate cements occurred after 2 days, and reached almost zero after 28 days of incubation (Foley & Blackwell, 2002). Similarly, the highest rate of Zn release detected by Osinaga *et al.* was within 24 h (Osinaga et al., 2003).

The Zn^{2+} ion is known to have a stimulatory influence on bone formation and mineralization and an inhibitory influence on bone resorption (Yamaguchi, 1998). About 85% of the bodily content of Zn (1.4-2.3 grams) is in bone and muscle and the remaining 15 % is found in other tissues (e.g. liver and skin). Zn concentration in the adult human skeleton is about $100 \mu g g^{-1}$ (Clayton, 1979; Tapiero & Tew, 2003). Zn deficiency is a common reason for bone growth retardation due to reduction in osteoblastic activity, in collagen, in proteoglycan synthesis, and in alkaline phosphatase (ALP) activity (Calhoun et al., 1974). Low Zn bioavailability can also lead to inadequate immunoresistance to infections in the elderly (Mocchegiani et al., 2001; Ripa & Ripa, 1994). It has also been found that osteoporotic patients have a lower skeletal Zn content than normal (Reginster et al., 1988). The oral administration of Zn compounds such as Zn-chelating dipeptide and Zn sulfate in rats has been shown to be effective in treatment of osteoporosis (Segawa et al., 1992). Excessive Zn content can also result in disorders such as growth retardation, anaemia and immunosuppression (Ripa & Ripa, 1994). For example, it has been reported that Zn concentrations in the range of 2–8 ppm may cause damage to human osteoblasts *via* oxidative stress (Goel et al., 2013). Thus, the beneficial effect of Zn is greatly dependent upon its dose and duration (Mocchegiani et al., 2001). It is also expected that the local delivery of Zn would have a significant impact on bone regeneration. The levels

of synergistic ion release from our materials correlates well with the levels of Ga^{3+} and Zn^{2+} ions typically associated with clinical benefits (cell responses).

4.13 Antibacterial tests

The effect of bioactive glass addition on the growth of both *E. coli* and *S. aureus* was investigated by monitoring culture turbidity for 10 h. The results are shown in Figures 4.13 and 4.14. It can be seen that the culture containing POC is slightly different from that of the negative control (LB broth) after 10 h. The low antibacterial activity of POC may be attributed to the presence of a large number of acid groups. As shown in Figure 4.13, the results indicate that both *E. coli* and *S. aureus* growth were significantly inhibited by the addition of bioactive glass. As the value of the optical density (OD) at 595 nm represents the absorbance of the bacteria, a decrease in OD implies bacterial depletion (L. Zhang et al., 2007). Consequently, the antibacterial efficacy of the materials was enhanced in proportion to the bioactive glass concentration. In particular, the culture including composite with 30 wt% bioactive glass inclusion had significantly less bacteria than the control during incubation at 37 °C. These data suggest that the antibacterial activity of composite scaffolds is dependent on glass content.

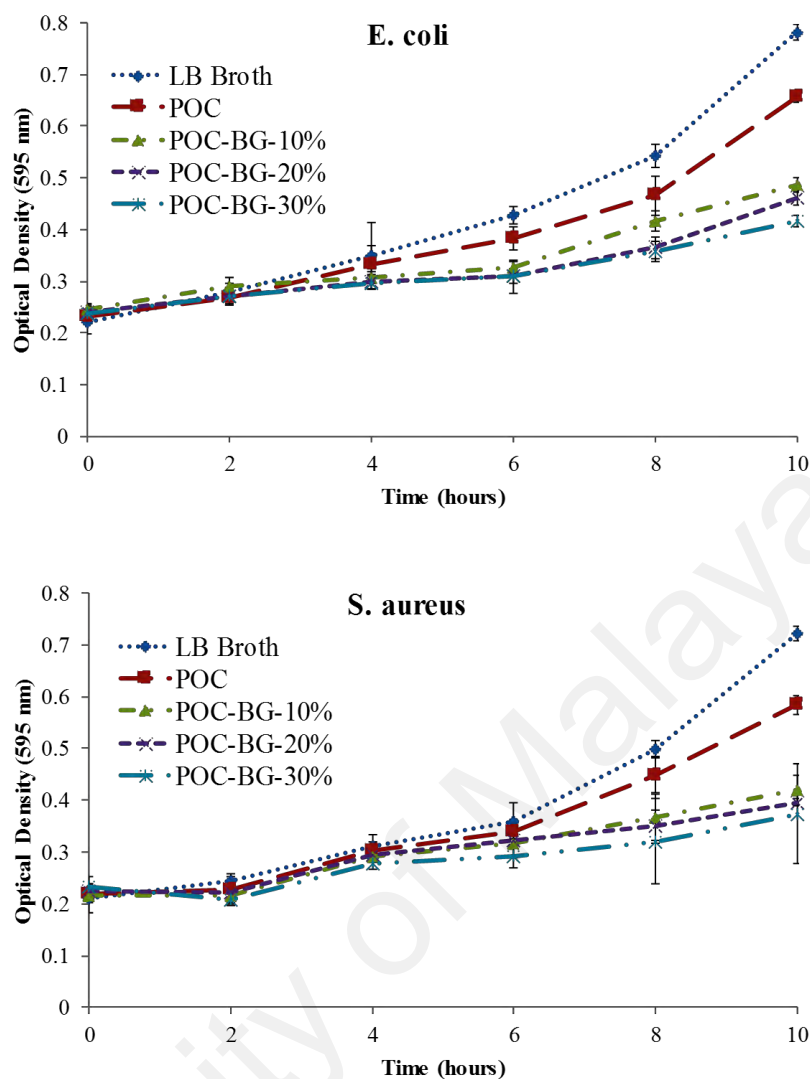


Figure 4.13: Effect of the composite scaffolds on the growth of *E. coli* and *S. aureus*; measured by monitoring the optical density at 595 nm.

Growing cultures after 10 h of growth were also plated to count viable bacteria, and the viable bacterium numbers are consistent with the OD of the growing cultures (Figure 4.14). Notably, at that time point, “viable bacteria recovered” decreased significantly with increasing glass content. As shown in Figure 4.15, POC-BG-30% scaffolds effectively limited the growth of both *E. coli* and *S. aureus*. Antibacterial testing against *E. coli* and *S. aureus* revealed bacteriostatic effects. However, the antibacterial activity of the composite scaffolds against *E. coli* was not as effective as that on *S. aureus*. This result might be attributed to the differences on membrane structure and composition of the

examined bacteria; *S. aureus*, a typical Gram-positive bacterium, is composed of a peptidoglycan layer which is a loosely-packed network structure with plenty of pores. Through these pores, foreign molecules can be transported across the cell into the interior with little obstruction. In contrast, *E. coli* is a typical Gram-negative bacterium which due to the presence of lipopolysaccharide molecule contains an outer membrane outside the porous peptidoglycan layer acting as drug barrier. The barrier can resist the permeation of large foreign molecules (Don et al., 2005). Thus, our composite scaffolds would be expected to have different antibacterial activity against these two bacteria due to the ions released.

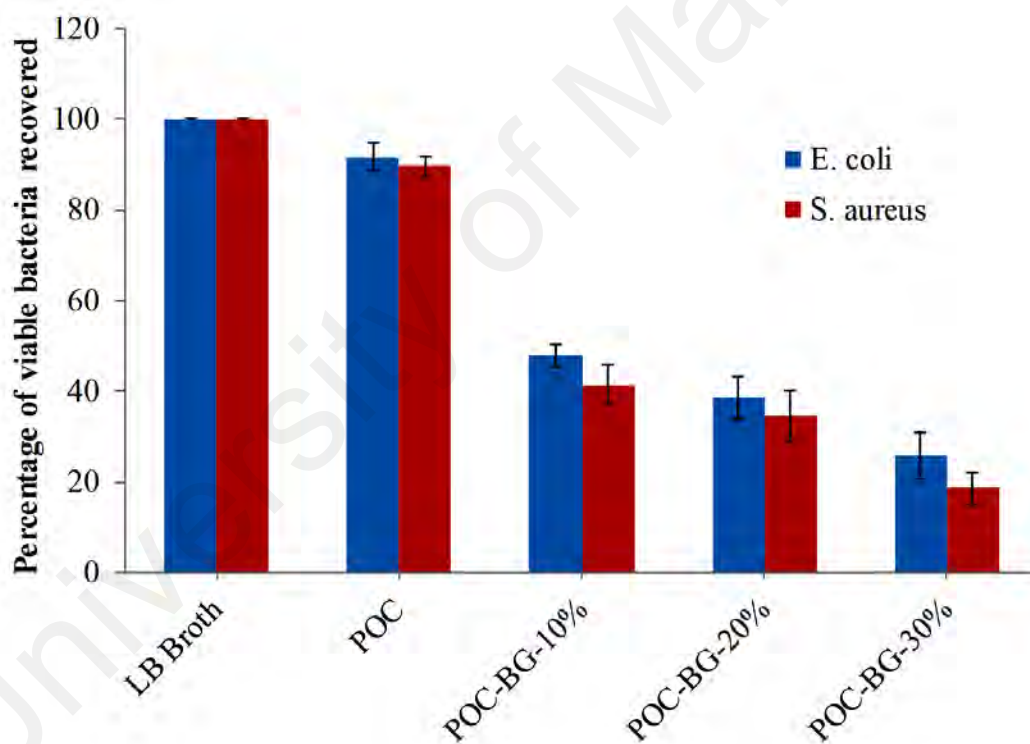


Figure 4.14: The viable *E. coli* and *S. aureus* recovered from agar plates after 10 h of incubation at 37 °C.

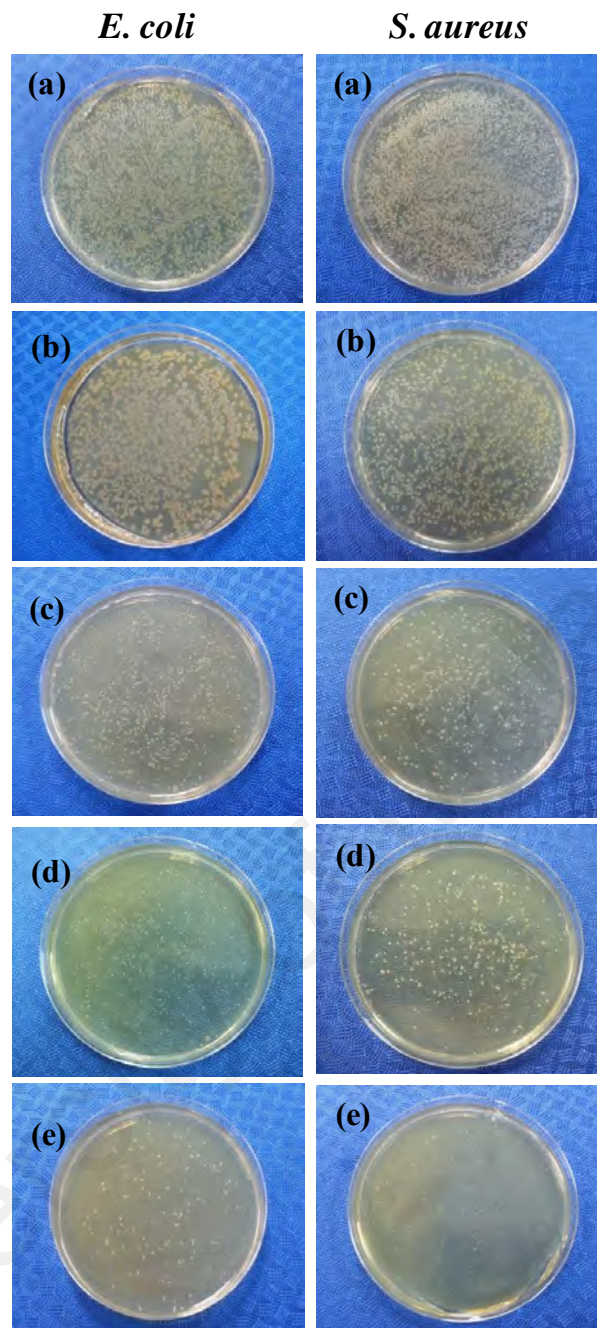


Figure 4.15: Plate assay of *E. coli* and *S. aureus* using (a) LB broth; (b) POC; (c) POC-BG-10%; (d) POC-BG-20%; (e) POC-BG-30% at 10 hours.

The antimicrobial effects of bioactive glasses are most likely a consequence of ion release, in addition to pH changes that they induce (Gubler et al., 2008). It is postulated that the antimicrobial effect of the composite scaffolds is based on the release of metal ions (Ga^{3+} and Zn^{2+}) to the cultures. Bioactive glasses doped with Ga^{3+} have antibacterial activity against both Gram-positive (*Staphylococcus aureus*, methicillin-resistant

Staphylococcus aureus, and *Clostridium difficile*) and Gram-negative (*Escherichia coli* and *Pseudomonas aeruginosa*) bacteria (Valappil et al., 2008). Due to the similarity of Ga^{3+} and Fe^{3+} in terms of ionic radius, coordination number and electronegativity, Ga^{3+} (redox inactive) can efficiently compete with Fe^{3+} (redox active) for binding to iron-containing enzymes, as well as to transferrin, lactoferrin, and microbial iron chelators (Franchini et al., 2012; Pickup et al., 2009). However, under the same conditions, unlike Fe^{3+} , Ga^{3+} cannot be reduced leading to inhibition of a number of essential biological reactions including those responsible for DNA and protein synthesis as well as energy production (Bernstein, 1998; Chitambar, 2010). Since only one-third of circulating transferrin is occupied by iron, Ga^{3+} can react with the remaining sites and form transferrin-Ga complexes and diminish the bacterial uptake of Fe^{3+} as well as the enhancement of a microorganism's vulnerability (Chitambar, 2010). The presence of Ga^{3+} has shown to retard localized infections (Valappil et al., 2008) alongside inhibiting *Pseudomonas aeruginosa* growth, preventing biofilm formation and imparting bactericidal activity against both free living bacteria and biofilm cells (Kaneko et al., 2007). Recently, it has been reported that low concentrations of Ga^{3+} inhibit biofilm formation from *E. coli* and *S. aureus* even when a high percentage of bacteria have survived the Ga_2O_3 treatment (Murthy et al., 2011). An explanation for this behavior is that Ga^{3+} decreased bacterial Fe^{3+} uptake in a concentration-dependent manner.

The antimicrobial activity of Zn^{2+} has been proven against various bacterial and fungal strains (Boyd et al., 2006; C. Wu et al., 2013). Recent reports have shown that Zn in micromolar concentrations can inhibit biofilm formation from several Gram-positive and negative bacteria (C. Wu et al., 2013). The antibacterial activity of Zn^{2+} against *Streptococcus mutans* and *Actinomyces viscosus* was found to be a result of Zn^{2+} migration (Boyd et al., 2006). The antibacterial activity of Zn^{2+} depends on its

concentration and contact duration. Two distinct mechanisms of actions have been proposed to explain the antimicrobial activities of Zn^{2+} leading to cell death:

- (i) a direct interaction with microorganism membrane proteins leading to membrane destabilization and enhanced permeability and finally destruction of their capability to transport through the plasma membrane;
- (ii) an interaction with nucleic acids and deactivation of enzymes of the respiratory system and electron transport system (Fang et al., 2006; Stanić et al., 2010).

It is reported that Gram-positive bacteria were the most susceptible bacterial group to Zn^{2+} but Gram-negative aerobic bacteria were usually not inhibited even at high concentrations (1024 μ l/ml) (Söderberg et al., 1990). However, Alhalawani *et al.* found that, in a glass series containing both Ga and Zn, the antibacterial activity was improved by the release of Zn^{2+} ions and not by Ga^{3+} ions (Alhalawani et al., 2014). It was found that the glass with lower Ga^{3+} content showed enhanced antibacterial properties against *E. coli*. Thus, in the work reported here, release of Zn^{2+} ions may be the reason for significant antibacterial activity of the composites against both Gram-positive and Gram-negative bacteria.

The release of both Ga^{3+} and Zn^{2+} ions at a controlled rate could offer significantly enhanced biological performance of materials for bone tissue regeneration. It has been reported that Ga^{3+} and Zn^{2+} in specific concentrations show therapeutic effects on the growth and proliferation of osteoblastic cells (Balamurugan et al., 2007; Elise Verron et al., 2010). Therefore, these ions can be doped into bioactive glasses with the aim of promoting bone forming ability as well as achieving anti-bacterial and anti-inflammatory properties. The findings in the present study indicate that adding bioactive glass into the

matrix improved the bacteriostatic properties of composites and the intensity of those effects corresponds with glass content in the composite. Thus, composites with bioactive glass containing therapeutic ions could not only improve antibacterial properties but also are expected to improve cell adhesion and proliferation. However, there is theoretically a threshold of glass content at which most of the desirable properties can be satisfactorily achieved. Our findings present a new approach in the production of tissue engineering scaffolds which would eventually enable a minimal risk of infection and reduce the need for revision surgery.

4.14 Osteoblast-scaffold interaction

4.14.1 Cell morphology and viability

FESEM was used to observe the cell morphology on the 3-D scaffolds seeded for 7 days. The results (Figure 4.16) show the cells are well-attached and spread throughout the surface and the walls of pores of both POC (control; Figure 4.16-A) and composite (Figures 4.16-B and C) scaffolds. It was observed that the cells well adhered on the surface of composites and preserved the characteristic morphology (insert) (Srinivasan et al., 2012). In addition, the penetration of cells into the pores expresses the suitable pore size for entrance of osteoblastic cells (Mozafari et al., 2010).

Cytotoxicity of the composite scaffolds were assessed using MTT assay (Figure 4.16-D). MTT assay measures the reduction of the tetrazolium component (MTT) into an insoluble formazan product by the mitochondria of viable cells. The results indicated that there are no significant differences between all the samples at day 1. Following 7 days of cell culture, the percentage of cells viability on POC-BG-10% remained almost constant, however decreased for the composites loaded with 20 % and 30 % bioglass. The cell

viability of composites was significantly decreased from day 14 to 28 as compared to pure POC. Furthermore, when compared the composite scaffolds, POC-BG-10% had a significantly higher cell viability for all the culture times studied. This results suggest that there is no significant difference between cell viability on POC and POC-BG-10% up to 7 days of culture. However, composite scaffolds with 20 % and 30 % bioactive glass were shown to have very low cytotoxicity.

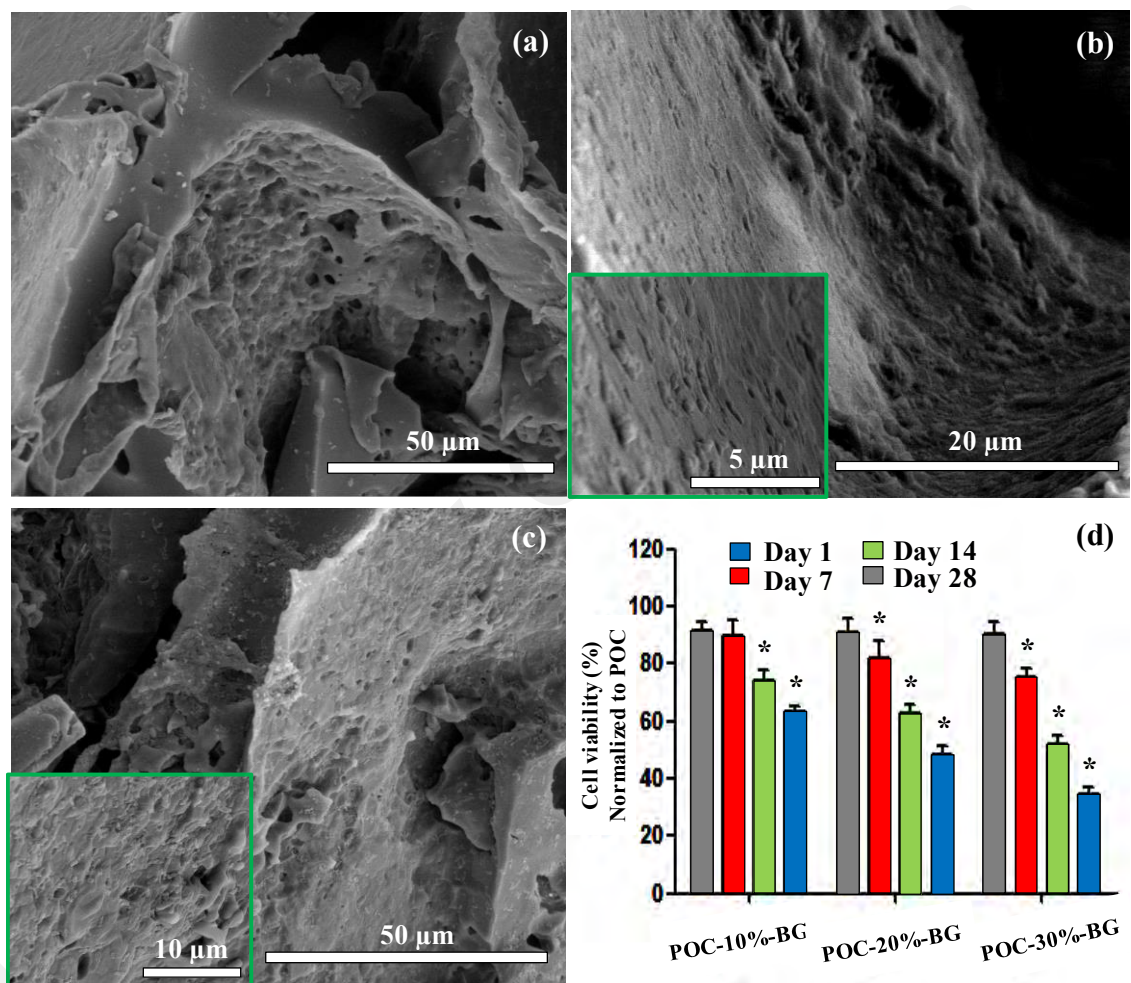


Figure 4.16: FESEM images of cell attachment of human osteoblast cells after 7 days in culture: (a) POC control; (b) POC-BG-10%; (c) POC-BG-20%; and (d) cell proliferation examined by MTT assay after 1, 7, 14 and 28 days culture; normalized to pure POC; (*P < 0.05) significantly different in comparison to respective pure POC.

4.14.2 Real-time PCR

The assessment of collagen synthesis is influential as collagen is a marker of matrix formation and about 95 % of bone matrix is composed of collagen (Alvarez & Nakajima, 2009). In addition, the major part of extracellular matrix (ECM) proteins of bone is composed of collagen which is known to be secreted in the early stage of *in vitro* cell culturing (Kim et al., 2008). Gene expression of bone marker-type I and III collagen in human osteoblast cells was assessed by real-time PCR at day 7 (Figure 4.17). The comparison of osteoblast types I and III collagen expression for prepared scaffolds are illustrated in Figure 4.16-D. Cells cultured on POC-BG-10% had remarkably higher expression of type I and III collagens in comparison to other composite scaffolds.

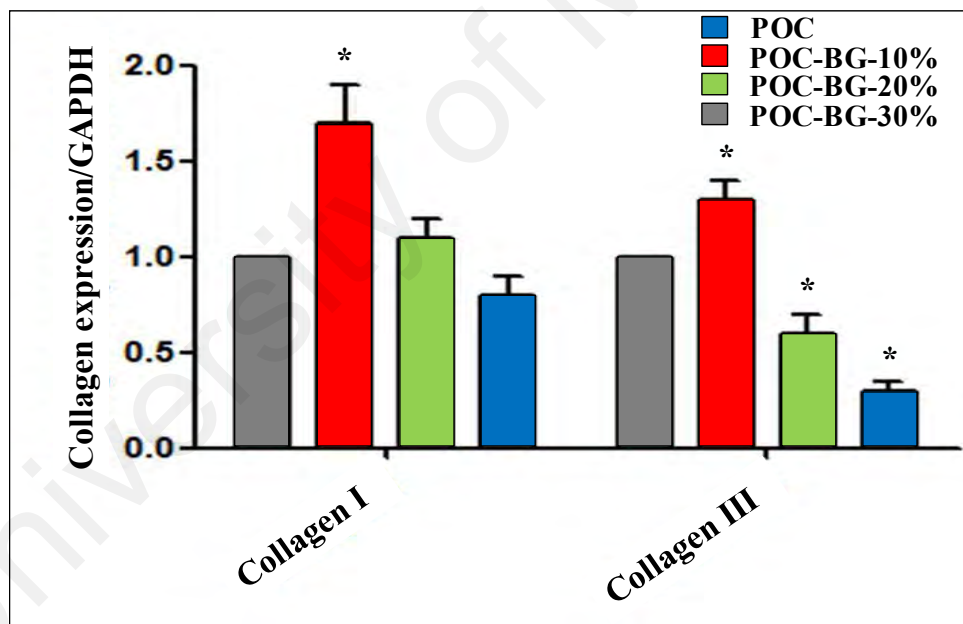


Figure 4.17: gene expression of collagen I and collagen III on composite scaffolds in comparison to POC scaffold used as control after 7 days in culture; (* $P < 0.05$) significantly different in comparison to respective pure POC.

4.14.2 Indirect Immunostaining

In order to evaluate an extracellular matrix proteins expression from human osteoblast, fluorescent immunostaining technique was performed to visualize type I and III collagens. The expression of type I and III collagen protein was indicated by green fluorescence (Figure 4.18). Immunostaining with mouse antibody against type I and III collagens showed a dot-like and fibrillary patterns for the composites respectively. Although type I and III collagens were positively expressed for all the scaffolds at day 7, the staining had significantly greater intensity and distribution for POC-BG-10% composite for both type I and III collagens. This may be as a result of dissolution products of bioglass which up-regulate the gene expression and increase the collagen production. Similar observation was made by Kim *et al.* (Kim et al., 2008) and Lu *et al.* (Lu et al., 2003). The authors have investigated the effect of bioglass on collagen production and observed that addition of 25 % of 45S5 bioglass to polymer led to promotion of collagen synthesis in respect to pure polymer matrix and polystyrene control. In our case, the increased protein synthesis may also be due to high release of Ga^{3+} as observed in release studies (Figures 4.8 and 4.9).

The effect of Ga on the secretion of proteins is well established in the literature (Jenis et al., 1993). For example, osteoblast cells treated with Ga nitrate also revealed increasing type I collagen synthesis (R. S. Bockman et al., 1993). In spite of Ga efficiency on protein synthesis the POC-BG-20% and POC-BG-30% composites illustrated the lower amount of protein as compared to pure POC which prove the dose-dependent manner of Ga containing materials. It was found that using noncytotoxic doses of Ga can effectively lead to proline incorporation which subsequently converts to hydroxy-proline and increasing collagen production (R. S. Bockman et al., 1993). It is believed that bioglasses doped with ions such as Ga^{3+} and Zn^{2+} offer antibacterial, anti-inflammatory, anti-tumor

and immunosuppressive properties (Ito et al., 2002; Mourino et al., 2010; E Verron et al., 2012). In addition, gallium increases the Lewis acidic strength of bioglass, make them suitable for interaction with biomolecules such as proteins and drugs (Aina et al., 2011). However, it has been reported that zinc ions do not have stimulatory effect on collagen synthesis. When bone marrow stromal cells were cultured in osteogenic medium containing basal or supplemented Zn^{2+} for up to 3 weeks, collagen expression was similar for all the samples (Popp et al., 2007).

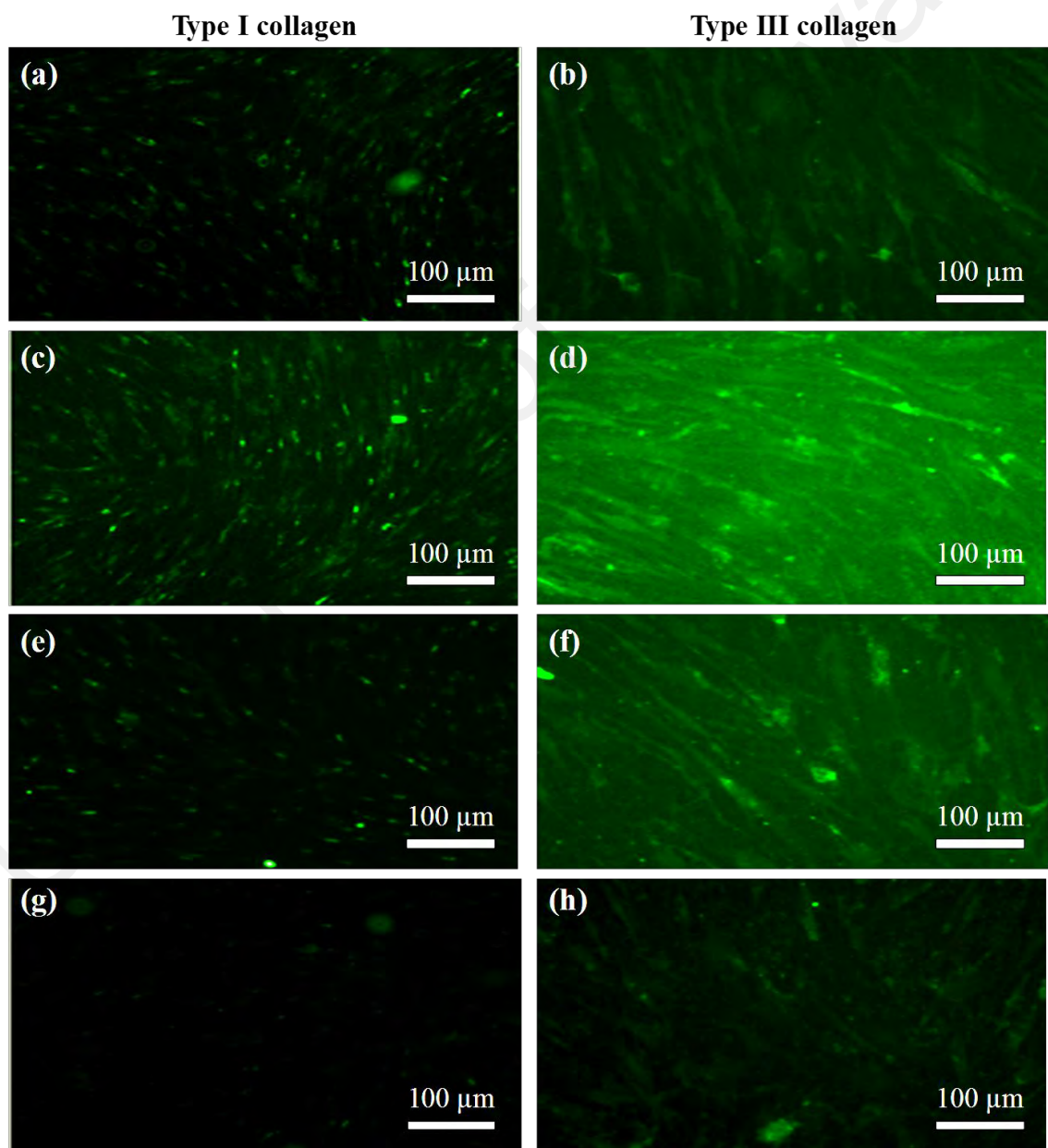


Figure 4.18: Fluorescent images of indirect immunostaining of collagen synthesis type I collagen and type III collagen on composite scaffolds after 7 days in culture: (a, b) pure POC; (c, d) POC-BG-10%; (e, f) POC-BG-20%; and (g, h) POC-BG-30%.

4.15 Stem cell-scaffold interaction

4.15.1 hBMSCs adhesion and proliferation

FESEM micrographs were used to study the cell attachment, morphology and spreading of hBMSCs on the prepared scaffolds (Figure 4.19). After 14 days, the cells were shown to be viable in the presence of both the composite materials and POC alone. The cells were well-attached to the materials with different morphological characteristics. The cells had flattened bodies on the pure POC yet kept their spherical morphology on the composite scaffolds, indicating both differentiated and undifferentiated states. The cells attached showed rounder morphology with an increase in bioactive glass concentration. Although the cells were well-attached to all the scaffolds, fewer cells were visually observed on the composites loaded with 20 % and 30 % bioactive glass, in comparison to POC-BG-10% and pure POC scaffolds.

Fluorescence microscopy was further used to study the attachment and distribution of hBMSCs using the nucleic acid staining dye Hoechst (Figure 4.19). Blue stained cells were observed on all the scaffolds, indicating that the composition of the scaffolds provided a physiologically appropriate environment for cell attachment. However, cell density was higher in the composite scaffold loaded with 10 % bioactive glass than the others.

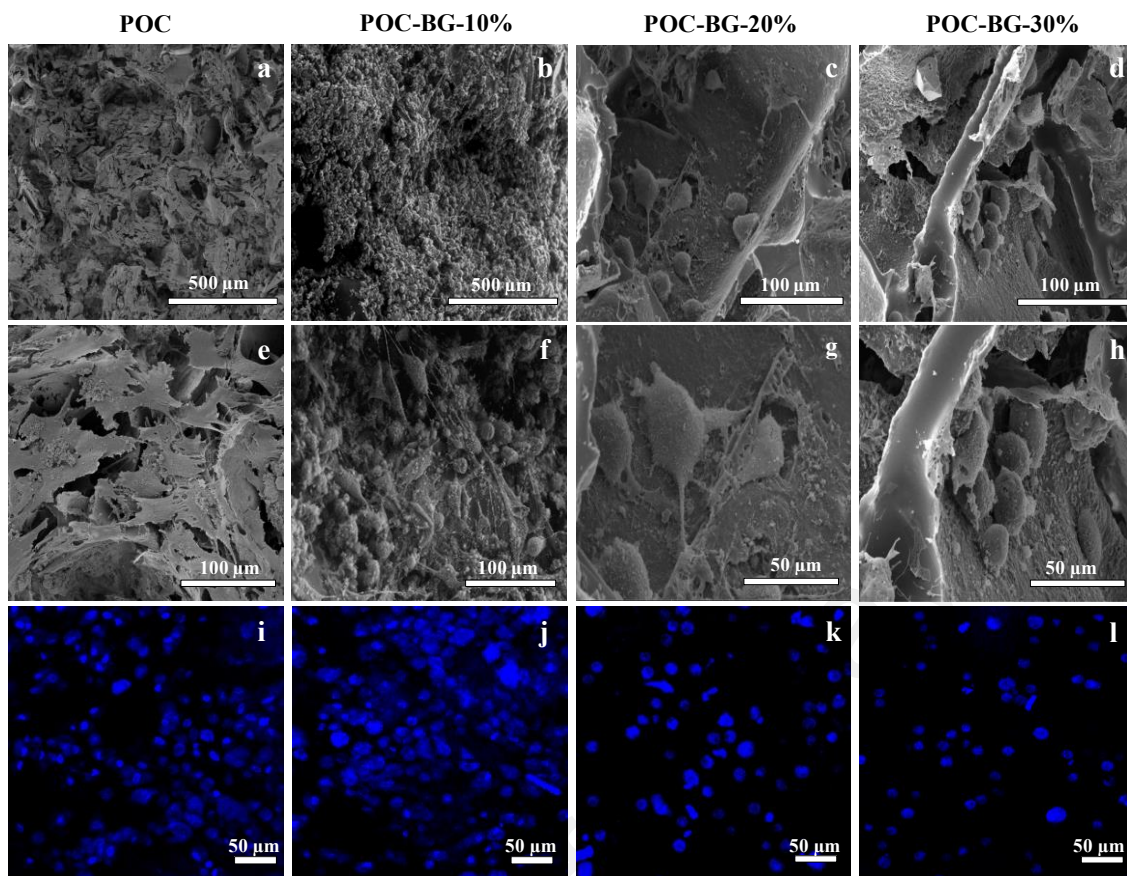


Figure 4.19: FESEM micrographs of hBMSCs for 2 weeks on (a, e) pure POC; (b, f) POC-BG-10%; (c, g) POC-BG-20%; (d, h) POC-BG-30% scaffolds at various magnifications. (i, j, k, l) Fluorescence microscopy of the cells attached to the scaffolds on day 14 – Hoechst's staining.

4.15.2 Cell proliferation

The quantitative *in vitro* growth of hBMSCs was assessed through the AlamarBlue[®] assay, as shown in Figure 4.20. No statistical difference was observed in the proliferation of hBMSCs on the composite scaffolds and the pure POC scaffold after 1 and 3 days of cell culture. Following 7 days of cell culture, the relative proliferation is found to be statistically greater on the POC samples compared to the composites loaded with 20 and 30% bioactive glass. At each time point, no significant differences were observed in cell proliferation between POC and POC-BG-10%. The highest level of cell proliferation in this experiment was measured on the POC scaffold.

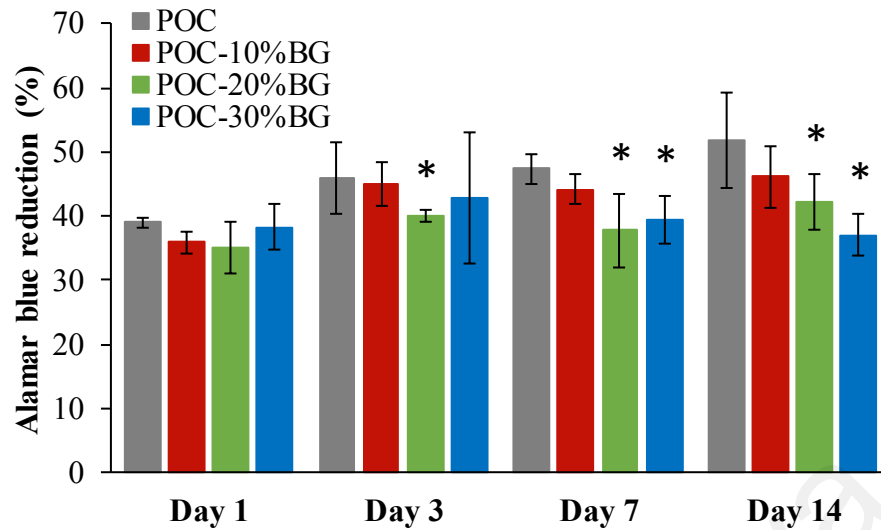


Figure 4.20: Proliferation of hBMSC on POC, POC-BG-10%, POC-BG-20% and POC-BG-30% scaffolds evaluated by AlamarBlue® assay on days 1, 3, 7, and 14; (* $P < 0.05$) significantly different in comparison to respective pure POC.

4.15.3 ALP activity

The ALP activity (Figure 4.21) was significantly higher on the composite scaffolds when compared to the pure POC scaffold on days 3 and 7. This is due to the presence of bioactive glass, which stimulates osteogenic differentiation. The ALP activity peaked at day 7 and decreased thereafter. However, no significant difference was observed between the composites with 10, 20, or 30% bioactive glass on day 14. The ALP activity was the highest on the POC-BG-10% in all time points. The ALP activity on the pure POC scaffold remained almost constant over culture time.

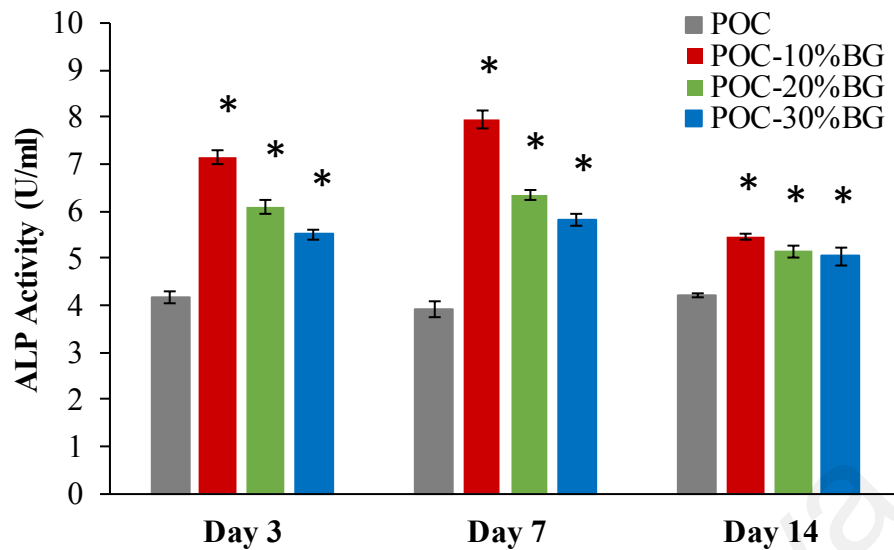


Figure 4.21: ALP activity of the hBMSC on the scaffolds was measured with the pNPP assay at 3, 7, and 14 days of culture; (* $P < 0.05$) significantly different in comparison to respective pure POC.

4.15.4 Quantitative RT-PCR

The differentiation of hBMSCs toward the osteogenic phenotype was further analyzed by RT-PCR. The analysis indicates the expression profiles of a series of specific genes that are usually associated with mineralization during osteogenesis; namely, RUNX2, COL I, BMP2, SPARC, and BGLAP over a 14-day culture period (Figure 4.22). The mRNA levels of all the selected genes increased for up to 14 days. For all markers and time points, the POC-BG-10% scaffold yielded higher gene expressions than other scaffolds. However, pure POC expressed a significantly higher level of BGLAP (the late osteogenic marker) in comparison to the composites loaded with 20 and 30 % bioactive glass at the two time points tested.

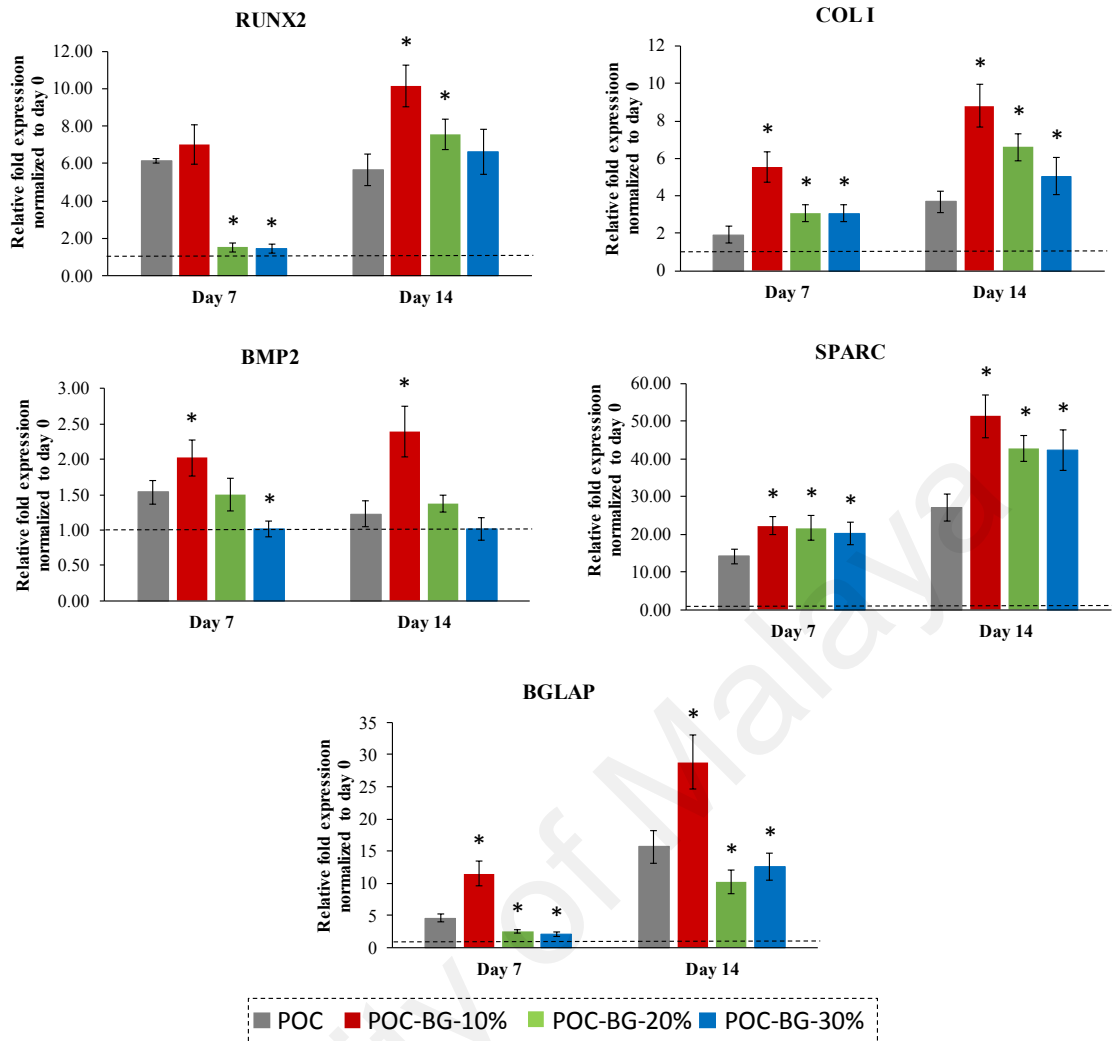


Figure 4.22: RT-PCR results showing transcript levels associated to osteoblastic marker expression of RUNX2, COL I, BMP2, SPARC, and BGLAP at 7 and 14 days after hBMSCs growth on the scaffolds. Data have been normalized to the gene expression levels on day 0; (*P< 0.05) significantly different in comparison to respective pure POC.

4.15.5 Calcium content

Cellular mineralization of scaffolds was determined by measuring the Ca content produced by the cells during 14 days culture, as shown in Figure 4.23. The results indicate that Ca has been increasing during the culture period. Ca concentration was higher in composites compared to the pure polymer. However, no significant difference was observed between the three composite scaffolds at up to day 7. Furthermore, when

compared to composite scaffolds, the POC-BG-10% had a significantly higher Ca deposition in the cell construct at day 14.

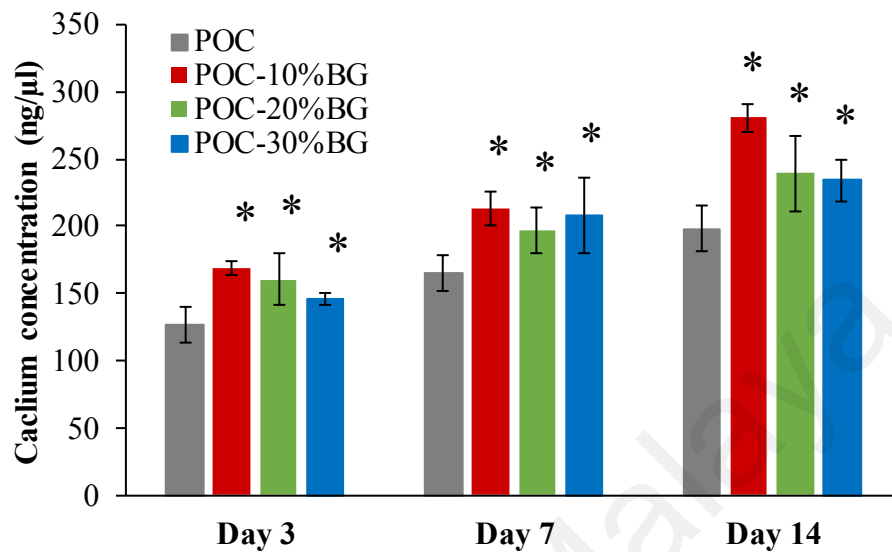


Figure 4.23: Calcium content measurements of hBMSC on the scaffolds during culture for 14 days; (* $P < 0.05$) significantly different in comparison to respective pure POC.

4.15 Discussion

It has been found that the delivery of stem cells on a polymer scaffold to treat large bony defects results in improved bone formation and enhanced mechanical properties compared to treatment with the scaffold alone (Dupont et al., 2010). However, transplanted cells often fail to promote the repair of the host tissue, not due to rejection, but rather due to poor scaffold selection leading to unfavourable delivery of viable cells. Our study sought to address this issue by fabrication of composite scaffolds made of POC and a therapeutic ion-releasing bioactive glass and evaluating their ability to support hBMSC attachment, proliferation, and differentiation. The results suggest that scaffold composition can play an essential role in the growth and osteogenic differentiation of hBMSCs. The scaffolds were shown to be flexible, suggesting their possible applicability as bone graft, while allowing a great deal of customization in the hands of the surgeon (Zaidman & Bosnakovski, 2012). Adhesion and morphology of hBMSCs on the materials

were observed by FESEM. The evaluation showed that the hBMSCs were well-attached to the composite scaffolds and maintained a rounded morphology. The morphology of cells attached to the scaffolds was dependent on the bioactive glass concentration, and the cell shape became more round with an increase in the bioactive glass content, while on the pure polymer cells assumed a more flattened form. This is in agreement with previous studies which demonstrated that cells keep their round morphology in the presence of bioactive glasses (Gomide et al., 2012; Salih et al., 2007). The results presented in this study indicate the excellent biocompatibility of the scaffolds. It was found that there is no significant difference between cell proliferation on POC and POC-BG-10% after 14 days of culture. However, composite scaffolds with 20 % and 30 % bioactive glass were shown to have very low cytotoxicity. The improved cytocompatibility of the composite scaffold loaded with 10% bioactive glass compared with higher percentages may be attributed to the smaller concentration of ionic dissolution products (Zn^{2+} and Ga^{3+}) released from the bioactive glass phase. It is most likely that the ions released from the bioactive glass phase during leaching and soaking of culture scaffolds had reabsorbed into the composites, leading to modification of scaffold surface properties. The results of the ion release showed that Zn^{2+} and Ga^{3+} were released and reabsorbed into the material itself and its surrounding after soaking in PBS, which confirms the above statement. Salih *et al.* also found that doping of ZnO to phosphate glasses (P_2O_5 -CaO- Na_2O) can increase attachment and proliferation of human osteoblastic cells as compared to Zn-free glass even though the cells did not spread and maintained their round morphology (Salih et al., 2007). Accordingly, they have suggested that the addition of a certain amount of Zn does not have a detrimental effect on osteoblast response, and that cells can still attach, which further creates a necessity for surface modification to allow cell spreading (Salih et al., 2007). In the current study, the round-shaped morphology of cells on the composite

scaffolds may be attributed to the differentiation of hBMSCs towards osteoblast-like cells.

The cellular differentiation into osteoblasts was highly affected by the amount of bioactive glass. ALP is considered as a marker of early osteoblastic differentiation and commitment of MSCs toward an osteogenic lineage (Ramalingam et al., 2012). ALP activity was highly influenced by the bioactive glass addition so that the entire composites showed a significantly higher ALP activity compared to pure POC. ALP activity was the highest for the POC scaffold incorporating 10% bioactive glass and after 2 weeks of culture. Since ALP can be expressed by other differentiated cells, it is essential to study other key markers of osteogenic differentiation. Accordingly, we have quantitatively evaluated the relative mRNA expression levels of the early osteogenic markers RUNX2, BMP2, COL I, and SPARC, and the osteogenic late stage marker BGLAP. RUNX2 is considered as a master gene involved in the osteoblast phenotype induction. It is a key regulator of osteogenesis and promotes an upregulation of ALP, BGLAP, osteopontin and bone sialoprotein (Teplyuk et al., 2008). COL I is the major protein of bone matrix and is essential for acceleration of osteogenic differentiation, matrix maturation and mineralization (Zhen-Ming et al., 2009). SPARC is a glycoprotein in the bone that binds to both calcium and collagen. It is secreted by osteoblasts during bone formation, thus initiating mineralization and promoting mineral crystal formation (Yan & Sage, 1999). BMP is a naturally occurring protein found in human bone and plays an essential role in angiogenesis and vascularisation of the periosteum (Zreiqat et al., 2015). BGLAP is one of the osteoblast specific genes and is a noncollagen matrix protein which is closely related to calcification of ECM (Raghavendran et al., 2016). The results presented in this study demonstrate that the hBMSC grown on the scaffolds expressed RUNX2, COL I, SPARC, BMP2, and BGLAP in the absence of osteogenic media (Figure 4.21). Our findings indicate that POC-BG-10% significantly up-regulated both early and late stages

of osteogenic differentiation of hBMSCs. The composite scaffolds also showed elevated mineralization as compared to the pure POC scaffold. Cell mineralization is a crucial indicator of osteogenesis *in vitro*. This result confirms that the inclusion of bioactive glass into the POC can stimulate cellular mineralization (Figure 4.22).

Observations of cell morphology, ALP activity, and gene expression suggest that osteoblastic differentiation may have occurred within the first two weeks of culture on the composite scaffolds. Furthermore, this response of hBMSCs on composite scaffolds was independent of stimulation with osteogenic media, indicating that the scaffolds alone can promote the osteogenic response. We found that hBMSCs grown on the composite scaffolds exhibited superior osteogenic potential (particularly, POC-BG-10%) than those found on the pure polymer scaffold. However, this raises the question as to why incorporation of 10% bioactive glass into the POC might improve the biological response more effectively than higher percentages.

Previous studies have demonstrated that ionic dissolution products released from bioactive glasses can stimulate angiogenesis and osteogenesis (Hench, 2009; I. D. Xynos et al., 2000). Silicate-based bioactive glasses have been shown to have the ability to support proliferation and differentiation of osteoblastic cells and MSCs either *in vitro* or *in vivo* (Brown et al., 2008; X. Liu et al., 2013). It has been reported that the formation of a calcium phosphate layer on the surface of bioactive glasses can stimulate the adjacent tissues to form new bone in the absence of any osteogenic supplements (Tsigkou et al., 2007). Ionic dissolution products released from glasses, particularly Si, play a crucial role in stimulating the proliferation of osteoblast-like cells, up-regulating the expression of a number of osteoblastic genes, and promoting the bone growth. Valerio *et al.* demonstrated that the higher osteoblasts proliferation and collagen synthesis after being treated by bioactive glass dissolution products are related to Si contact but not Ca, because no enhanced osteoblast activity was observed in the absence of Si release (Valerio et al.,

2004). Based on the results discussed above, we believe that the effect of therapeutic ions (i.e. Zn^{2+} and Ga^{3+}) on the hBMSCs function can be considered more dominant than Si since the POC-BG-30% showed a higher SiO_3^{2-} release but poorer biological response as compared to POC-BG-10%. Furthermore, we found that the concentration of Ga^{3+} and Zn^{2+} in physiological solution increased by enhancing the bioactive glass amount. Therefore, it could be inferred that the presence of high concentration of mentioned ions may exert very low cytotoxicity. Even so, the stimulated osteogenic differentiation of hBMSCs observed in the present study is possibly the result of the combined effects of all the ions.

In order to improve the bioactivity of bioactive glasses towards a specific biological response, various therapeutic metal ions have been incorporated into the glass structure. A few recent studies have investigated the effect of Zn within the bioactive glass composition on the osteogenic differentiation of stem cells (Oh et al., 2010; Oh et al., 2011; Salih et al., 2007). Zinc addition to bioactive glasses has contradictory effects on cell responses, with some studies mentioning the stimulatory effect of Zn on bone formation at up to 5 mol%, and others reporting the optimal amount of Zn being less than 1 mol% (Balamurugan et al., 2007; Haimi et al., 2009). This effect can be more highlighted by the glass formulation as it effects on dissolution properties. Zinc is one of the most important nutritional trace elements in the human body and plays a vital role in activation of bone cells. The beneficial effect of Zn is greatly reliant on the dose and duration of treatment (Mocchegiani et al., 2001). Not only Zn compounds indicate a stimulatory effect on the proliferation of mouse marrow cells but they also showed an inhibitory effect on osteoclast-like cell formation (Kishi & Yamaguchi, 1994). Oh *et al.* reported that Zn-containing bioactive glasses stimulated the osteogenic differentiation of MSCs as determined by ALP and BSP at levels equal to or even greater than Zn-free glass (Oh et al., 2010). However, Haimi *et al.* reported that substitution of CaO with ZnO in a

bioactive glass resulted in the suppression of osteogenic fate in the commitment of human adipose stem cell in respect to the Zn-free glass and it was attributed to the reduction in the degradation profile after Zn addition (Haimi et al., 2009). In another study, Wang *et al.* investigated the effect of Zn ions on the osteogenic and adipogenic differentiation of mouse primary bone marrow stromal cells and the adipogenic trans-differentiation of mouse primary osteoblasts (T. Wang et al., 2007). They found that Zn ions may have an inhibitory effect on osteogenic and adipogenic differentiation of the cells. According to their findings, inhibition of adipogenic may lead to an indirect protective influence of Zn ions on bone by modulating osteoblast formation and inhibiting osteoclast formation.

Very few studies have been conducted to assess the interaction between Ga-containing bioactive glasses and cells (Deliormanlı, 2016; Pourshahrestani et al., 2016). Ga has a beneficial influence on the secretion and synthesis of type I collagen while it decreases osteocalcin gene expression without affecting the viability of osteoblasts (Elise Verron et al., 2010). Furthermore, *in vivo* implantation of Ga doped apatitic calcium phosphate cement into a rabbit bone critical defect exhibited an excellent implant-bone tissue interface without any adverse effects (Mellier et al., 2015). The biological function of gallium *in vivo* and its low toxicity effects on osteoblasts and osteoclasts led to it being approved by the FDA (Chitambar, 2010). However it is dose-dependent and only up to 14 ppm does not induce apoptosis (Bernstein, 1998; Franchini et al., 2012). The results of the current study also confirm that the presence of the mentioned elements in the bioactive glass phase in a very low concentration can promote the osteogenic potential of hBMSCs.

This study indicated that, of the studied scaffolds, composite scaffolds supported proliferation of hBMSCs less well than pure POC, although hBMSCs showed a stronger differentiation capacity when cultured on composite scaffolds. Scaffolds for self-

regenerative applications are expected to provide a framework for tissue repair and at the same time act as carriers for antimicrobial agents. The scaffold should be designed to promote cell adhesion, proliferation, and differentiation for target tissues whilst also inhibiting bacterial adhesion and biofilm formation. The results of the present study, suggest that POC/bioglass composites not only support hBMSC growth and differentiation but can also impart antibacterial activity with a controlled release of antibacterial ions, which adds another advantage required for an ideal bone tissue construct.

University of Malaya

CHAPTER 5: CONCLUSION AND FUTURE DIRECTIONS

5.1 Introduction

This chapter presents firstly, a summary of the key findings of the research, followed by some suggestions for future research in this area.

5.2 Summary and conclusions

In the present study, microcomposite scaffolds of POC and a therapeutic ion-releasing bioglass were successfully fabricated using a salt-leaching method. The scaffolds have a highly porous structure with a porosity of greater than 80 % and pore size in the range of 200-300 μm which is found to be optimum for bone tissue ingrowth. The contact angle decreased with increased bioglass content indicating the enhanced hydrophilicity of composite scaffolds. It was observed that increased physical crosslinks, as a result of metallic carboxylate formation in composite scaffolds, had a significant influence on compression moduli, storage moduli and glass transition temperatures. The values of measured composite properties increased proportionally with added bioglass content (ranging from 10 % to 30 %). The effect of bioglass on weight loss was a result of lower dissolution rate of bioglass and neutralized pH. Ion release into both PBS and SBF revealed that Ga^{3+} release was similar in both solutions while Zn^{2+} release was slightly higher in SBF after 28 days of incubation. It was found that apatite formation was significantly inhibited due to the release of these ions from composite scaffolds. In a bovine bone model, it was found that Zn^{2+} was released and penetrated into the bones by as far as 4500 μm from the scaffold-bone interface. However, the presence of Zn^{2+} on the bone surface did not affect Ca/P ratio at the measured points. The resulting composite

scaffolds were found to be highly effective against both Gram-positive *S. aureus* and Gram-negative *E. coli* bacteria. The antibacterial activity of composites increased with glass concentration. It was found that the bacteria were significantly inhibited by the release of Zn^{2+} and Ga^{3+} ions.

The assessment of hFOB response to the scaffolds revealed that incorporation of bioglass up to 10 % into polymer matrix lead to enhanced osteoblast cell attachment and collagen secretion which suggest that there is threshold of bioglass content for optimal cellular response. This *in vitro* study also indicated the response of hBMSCs to the composite scaffolds. The cells adhered to, proliferated and differentiated on the scaffolds, even though the morphology, growth and osteogenic differentiation of the hBMSCs was dependent upon the bioactive glass amount. The cells were flatter on the pure POC while they were in a round shape on the composite scaffolds after 14 days of culture. It was found that pure POC had the highest hBMSC proliferation rate, but the weakest effect will be on osteogenic differentiation. The ionic dissolution products released from composite scaffolds were found to contribute to the solution-mediated effect on osteogenesis of hBMSC. Low levels of bioactive glass content remarkably enhanced the osteogenesis of hBMSCs. The addition of 10% bioactive glass to the POC was proved to significantly promote ALP activity, and the mRNA expression of early and late osteogenic markers such as RUNX2, BMP2, COL I, SPARC, and BGLAP, as well as cellular mineralization, suggesting that there is a threshold of bioactive glass content for optimal cellular response. The results further demonstrate that composite scaffolds can be used as a potential bone regenerative biomaterial for stem cell based therapies.

5.3 Direction for future research

Our study proposed promising therapeutic bioactive composite scaffolds for hard tissue engineering with improved antibacterial activity and enhanced osteogenesis. However, we provide suggestions for future research that might address other concerns. Addition of bioactive glasses can improve most elastomer properties but there is a threshold limit for bioactive glass incorporation beyond which composite properties such as strength and cellular response become compromised. Apart from content, other parameters such as glass size, shape and composition can influence the final properties of composites. Smaller glass particles are more effective in improving both mechanical stability and bioactivity. Nonetheless, the strength of pure elastomers and their composites are orders of magnitude weaker than natural human bone meaning that, currently, such materials only have applicability as bone filling agents with external support.

A future focus should be on the fabrication of composite scaffolds with enhanced mechanical stability which can withstand cyclic mechanical loading. Moreover, there is a growing need for more research on the antibacterial properties of composites that would prevent infections upon surgery. A promising solution could be doping of the proper concentration of antibacterial ions to the glass such that cell adhesion and growth could be improved simultaneously. A better understanding of how specific scaffold properties affect cell behavior will also allow optimization of scaffold based tissue engineering constructs toward bone regeneration. A continuation in stem cell research with composite biomaterials is necessary due the unique properties of stem cells such as self-renewal, differentiation into other specialized cell types, and each new cell type attaining a specialized function (Bongso et al., 2008). Indeed, the stimulatory role of the biological apatite layer formed on the surface of bioactive glasses on osteoblastic differentiation of

stem cells without addition of osteogenic induction factor makes bioactive glasses promising candidate for bone tissue engineering. On the other hand, the elasticity of materials is a crucial parameter in cellular responses both *in vitro* and *in vivo* (Engler et al., 2006; Rohman et al., 2007). The high elasticity of elastomers provides a large capacity for filler loading and so the addition of bioactive glasses to the elastomers offers a unique opportunity to tune the elasticity and control the differentiation of stem cells by the presence of bioglass materials within the polymer matrix. In addition, more research needs to evaluate the biological response of elastomeric composites under dynamic conditions. Using bioreactors offers an incremental improvement over traditional static culture techniques since they can satisfy the external requirement for medium flow and usually mimic *in vivo* cellular microenvironments. There is only limited knowledge on *in vivo* cell–elastomer interaction. Elastomeric composites may show completely different behavior *in vivo*. Associated cytotoxicity with polymeric degradation products and release of high concentrations of some trace elements from bioactive glasses detected in the confined culture wells may have been modulated *in vivo*. Therefore, *in vivo* investigations should be the focus of future studies to continue the scaffold development.

REFERENCES

- Ahmed, A., Ali, A., Mahmoud, D. A., & El-Fiqi, A. (2011). Preparation and characterization of antibacterial P2O5–CaO–Na2O–Ag2O glasses. *Journal of Biomedical Materials Research Part A*, 98(1), 132-142.
- Ahmed, I., Parsons, A., Palmer, G., Knowles, J., Walker, G., & Rudd, C. (2008). Weight loss, ion release and initial mechanical properties of a binary calcium phosphate glass fibre/PCL composite. *Acta Biomaterialia*, 4(5), 1307-1314.
- Aina, V., Morterra, C., Lusvardi, G., Malavasi, G., Menabue, L., Shruti, S., . . . Bolis, V. (2011). Ga-Modified (Si–Ca–P) Sol–Gel Glasses: Possible Relationships between Surface Chemical Properties and Bioactivity. *The Journal of Physical Chemistry C*, 115(45), 22461-22474.
- Akmaz, I., Kiral, A., Pehlivan, O., Mahirogulları, M., Solakoglu, C., & Rodop, O. (2004). Biodegradable implants in the treatment of scaphoid nonunions. *International orthopaedics*, 28(5), 261-266.
- Alhalawani, A. M., Placek, L., Wren, A. W., Curran, D. J., Boyd, D., & Towler, M. R. (2014). Influence of gallium on the surface properties of zinc based glass polyalkenoate cements. *Materials Chemistry and Physics*, 147(3), 360-364.
- Allo, B. A., Costa, D. O., Dixon, S. J., Mequanint, K., & Rizkalla, A. S. (2012). Bioactive and biodegradable nanocomposites and hybrid biomaterials for bone regeneration. *Journal of Functional Biomaterials*, 3(2), 432-463.
- Alperin, C., Zandstra, P., & Woodhouse, K. (2005). Polyurethane films seeded with embryonic stem cell-derived cardiomyocytes for use in cardiac tissue engineering applications. *Biomaterials*, 26(35), 7377-7386.
- Alvarez, K., & Nakajima, H. (2009). Metallic scaffolds for bone regeneration. *Materials*, 2(3), 790-832.
- Amsden, B. (2007). Curable, biodegradable elastomers: emerging biomaterials for drug delivery and tissue engineering. *Soft Matter*, 3(11), 1335-1348.
- Anselme, K. (2000). Osteoblast adhesion on biomaterials. *Biomaterials*, 21(7), 667-681.

- Asefnejad, A., Khorasani, M. T., Behnamghader, A., Farsadzadeh, B., & Bonakdar, S. (2011). Manufacturing of biodegradable polyurethane scaffolds based on polycaprolactone using a phase separation method: physical properties and in vitro assay. *International journal of nanomedicine*, 6, 2375.
- Baino, F., Verné, E., & Vitale-Brovarone, C. (2009). Feasibility, tailoring and properties of polyurethane/bioactive glass composite scaffolds for tissue engineering. *Journal of Materials Science: Materials in Medicine*, 20(11), 2189-2195.
- Baino, F., & Vitale-Brovarone, C. (2011). Three-dimensional glass-derived scaffolds for bone tissue engineering: Current trends and forecasts for the future. *Journal of Biomedical Materials Research Part A*, 97(4), 514-535.
- Balamurugan, A., Balossier, G., Kannan, S., Michel, J., Rebelo, A. H., & Ferreira, J. M. (2007). Development and in vitro characterization of sol-gel derived CaO-P2O5-SiO2-ZnO bioglass. *Acta Biomaterialia*, 3(2), 255-262.
- Barrett, D. G., & Yousaf, M. N. (2009). Design and applications of biodegradable polyester tissue scaffolds based on endogenous monomers found in human metabolism. *Molecules*, 14(10), 4022-4050.
- Bayer, O., Rinke, H., Siefken, W., Ortner, L., & Schild, H. (1937). A process for the production of polyurethanes and polyureas [Verfahren zur Herstellung von Polyurethanen bzw]. *Polyharnstoffen. German Patent*, 728.
- Belt, H. v. d., Neut, D., Schenk, W., Horn, J. R. v., Mei, H. C. v. d., & Busscher, H. J. (2001). Infection of orthopedic implants and the use of antibiotic-loaded bone cements: a review. *Acta Orthopaedica Scandinavica*, 72(6), 557-571.
- Bernstein, L. R. (1998). Mechanisms of therapeutic activity for gallium. *Pharmacological reviews*, 50(4), 665-682.
- Bettinger, C. J. (2011). Biodegradable elastomers for tissue engineering and cell-biomaterial interactions. *Macromolecular Bioscience*, 11(4), 467-482.
- Bianco, P., Riminucci, M., Gronthos, S., & Robey, P. G. (2001). Bone marrow stromal stem cells: nature, biology, and potential applications. *Stem Cells*, 19(3), 180-192.
- Bigi, A., Cojazzi, G., Panzavolta, S., Rubini, K., & Roveri, N. (2001). Mechanical and thermal properties of gelatin films at different degrees of glutaraldehyde crosslinking. *Biomaterials*, 22(8), 763-768.

- Bil, M., Ryszkowska, J., Roether, J., Bretcanu, O., & Boccaccini, A. (2007). Bioactivity of polyurethane-based scaffolds coated with Bioglass®. *Biomedical Materials*, 2(2), 93.
- Blaker, J. J., Maquet, V., Jérôme, R., Boccaccini, A. R., & Nazhat, S. (2005). Mechanical properties of highly porous PDLLA/Bioglass® composite foams as scaffolds for bone tissue engineering. *Acta Biomaterialia*, 1(6), 643-652.
- Blumenthal, N. C., Cosma, V., & Levine, S. (1989). Effect of gallium on their vitro formation, growth, and solubility of hydroxyapatite. *Calcified tissue international*, 45(2), 81-87.
- Boccaccini, A. R., Erol, M., Stark, W. J., Mohn, D., Hong, Z., & Mano, J. F. (2010). Polymer/bioactive glass nanocomposites for biomedical applications: a review. *Composites Science and Technology*, 70(13), 1764-1776.
- Boccaccini, A. R., Notingher, I., Maquet, V., & Jérôme, R. (2003). Bioresorbable and bioactive composite materials based on polylactide foams filled with and coated by Bioglass® particles for tissue engineering applications. *Journal of Materials Science: Materials in Medicine*, 14(5), 443-450.
- Bockman, R., Boskey, A., Blumenthal, N., Alcock, N., & Warrell Jr, R. (1986). Gallium increases bone calcium and crystallite perfection of hydroxyapatite. *Calcified tissue international*, 39(6), 376-381.
- Bockman, R. S., Guidon, P. T., Pan, L. C., Salvatori, R., & Kawaguchi, A. (1993). Gallium nitrate increases type I collagen and fibronectin mRNA and collagen protein levels in bone and fibroblast cells. *Journal of cellular biochemistry*, 52(4), 396-403.
- Bohner, M., & Lemaître, J. (2009). Can bioactivity be tested in vitro with SBF solution? *Biomaterials*, 30(12), 2175-2179.
- Bonfield, W., Grynepas, M., Tully, A., Bowman, J., & Abram, J. (1981). Hydroxyapatite reinforced polyethylene—a mechanically compatible implant material for bone replacement. *Biomaterials*, 2(3), 185-186.
- Bongso, A., Fong, C. Y., & Gauthaman, K. (2008). Taking stem cells to the clinic: major challenges. *Journal of cellular biochemistry*, 105(6), 1352-1360.
- Bose, S., Roy, M., & Bandyopadhyay, A. (2012). Recent advances in bone tissue engineering scaffolds. *Trends in biotechnology*, 30(10), 546-554.

- Boyd, D., Li, H., Tanner, D., Towler, M., & Wall, J. (2006). The antibacterial effects of zinc ion migration from zinc-based glass polyalkenoate cements. *Journal of Materials Science-Materials in Medicine*, 17(6), 489-494.
- Boyd, D., Towler, M., Wren, A., Clarkin, O., & Tanner, D. (2008). TEM analysis of apatite surface layers observed on zinc based glass polyalkenoate cements. *Journal of materials science*, 43(3), 1170-1173.
- Bretcanu, O., Boccaccini, A. R., & Salih, V. (2012). Poly-dl-lactic acid coated Bioglass® scaffolds: toughening effects and osteosarcoma cell proliferation. *Journal of materials science*, 47(15), 5661-5672.
- Brown, R. F., Day, D. E., Day, T. E., Jung, S., Rahaman, M. N., & Fu, Q. (2008). Growth and differentiation of osteoblastic cells on 13–93 bioactive glass fibers and scaffolds. *Acta Biomaterialia*, 4(2), 387-396.
- Bruellhoff, K., Fiedler, J., Möller, M., Groll, J., & Brenner, R. E. (2010). Surface coating strategies to prevent biofilm formation on implant surfaces. *Int J Artif Organs*, 33(9), 646-653.
- Calhoun, N. R., Smith Jr, J. C., & Becker, K. L. (1974). The role of zinc in bone metabolism. *Clinical orthopaedics and related research*, 103, 212-234.
- Cannillo, V., Chiellini, F., Fabbri, P., & Sola, A. (2010). Production of Bioglass® 45S5–Polycaprolactone composite scaffolds via salt-leaching. *Composite Structures*, 92(8), 1823-1832.
- Cao, Y., Mitchell, G., Messina, A., Price, L., Thompson, E., Penington, A., . . . Cooper-White, J. (2006). The influence of architecture on degradation and tissue ingrowth into three-dimensional poly (lactic-co-glycolic acid) scaffolds in vitro and in vivo. *Biomaterials*, 27(14), 2854-2864.
- Caplan, A. I. (2000). Mesenchymal stem cells and gene therapy. *Clinical orthopaedics and related research*, 379, S67-S70.
- Caridade, S. G., Merino, E. G., Alves, N. M., Bermudez, V. d. Z., Boccaccini, A. R., & Mano, J. F. (2013). Chitosan membranes containing micro or nano-size bioactive glass particles: evolution of biomineralization followed by in situ dynamic mechanical analysis. *Journal of the mechanical behavior of biomedical materials*, 20, 173-183.

- Caridade, S. G., Merino, E. G., Alves, N. M., & Mano, J. F. (2012). Bioactivity and viscoelastic characterization of chitosan/bioglass® composite membranes. *Macromolecular Bioscience*, 12(8), 1106-1113.
- Carlisle, E. M. (1986). *Silicon as an essential trace element in animal nutrition*. Paper presented at the Ciba Foundation Symposium 121-Silicon Biochemistry.
- Cascone, M. G., Polacco, G., Lazzeri, L., & Barbani, N. (1997). Dextran/poly (acrylic acid) mixtures as miscible blends. *Journal of applied polymer science*, 66(11), 2089-2094.
- Catauro, M., Raucci, M., De Gaetano, F., & Marotta, A. (2004). Antibacterial and bioactive silver-containing Na₂O·CaO·2SiO₂ glass prepared by sol-gel method. *Journal of Materials Science: Materials in Medicine*, 15(7), 831-837.
- Chen, Q., & Boccaccini, A. R. (2006). Coupling Mechanical Competence and Bioresorbability in Bioglass®-Derived Tissue Engineering Scaffolds. *Advanced Engineering Materials*, 8(4), 285-289.
- Chen, Q., Jin, L., Cook, W. D., Mohn, D., Lagerqvist, E. L., Elliott, D. A., . . . Pouton, C. W. (2010). Elastomeric nanocomposites as cell delivery vehicles and cardiac support devices. *Soft Matter*, 6(19), 4715-4726.
- Chen, Q., Liang, S., & Thouas, G. A. (2013). Elastomeric biomaterials for tissue engineering. *Progress in Polymer Science*, 38(3), 584-671.
- Chen, Q., Zhu, C., & Thouas, G. (2012). Progress and challenges in biomaterials used for bone tissue engineering: bioactive glasses and elastomeric composites. *Progress in Biomaterials*, 1(1), 1-22.
- Chitambar, C. R. (2010). Medical applications and toxicities of gallium compounds. *International journal of environmental research and public health*, 7(5), 2337-2361.
- Chung, E. J., Kodali, P., Laskin, W., Koh, J. L., & Ameer, G. A. (2011). Long-term in vivo response to citric acid-based nanocomposites for orthopaedic tissue engineering. *Journal of Materials Science: Materials in Medicine*, 22(9), 2131-2138.
- Chung, E. J., Qiu, H., Kodali, P., Yang, S., Sprague, S. M., Hwong, J., . . . Ameer, G. A. (2011). Early tissue response to citric acid-based micro-and nanocomposites. *Journal of Biomedical Materials Research Part A*, 96(1), 29-37.

- Clayton, B. (1979). The Elemental Composition of Human Tissues and Body Fluids. *Journal of clinical pathology*, 32(3), 311-311.
- Collery, P., Keppler, B., Madoulet, C., & Desoize, B. (2002). Gallium in cancer treatment. *Critical reviews in oncology/hematology*, 42(3), 283-296.
- Cordier, P., Tournilhac, F., Soulié-Ziakovic, C., & Leibler, L. (2008). Self-healing and thermoreversible rubber from supramolecular assembly. *Nature*, 451(7181), 977-980.
- Courthéoux, L., Lao, J., Nedelec, J.-M., & Jallot, E. (2008). Controlled bioactivity in zinc-doped sol-gel-derived binary bioactive glasses. *The Journal of Physical Chemistry C*, 112(35), 13663-13667.
- Day, R. M. (2005). Bioactive glass stimulates the secretion of angiogenic growth factors and angiogenesis in vitro. *Tissue Engineering*, 11(5-6), 768-777.
- de Oliveira, A. A. R., de Carvalho, S. M., de Fátima Leite, M., Oréfice, R. L., & de Magalhães Pereira, M. (2012). Development of biodegradable polyurethane and bioactive glass nanoparticles scaffolds for bone tissue engineering applications. *Journal of Biomedical Materials Research Part B: Applied Biomaterials*, 100(5), 1387-1396.
- Deliormanlı, A. M. (2016). Electrospun cerium and gallium-containing silicate based 13-93 bioactive glass fibers for biomedical applications. *Ceramics International*, 42(1), 897-906.
- Detsch, R., Alles, S., Hum, J., Westenberger, P., Sieker, F., Heusinger, D., . . . Boccaccini, A. R. (2014). Osteogenic differentiation of umbilical cord and adipose derived stem cells onto highly porous 45S5 Bioglass®-based scaffolds. *Journal of Biomedical Materials Research Part A*, 103(3), 1029-1037.
- Dey, J., Xu, H., Shen, J., Thevenot, P., Gondi, S. R., Nguyen, K. T., . . . Yang, J. (2008). Development of biodegradable crosslinked urethane-doped polyester elastomers. *Biomaterials*, 29(35), 4637-4649.
- Dhandayuthapani, B., Yoshida, Y., Maekawa, T., & Kumar, D. S. (2011). Polymeric scaffolds in tissue engineering application: a review. *International Journal of Polymer Science*, 2011.
- Dimitriou, R., Jones, E., McGonagle, D., & Giannoudis, P. V. (2011). Bone regeneration: current concepts and future directions. *BMC medicine*, 9(1), 66.

- Djordjevic, I., Choudhury, N. R., Dutta, N. K., & Kumar, S. (2009). Synthesis and characterization of novel citric acid-based polyester elastomers. *Polymer*, *50*(7), 1682-1691.
- Don, T.-M., Chen, C.-C., Lee, C.-K., Cheng, W.-Y., & Cheng, L.-P. (2005). Preparation and antibacterial test of chitosan/PAA/PEGDA bi-layer composite membranes. *Journal of Biomaterials Science, Polymer Edition*, *16*(12), 1503-1519.
- Du, R. L., Chang, J., Ni, S. Y., Zhai, W. Y., & Wang, J. Y. (2006). Characterization and in vitro bioactivity of zinc-containing bioactive glass and glass-ceramics. *Journal of biomaterials applications*, *20*(4), 341-360.
- Du, Y., Ge, J., Shao, Y., Ma, P. X., Chen, X., & Lei, B. (2015). Development of silica grafted poly (1, 8-octanediol-co-citrates) hybrid elastomers with highly tunable mechanical properties and biocompatibility. *Journal of Materials Chemistry B*, *3*(15), 2986-3000.
- Dupont, K. M., Sharma, K., Stevens, H. Y., Boerckel, J. D., García, A. J., & Guldberg, R. E. (2010). Human stem cell delivery for treatment of large segmental bone defects. *Proceedings of the National Academy of Sciences*, *107*(8), 3305-3310.
- El-Kady, A. M., Saad, E. A., El-Hady, B. M. A., & Farag, M. M. (2010). Synthesis of silicate glass/poly (L-lactide) composite scaffolds by freeze-extraction technique: characterization and in vitro bioactivity evaluation. *Ceramics International*, *36*(3), 995-1009.
- Engelberg, I., & Kohn, J. (1991). Physico-mechanical properties of degradable polymers used in medical applications: A comparative study. *Biomaterials*, *12*(3), 292-304.
- Engler, A. J., Sen, S., Sweeney, H. L., & Discher, D. E. (2006). Matrix elasticity directs stem cell lineage specification. *Cell*, *126*(4), 677-689.
- Fabbri, P., Cannillo, V., Sola, A., Dorigato, A., & Chiellini, F. (2010). Highly porous polycaprolactone-45S5 Bioglass® scaffolds for bone tissue engineering. *Composites Science and Technology*, *70*(13), 1869-1878.
- Fang, M., Chen, J.-H., Xu, X.-L., Yang, P.-H., & Hildebrand, H. F. (2006). Antibacterial activities of inorganic agents on six bacteria associated with oral infections by two susceptibility tests. *International Journal of Antimicrobial Agents*, *27*(6), 513-517.

- Fernandes, J. S., Gentile, P., Moorehead, R., Crawford, A., Miller, C., Pires, R. A., . . . Reis, R. L. (2016). The Design and Properties of Novel Substituted Borosilicate Bioactive Glasses and Their Glass-Ceramic Derivatives. *Crystal Growth & Design*.
- Foley, J., & Blackwell, A. (2002). In vivo cariostatic effect of black copper cement on carious dentine. *Caries research*, 37(4), 254-260.
- Franchini, M., Lusvardi, G., Malavasi, G., & Menabue, L. (2012). Gallium-containing phospho-silicate glasses: Synthesis and in vitro bioactivity. *Materials Science and Engineering: C*, 32(6), 1401-1406.
- Fu, Q., Rahaman, M. N., Bal, B. S., Kuroki, K., & Brown, R. F. (2010). In vivo evaluation of 13-93 bioactive glass scaffolds with trabecular and oriented microstructures in a subcutaneous rat implantation model. *Journal of Biomedical Materials Research Part A*, 95(1), 235-244.
- Fu, Q., Saiz, E., Rahaman, M. N., & Tomsia, A. P. (2011). Bioactive glass scaffolds for bone tissue engineering: state of the art and future perspectives. *Materials Science and Engineering: C*, 31(7), 1245-1256.
- Fu, S.-Y., Feng, X.-Q., Lauke, B., & Mai, Y.-W. (2008). Effects of particle size, particle/matrix interface adhesion and particle loading on mechanical properties of particulate-polymer composites. *Composites Part B: Engineering*, 39(6), 933-961.
- Fuierer, T. A., LoRe, M., Puckett, S. A., & Nancollas, G. H. (1994). A mineralization adsorption and mobility study of hydroxyapatite surfaces in the presence of zinc and magnesium ions. *Langmuir*, 10(12), 4721-4725.
- Gan, Z., Yu, D., Zhong, Z., Liang, Q., & Jing, X. (1999). Enzymatic degradation of poly (ϵ -caprolactone)/poly (DL-lactide) blends in phosphate buffer solution. *Polymer*, 40(10), 2859-2862.
- Gerhardt, L.-C., & Boccaccini, A. R. (2010). Bioactive glass and glass-ceramic scaffolds for bone tissue engineering. *Materials*, 3(7), 3867-3910.
- Gerhardt, L.-C., Widdows, K. L., Erol, M. M., Burch, C. W., Sanz-Herrera, J. A., Ochoa, I., . . . Ansari, T. (2011). The pro-angiogenic properties of multi-functional bioactive glass composite scaffolds. *Biomaterials*, 32(17), 4096-4108.

- Goel, A., Kapoor, S., Tilocca, A., Rajagopal, R. R., & Ferreira, J. M. (2013). Structural role of zinc in biodegradation of alkali-free bioactive glasses. *Journal of Materials Chemistry B*, 1(24), 3073-3082.
- Gogolewski, S., & Pennings, A. J. (1983). An artificial skin based on biodegradable mixtures of polylactides and polyurethanes for full-thickness skin wound covering. *Die Makromolekulare Chemie, Rapid Communications*, 4(10), 675-680.
- Gomide, V. S., Zonari, A., Ocarino, N. M., Goes, A. M., Serakides, R., & Pereira, M. M. (2012). In vitro and in vivo osteogenic potential of bioactive glass-PVA hybrid scaffolds colonized by mesenchymal stem cells. *Biomedical Materials*, 7(1), 015004.
- Gorustovich, A. A., Roether, J. A., & Boccaccini, A. R. (2009). Effect of bioactive glasses on angiogenesis: a review of in vitro and in vivo evidences. *Tissue Engineering Part B: Reviews*, 16(2), 199-207.
- Grynopas, M., Pritzker, K., & Hancock, R. (1987). Neutron activation analysis of bulk and selected trace elements in bones using a low flux SLOWPOKE reactor. *Biological trace element research*, 13(1), 333-344.
- Guarino, V., Causa, F., Taddei, P., di Foggia, M., Ciapetti, G., Martini, D., . . . Ambrosio, L. (2008). Polylactic acid fibre-reinforced polycaprolactone scaffolds for bone tissue engineering. *Biomaterials*, 29(27), 3662-3670.
- Gubler, M., Brunner, T., Zehnder, M., Waltimo, T., Sener, B., & Stark, W. (2008). Do bioactive glasses convey a disinfecting mechanism beyond a mere increase in pH? *International endodontic journal*, 41(8), 670-678.
- Gunatillake, P. A., Martin, D. J., Meijs, G. F., McCarthy, S. J., & Adhikari, R. (2003). Designing biostable polyurethane elastomers for biomedical implants. *Australian journal of chemistry*, 56(6), 545-557.
- Hacker, M., & Mikos, A. (2009). Synthetic polymers. *Foundations of Regenerative Medicine: Clinical and Therapeutic Applications*, 336.
- Haimi, S., Gorianc, G., Moimas, L., Lindroos, B., Huhtala, H., Rätty, S., . . . Miettinen, S. (2009). Characterization of zinc-releasing three-dimensional bioactive glass scaffolds and their effect on human adipose stem cell proliferation and osteogenic differentiation. *Acta Biomaterialia*, 5(8), 3122-3131.

- Hajiali, H., Karbasi, S., Hosseinalipour, M., & Rezaie, H. R. (2010). Preparation of a novel biodegradable nanocomposite scaffold based on poly (3-hydroxybutyrate)/bioglass nanoparticles for bone tissue engineering. *Journal of Materials Science: Materials in Medicine*, 21(7), 2125-2132.
- Hall, T. J., & Chambers, T. J. (1990). Gallium inhibits bone resorption by a direct effect on osteoclasts. *Bone and mineral*, 8(3), 211-216.
- Hamed, E., & Jasiuk, I. (2012). Elastic modeling of bone at nanostructural level. *Materials Science and Engineering: R: Reports*, 73(3-4), 27-49.
- Haugh, M. G., Jaasma, M. J., & O'Brien, F. J. (2009). The effect of dehydrothermal treatment on the mechanical and structural properties of collagen-GAG scaffolds. *Journal of Biomedical Materials Research Part A*, 89(2), 363-369.
- Hench, L. L. (1998). Bioceramics. *Journal of the American Ceramic Society*, 81(7), 1705-1728.
- Hench, L. L. (1998). Biomaterials: a forecast for the future. *Biomaterials*, 19(16), 1419-1423.
- Hench, L. L. (2009). Genetic design of bioactive glass. *Journal of the European Ceramic Society*, 29(7), 1257-1265.
- Hench, L. L., Splinter, R. J., Allen, W., & Greenlee, T. (1971). Bonding mechanisms at the interface of ceramic prosthetic materials. *Journal of Biomedical Materials Research*, 5(6), 117-141.
- Hild, N., Tawakoli, P. N., Halter, J. G., Sauer, B., Buchalla, W., Stark, W. J., & Mohn, D. (2013). pH-dependent antibacterial effects on oral microorganisms through pure PLGA implants and composites with nanosized bioactive glass. *Acta Biomaterialia*, 9(11), 9118-9125.
- Holmbom, J., Södergård, A., Ekholm, E., Mårtson, M., Kuusilehto, A., Saukko, P., & Penttinen, R. (2005). Long-term evaluation of porous poly (ϵ -caprolactone-co-L-lactide) as a bone-filling material. *Journal of Biomedical Materials Research Part A*, 75(2), 308-315.
- Hoppe, A., Güldal, N. S., & Boccaccini, A. R. (2011). A review of the biological response to ionic dissolution products from bioactive glasses and glass-ceramics. *Biomaterials*, 32(11), 2757-2774.

- Howard, G. T. (2002). Biodegradation of polyurethane: a review. *International Biodeterioration & Biodegradation*, 49(4), 245-252.
- Huang, W., Day, D. E., Kittiratanapiboon, K., & Rahaman, M. N. (2006). Kinetics and mechanisms of the conversion of silicate (45S5), borate, and borosilicate glasses to hydroxyapatite in dilute phosphate solutions. *Journal of Materials Science: Materials in Medicine*, 17(7), 583-596.
- Ito, A., Kawamura, H., Otsuka, M., Ikeuchi, M., Ohgushi, H., Ishikawa, K., . . . Ichinose, N. (2002). Zinc-releasing calcium phosphate for stimulating bone formation. *Materials Science and Engineering: C*, 22(1), 21-25.
- Jaakkola, T., Rich, J., Tirri, T., Närhi, T., Jokinen, M., Seppälä, J., & Yli-Urpo, A. (2004). In vitro Ca-P precipitation on biodegradable thermoplastic composite of poly(ϵ -caprolactone-co-dl-lactide) and bioactive glass (S53P4). *Biomaterials*, 25(4), 575-581.
- Jenis, L. G., Waud, C. E., Stein, G. S., Lian, J. B., & Baran, D. T. (1993). Effect of gallium nitrate in vitro and in normal rats. *Journal of cellular biochemistry*, 52(3), 330-336.
- Ji, L., Wang, W., Jin, D., Zhou, S., & Song, X. (2015). In vitro bioactivity and mechanical properties of bioactive glass nanoparticles/polycaprolactone composites. *Materials Science and Engineering: C*, 46, 1-9.
- Jo, J.-H., Lee, E.-J., Shin, D.-S., Kim, H.-E., Kim, H.-W., Koh, Y.-H., & Jang, J.-H. (2009). In vitro/in vivo biocompatibility and mechanical properties of bioactive glass nanofiber and poly (ϵ -caprolactone) composite materials. *Journal of Biomedical Materials Research Part B: Applied Biomaterials*, 91(1), 213-220.
- Jugdaohsingh, R. (2007). Silicon and bone health. *The journal of nutrition, health & aging*, 11(2), 99.
- Jung, S. B. (2012). Bioactive Borate Glasses *Bio-Glasses* (pp. 75-95): John Wiley & Sons, Ltd.
- Kamitakahara, M., Ohtsuki, C., Inada, H., Tanihara, M., & Miyazaki, T. (2006). Effect of ZnO addition on bioactive CaO–SiO₂–P₂O₅–CaF₂ glass–ceramics containing apatite and wollastonite. *Acta Biomaterialia*, 2(4), 467-471.

- Kaneko, Y., Thoendel, M., Olakanmi, O., Britigan, B. E., & Singh, P. K. (2007). The transition metal gallium disrupts *Pseudomonas aeruginosa* iron metabolism and has antimicrobial and antibiofilm activity. *The Journal of clinical investigation*, *117*(4), 877.
- Kang, Y., Yang, J., Khan, S., Anissian, L., & Ameer, G. A. (2006). A new biodegradable polyester elastomer for cartilage tissue engineering. *Journal of Biomedical Materials Research Part A*, *77*(2), 331-339.
- Kaur, G., Pandey, O. P., Singh, K., Homa, D., Scott, B., & Pickrell, G. (2014). A review of bioactive glasses: Their structure, properties, fabrication and apatite formation. *Journal of Biomedical Materials Research Part A*, *102*(1), 254-274.
- Keenan, T., Placek, L., Coughlan, A., Bowers, G., Hall, M., & Wren, A. (2016). Structural characterization and anti-cancerous potential of gallium bioactive glass/hydrogel composites. *Carbohydrate Polymers*, *153*, 482-491.
- Keenan, T., Placek, L., Hall, M., & Wren, A. (2016). Antibacterial and antifungal potential of Ga-bioactive glass and Ga-bioactive glass/polymeric hydrogel composites. *Journal of Biomedical Materials Research Part B: Applied Biomaterials*.
- Keenan, T., Placek, L., Keenan, N., Hall, M., & Wren, A. (2016). Synthesis, characterization, and in vitro cytocompatibility of Ga-bioactive glass/polymer hydrogel composites. *Journal of biomaterials applications*, 0885328216646655.
- Kim, H. W., Lee, H. H., & Chun, G. S. (2008). Bioactivity and osteoblast responses of novel biomedical nanocomposites of bioactive glass nanofiber filled poly (lactic acid). *Journal of Biomedical Materials Research Part A*, *85*(3), 651-663.
- Kishi, S., & Yamaguchi, M. (1994). Inhibitory effect of zinc compounds on osteoclast-like cell formation in mouse marrow cultures. *Biochemical pharmacology*, *48*(6), 1225-1230.
- Kneser, U., Schaefer, D., Polykandriotis, E., & Horch, R. (2006). Tissue engineering of bone: the reconstructive surgeon's point of view. *Journal of cellular and molecular medicine*, *10*(1), 7-19.
- Kokubo, T. (1998). Apatite formation on surfaces of ceramics, metals and polymers in body environment. *Acta Mater.*, *46*(7), 2519-2527.

- Kokubo, T., & Takadama, H. (2006). How useful is SBF in predicting in vivo bone bioactivity? *Biomaterials*, 27(15), 2907-2915.
- Korbas, M., Rokita, E., Meyer-Klaucke, W., & Ryczek, J. (2004). Bone tissue incorporates in vitro gallium with a local structure similar to gallium-doped brushite. *JBIC Journal of Biological Inorganic Chemistry*, 9(1), 67-76.
- Kramschuster, A., & Turng, L.-S. (2012). 17 Fabrication of Tissue Engineering Scaffolds. *Handbook of Biopolymers and Biodegradable Plastics: Properties, Processing and Applications*, 427.
- Kuhn, L. T., Grynepas, M. D., Rey, C. C., Wu, Y., Ackerman, J. L., & Glimcher, M. J. (2008). A comparison of the physical and chemical differences between cancellous and cortical bovine bone mineral at two ages. *Calcified tissue international*, 83(2), 146-154.
- Lai, W., Garino, J., & Ducheyne, P. (2002). Silicon excretion from bioactive glass implanted in rabbit bone. *Biomaterials*, 23(1), 213-217.
- Langer, R., & Peppas, N. A. (2003). Advances in biomaterials, drug delivery, and bionanotechnology. *AIChE Journal*, 49(12), 2990-3006.
- Lansdown, A. (1996). Zinc in the healing wound. *The Lancet*, 347(9003), 706-707.
- Lee, H.-H., Yu, H.-S., Jang, J.-H., & Kim, H.-W. (2008). Bioactivity improvement of poly (ϵ -caprolactone) membrane with the addition of nanofibrous bioactive glass. *Acta Biomaterialia*, 4(3), 622-629.
- Lee, S.-H., & Shin, H. (2007). Matrices and scaffolds for delivery of bioactive molecules in bone and cartilage tissue engineering. *Advanced drug delivery reviews*, 59(4), 339-359.
- Lee, S. H., Kim, B. S., Kim, S. H., Choi, S. W., Jeong, S. I., Kwon, I. K., . . . Han, Y. K. (2003). Elastic biodegradable poly (glycolide-co-caprolactone) scaffold for tissue engineering. *Journal of Biomedical Materials Research Part A*, 66(1), 29-37.
- Leong, K., Cheah, C., & Chua, C. (2003). Solid freeform fabrication of three-dimensional scaffolds for engineering replacement tissues and organs. *Biomaterials*, 24(13), 2363-2378.

- Leong, N. L., Jiang, J., & Lu, H. H. (2006). *Polymer-ceramic composite scaffold induces osteogenic differentiation of human mesenchymal stem cells*. Paper presented at the Engineering in Medicine and Biology Society, 2006. EMBS'06. 28th Annual International Conference of the IEEE.
- Leppäranta, O., Vaahtio, M., Peltola, T., Zhang, D., Hupa, L., Hupa, M., . . . Eerola, E. (2008). Antibacterial effect of bioactive glasses on clinically important anaerobic bacteria in vitro. *Journal of Materials Science: Materials in Medicine*, 19(2), 547-551.
- Li, H., Du, R., & Chang, J. (2005). Fabrication, characterization, and in vitro degradation of composite scaffolds based on PHBV and bioactive glass. *Journal of biomaterials applications*, 20(2), 137-155.
- Li, S., Garreau, H., & Vert, M. (1990). Structure-property relationships in the case of the degradation of massive poly (α -hydroxy acids) in aqueous media. *Journal of Materials Science: Materials in Medicine*, 1(4), 198-206.
- Li, W.-J., & Cooper Jr, J. A. (2011). Fibrous Scaffolds for Tissue Engineering. *Biomaterials for Tissue Engineering Applications: A Review of the Past and Future Trends*, 47.
- Li, Y., Thouas, G. A., & Chen, Q.-Z. (2012). Biodegradable soft elastomers: synthesis/properties of materials and fabrication of scaffolds. *RSC Advances*, 2(22), 8229-8242.
- Liang, S.-L., Cook, W. D., Thouas, G. A., & Chen, Q.-Z. (2010). The mechanical characteristics and in vitro biocompatibility of poly (glycerol sebacate)-Bioglass® elastomeric composites. *Biomaterials*, 31(33), 8516-8529.
- Liang, S.-L., Yang, X.-Y., Fang, X.-Y., Cook, W. D., Thouas, G. A., & Chen, Q.-Z. (2011). In Vitro enzymatic degradation of poly (glycerol sebacate)-based materials. *Biomaterials*, 32(33), 8486-8496.
- Liang, S., Cook, W. D., & Chen, Q. (2012). Physical characterization of poly (glycerol sebacate)/Bioglass® composites. *Polymer International*, 61(1), 17-22.
- Liebschner, M., Wettergreen, M., Ashammakhi, N., & Ferretti, P. (2003). Optimization of bone scaffold engineering for load bearing applications. *Topics in tissue engineering*, 1-39.

- Liu, C., Xia, Z., & Czernuszka, J. (2007). Design and development of three-dimensional scaffolds for tissue engineering. *Chemical Engineering Research and Design*, 85(7), 1051-1064.
- Liu, Q., Jiang, L., Shi, R., & Zhang, L. (2012). Synthesis, preparation, in vitro degradation, and application of novel degradable bioelastomers—A review. *Progress in Polymer Science*, 37(5), 715-765.
- Liu, X., Rahaman, M. N., & Fu, Q. (2013). Bone regeneration in strong porous bioactive glass (13-93) scaffolds with an oriented microstructure implanted in rat calvarial defects. *Acta Biomaterialia*, 9(1), 4889-4898.
- Lu, H. H., El-Amin, S. F., Scott, K. D., & Laurencin, C. T. (2003). Three-dimensional, bioactive, biodegradable, polymer–bioactive glass composite scaffolds with improved mechanical properties support collagen synthesis and mineralization of human osteoblast-like cells in vitro. *Journal of Biomedical Materials Research Part A*, 64(3), 465-474.
- Lu, H. H., Tang, A., Oh, S. C., Spalazzi, J. P., & Dionisio, K. (2005). Compositional effects on the formation of a calcium phosphate layer and the response of osteoblast-like cells on polymer-bioactive glass composites. *Biomaterials*, 26(32), 6323-6334.
- Lü, J.-M., Wang, X., Marin-Muller, C., Wang, H., Lin, P. H., Yao, Q., & Chen, C. (2009). Current advances in research and clinical applications of PLGA-based nanotechnology.
- Lusvardi, G., Malavasi, G., Menabue, L., & Shruti, S. (2013). Gallium-Containing Phosphosilicate Glasses: Functionalization and in-vitro Bioactivity. *Materials Science and Engineering: C*.
- Malavasi, G., Pedone, A., & Menziani, M. C. (2013). Study of the Structural Role of Gallium and Aluminum in 45S5 Bioactive Glasses by Molecular Dynamics Simulations. *The Journal of Physical Chemistry B*, 117(15), 4142-4150.
- Mano, J., Silva, G., Azevedo, H. S., Malafaya, P., Sousa, R., Silva, S., . . . Marques, A. (2007). Natural origin biodegradable systems in tissue engineering and regenerative medicine: present status and some moving trends. *Journal of the Royal Society Interface*, 4(17), 999-1030.
- Marolt, D., Knezevic, M., & Novakovic, G. V. (2010). Bone tissue engineering with human stem cells. *Stem cell research & therapy*, 1(10), 20637059.

- Marquez-Curtis, L. A., Janowska-Wieczorek, A., McGann, L. E., & Elliott, J. A. (2015). Mesenchymal stromal cells derived from various tissues: Biological, clinical and cryopreservation aspects. *Cryobiology*, 71(2), 181-197.
- Mellier, C., Fayon, F., Boukhechba, F., Verron, E., LeFerrec, M., Montavon, G., . . . Janvier, P. (2015). Design and properties of novel gallium-doped injectable apatitic cements. *Acta Biomaterialia*, 24, 322-332.
- Mellier, C., Fayon, F., Schnitzler, V., Deniard, P., Allix, M., Quillard, S., . . . Janvier, P. (2011). Characterization and properties of novel gallium-doped calcium phosphate ceramics. *Inorganic chemistry*, 50(17), 8252-8260.
- Melnikov, P., Teixeira, A., Malzac, A., & Coelho, M. d. B. (2009). Gallium-containing hydroxyapatite for potential use in orthopedics. *Materials Chemistry and Physics*, 117(1), 86-90.
- Meretoja, V., Helminen, A., Korventausta, J., Haapa-aho, V., Seppälä, J., & Närhi, T. (2006). Crosslinked poly (ϵ -caprolactone/D, L-lactide)/bioactive glass composite scaffolds for bone tissue engineering. *Journal of Biomedical Materials Research Part A*, 77(2), 261-268.
- Meretoja, V. V., Tirri, T., Malin, M., Seppälä, J. V., & Närhi, T. O. (2014). Ectopic bone formation in and soft-tissue response to P (CL/DLLA)/bioactive glass composite scaffolds. *Clinical oral implants research*, 25(2), 159-164.
- Misra, S. K., Ansari, T., Mohn, D., Valappil, S. P., Brunner, T. J., Stark, W. J., . . . Jones, E. V. (2009). Effect of nanoparticulate bioactive glass particles on bioactivity and cytocompatibility of poly (3-hydroxybutyrate) composites. *Journal of the Royal Society Interface*, rsif20090255.
- Misra, S. K., Mohn, D., Brunner, T. J., Stark, W. J., Philip, S. E., Roy, I., . . . Boccaccini, A. R. (2008). Comparison of nanoscale and microscale bioactive glass on the properties of P (3HB)/Bioglass® composites. *Biomaterials*, 29(12), 1750-1761.
- Misra, S. K., Nazhat, S. N., Valappil, S. P., Moshrefi-Torbati, M., Wood, R. J., Roy, I., & Boccaccini, A. R. (2007). Fabrication and characterization of biodegradable poly (3-hydroxybutyrate) composite containing bioglass. *Biomacromolecules*, 8(7), 2112-2119.
- Misra, S. K., Valappil, S. P., Roy, I., & Boccaccini, A. R. (2006). Polyhydroxyalkanoate (PHA)/inorganic phase composites for tissue engineering applications. *Biomacromolecules*, 7(8), 2249-2258.

- Mocchegiani, E., Giacconi, R., Muzzioli, M., & Cipriano, C. (2001). Zinc, infections and immunosenescence. *Mechanisms of ageing and development*, 121(1), 21-35.
- Mourino, V., Newby, P., & Boccaccini, A. R. (2010). Preparation and Characterization of Gallium Releasing 3-D Alginate Coated 45S5 Bioglass® Based Scaffolds for Bone Tissue Engineering. *Advanced Engineering Materials*, 12(7), B283-B291.
- Mozafari, M., Rabiee, M., Azami, M., & Maleknia, S. (2010). Biomimetic formation of apatite on the surface of porous gelatin/bioactive glass nanocomposite scaffolds. *Applied Surface Science*, 257(5), 1740-1749.
- Murthy, P. S., Venugopalan, V., Sahoo, P., Dhara, S., Das, A., Tyagi, A., & Saini, G. (2011). *Gallium oxide nanoparticle induced inhibition of bacterial adhesion and biofilm formation*. Paper presented at the Nanoscience, Engineering and Technology (ICONSET), 2011 International Conference on.
- Nadeem, D., Kiamehr, M., Yang, X., & Su, B. (2013). Fabrication and in vitro evaluation of a sponge-like bioactive-glass/gelatin composite scaffold for bone tissue engineering. *Materials Science and Engineering: C*, 33(5), 2669-2678.
- Narayan, R. (2009). *Biomedical materials*: Springer Science & Business Media.
- Nawaz, M., Fatima, F., Vallabhaneni, K. C., Penfornis, P., Valadi, H., Ekström, K., . . . Pochampally, R. (2015). Extracellular Vesicles: Evolving Factors in Stem Cell Biology. *Stem cells international*, 2016.
- Nordin, B. C. (1997). Calcium and osteoporosis. *Nutrition*, 13(7), 664-686.
- Oh, S.-A., Kim, S.-H., Won, J.-E., Kim, J.-J., Shin, U. S., & Kim, H.-W. (2010). Effects on growth and osteogenic differentiation of mesenchymal stem cells by the zinc-added sol-gel bioactive glass granules. *Journal of tissue engineering*, 1(1), 475260.
- Oh, S.-A., Won, J.-E., & Kim, H.-W. (2011). Composite membranes of poly (lactic acid) with zinc-added bioactive glass as a guiding matrix for osteogenic. *Journal of biomaterials applications*, 0885328211408944.
- Ohgushi, H., Dohi, Y., Yoshikawa, T., Tamai, S., Tabata, S., Okunaga, K., & Shibuya, T. (1996). Osteogenic differentiation of cultured marrow stromal stem cells on the surface of bioactive glass ceramics. *Journal of Biomedical Materials Research*, 32(3), 341-348.

- Okamoto, M., & John, B. (2013). Synthetic biopolymer nanocomposites for tissue engineering scaffolds. *Progress in Polymer Science*, 38(10), 1487-1503.
- Okamoto, Y., & Hidaka, S. (1994). Studies on calcium phosphate precipitation: effects of metal ions used in dental materials. *Journal of Biomedical Materials Research*, 28(12), 1403-1410.
- Olsen-Claire, J., Blaker, J. J., Roether, J. A., Boccaccini, A. R., Schmack, G., & Gliesche, K. (2006). Bioglass® Coatings on Biodegradable Poly(3-hydroxybutyrate) (P3HB) Meshes for Tissue Engineering Scaffolds. *Materialwissenschaft und Werkstofftechnik*, 37(7), 577-583.
- Olszta, M. J., Cheng, X., Jee, S. S., Kumar, R., Kim, Y.-Y., Kaufman, M. J., . . . Gower, L. B. (2007). Bone structure and formation: A new perspective. *Materials Science and Engineering: R: Reports*, 58(3-5), 77-116.
- Oryan, A., Alidadi, S., Moshiri, A., & Maffulli, N. (2014). Bone regenerative medicine: classic options, novel strategies, and future directions. *Journal of orthopaedic surgery and research*, 9(1), 1.
- Osinaga, P. W., Grande, R. H. M., Ballester, R. Y., Simionato, M. R. L., Rodrigues, C. R. M. D., & Muench, A. (2003). Zinc sulfate addition to glass-ionomer-based cements: influence on physical and antibacterial properties, zinc and fluoride release. *Dental Materials*, 19(3), 212-217.
- Oudadesse, H., Dietrich, E., Gal, Y., Pellen, P., Bureau, B., Mostafa, A., & Cathelineau, G. (2011). Apatite forming ability and cytocompatibility of pure and Zn-doped bioactive glasses. *Biomedical Materials*, 6(3), 035006.
- Pamula, E., Kokoszka, J., Cholewa-Kowalska, K., Laczka, M., Kantor, L., Niedzwiedzki, L., . . . Kolodziejczyk, M. (2011). Degradation, bioactivity, and osteogenic potential of composites made of PLGA and two different sol-gel bioactive glasses. *Annals of biomedical engineering*, 39(8), 2114-2129.
- Pan, H., Zhao, X., Zhang, X., Zhang, K., Li, L., Li, Z., . . . Huang, W. (2010). Strontium borate glass: potential biomaterial for bone regeneration. *Journal of the Royal Society Interface*, 7(48), 1025-1031.
- Pasquet, J., Chevalier, Y., Pelletier, J., Couval, E., Bouvier, D., & Bolzinger, M.-A. (2014). The contribution of zinc ions to the antimicrobial activity of zinc oxide. *Colloids and Surfaces A: Physicochemical and Engineering Aspects*, 457, 263-274.

- Peltola, S. M., Melchels, F. P., Grijpma, D. W., & Kellomäki, M. (2008). A review of rapid prototyping techniques for tissue engineering purposes. *Annals of medicine*, 40(4), 268-280.
- Peng, H. T., Martineau, L., & Shek, P. N. (2007). Hydrogel–elastomer composite biomaterials: 1. Preparation of interpenetrating polymer networks and in vitro characterization of swelling stability and mechanical properties. *Journal of Materials Science: Materials in Medicine*, 18(6), 975-986.
- Perez, R. A., Won, J.-E., Knowles, J. C., & Kim, H.-W. (2013). Naturally and synthetic smart composite biomaterials for tissue regeneration. *Advanced drug delivery reviews*, 65(4), 471-496.
- Peter, M., Binulal, N., Nair, S., Selvamurugan, N., Tamura, H., & Jayakumar, R. (2010). Novel biodegradable chitosan–gelatin/nano-bioactive glass ceramic composite scaffolds for alveolar bone tissue engineering. *Chemical Engineering Journal*, 158(2), 353-361.
- Pickup, D., Moss, R., Qiu, D., Newport, R., Valappil, S., Knowles, J., & Smith, M. E. (2009). Structural characterization by x-ray methods of novel antimicrobial gallium-doped phosphate-based glasses. *Journal of Chemical Physics*, 130, 064708.
- Poh, P. S., Hutmacher, D. W., Stevens, M. M., & Woodruff, M. A. (2013). Fabrication and in vitro characterization of bioactive glass composite scaffolds for bone regeneration. *Biofabrication*, 5(4), 045005.
- Popp, J. R., Love, B. J., & Goldstein, A. S. (2007). Effect of soluble zinc on differentiation of osteoprogenitor cells. *Journal of Biomedical Materials Research Part A*, 81(3), 766-769.
- Pourshahrestani, S., Zeimaran, E., Kadri, N. A., Gargiulo, N., Samuel, S., Naveen, S. V., . . . Towler, M. R. (2016). Gallium-containing mesoporous bioactive glass with potent hemostatic activity and antibacterial efficacy. *Journal of Materials Chemistry B*, 4(1), 71-86.
- Prabhakaran, M. P., Nair, A. S., Kai, D., & Ramakrishna, S. (2012). Electrospun composite scaffolds containing poly (octanediol-co-citrate) for cardiac tissue engineering. *Biopolymers*, 97(7), 529-538.
- Pravina, P., Sayaji, D., & Avinash, M. (2013). Calcium and its role in human body. *International Journal of Research in Pharmaceutical and Biomedical Sciences*, 4(2), 659-668.

- Puppi, D., Chiellini, F., Piras, A. M., & Chiellini, E. (2010). Polymeric materials for bone and cartilage repair. *Progress in Polymer Science*, 35(4), 403-440.
- Qiu, H., Yang, J., Kodali, P., Koh, J., & Ameer, G. A. (2006). A citric acid-based hydroxyapatite composite for orthopedic implants. *Biomaterials*, 27(34), 5845-5854.
- Raghavendran, H. R. B., Mohan, S., Genasan, K., Murali, M. R., Naveen, S. V., Talebian, S., . . . Kamarul, T. (2016). Synergistic interaction of platelet derived growth factor (PDGF) with the surface of PLLA/Col/HA and PLLA/HA scaffolds produces rapid osteogenic differentiation. *Colloids and Surfaces B: Biointerfaces*, 139, 68-78.
- Rahaman, M. N., Day, D. E., Bal, B. S., Fu, Q., Jung, S. B., Bonewald, L. F., & Tomsia, A. P. (2011). Bioactive glass in tissue engineering. *Acta Biomaterialia*, 7(6), 2355-2373.
- Rahman, R. A., Sukri, N. M., Nazir, N. M., Radzi, M. A. z. A., Zulkifly, A. H., Ahmad, A. C., . . . Sha'ban, M. (2015). The potential of 3-dimensional construct engineered from poly (lactic-co-glycolic acid)/fibrin hybrid scaffold seeded with bone marrow mesenchymal stem cells for in vitro cartilage tissue engineering. *Tissue and Cell*, 47(4), 420-430.
- Ramalingam, M., Ramakrishna, S., & Best, S. (2012). *Biomaterials and stem cells in regenerative medicine*: CRC Press.
- Reginster, J.-Y., Strause, L., Saltman, P., & Franchimont, P. (1988). Trace elements and postmenopausal osteoporosis: a preliminary report of decreased serum manganese. *Medical Science Research*, 16.
- Reilly, G. C., Radin, S., Chen, A. T., & Ducheyne, P. (2007). Differential alkaline phosphatase responses of rat and human bone marrow derived mesenchymal stem cells to 45S5 bioactive glass. *Biomaterials*, 28(28), 4091-4097.
- Rezwan, K., Chen, Q., Blaker, J., & Boccaccini, A. R. (2006). Biodegradable and bioactive porous polymer/inorganic composite scaffolds for bone tissue engineering. *Biomaterials*, 27(18), 3413-3431.
- Rich, J., Jaakkola, T., Tirri, T., Närhi, T., Yli-Urpo, A., & Seppälä, J. (2002). In vitro evaluation of poly (ϵ -caprolactone-co-DL-lactide)/bioactive glass composites. *Biomaterials*, 23(10), 2143-2150.

- Ripa, S., & Ripa, R. (1994). Zinc and immune function. *MINERVA MED*, 86(7-8), 315-318.
- Ródenas-Rochina, J., Ribelles, J. L. G., & Lebourg, M. (2013). Comparative study of PCL-HAp and PCL-bioglass composite scaffolds for bone tissue engineering. *Journal of Materials Science: Materials in Medicine*, 24(5), 1293-1308.
- Rodríguez-Galán, A., Franco, L., & Puiggali, J. (2011). Biodegradable Polyurethanes and Poly (ester amide) s. *Handbook of Biodegradable Polymers: Isolation, Synthesis, Characterization and Applications*, 133-154.
- Roether, J., Gough, J., Boccaccini, A. R., Hench, L., Maquet, V., & Jérôme, R. (2002). Novel bioresorbable and bioactive composites based on bioactive glass and polylactide foams for bone tissue engineering. *Journal of Materials Science: Materials in Medicine*, 13(12), 1207-1214.
- Rohman, G., Pettit, J. J., Isaure, F., Cameron, N. R., & Southgate, J. (2007). Influence of the physical properties of two-dimensional polyester substrates on the growth of normal human urothelial and urinary smooth muscle cells in vitro. *Biomaterials*, 28(14), 2264-2274.
- Ryszkowska, J. L., Auguścik, M., Sheikh, A., & Boccaccini, A. R. (2010). Biodegradable polyurethane composite scaffolds containing Bioglass® for bone tissue engineering. *Composites Science and Technology*, 70(13), 1894-1908.
- Salih, V., Patel, A., & Knowles, J. (2007). Zinc-containing phosphate-based glasses for tissue engineering. *Biomedical Materials*, 2(1), 11.
- Salinas, A. J., & Vallet-Regí, M. (2013). Bioactive ceramics: from bone grafts to tissue engineering. *RSC Advances*, 3(28), 11116-11131.
- Segawa, Y., Tsuzuike, N., Tagashira, E., & Yamaguchi, M. (1992). Preventive effect of β -analyl-l-histidinato zinc on bone metabolism in rats fed on low-calcium and vitamin D-deficient diets. *Research in experimental medicine*, 192(1), 213-219.
- Selling, G. W. (2010). The effect of extrusion processing on Zein. *Polymer degradation and stability*, 95(12), 2241-2249.
- Serrano, M. C., Chung, E. J., & Ameer, G. (2010). Advances and applications of biodegradable elastomers in regenerative medicine. *Advanced Functional Materials*, 20(2), 192-208.

- Sharma, A. K., Hota, P. V., Matoka, D. J., Fuller, N. J., Jandali, D., Thaker, H., . . . Cheng, E. Y. (2010). Urinary bladder smooth muscle regeneration utilizing bone marrow derived mesenchymal stem cell seeded elastomeric poly (1, 8-octanediol-co-citrate) based thin films. *Biomaterials*, 31(24), 6207-6217.
- Shi, R., Chen, D., Liu, Q., Wu, Y., Xu, X., Zhang, L., & Tian, W. (2009). Recent advances in synthetic bioelastomers. *International journal of molecular sciences*, 10(10), 4223-4256.
- Shirazi, F., Moghaddam, E., Mehrali, M., Oshkour, A., Metselaar, H., Kadri, N., . . . Abu, N. (2014). In vitro characterization and mechanical properties of β -calcium silicate/POC composite as a bone fixation device. *Journal of Biomedical Materials Research Part A*.
- Shogren, R., & Bagley, E. (1999). Natural polymers as advanced materials: some research needs and directions.
- Silva, A., Paula, A., Martins, T., Goes, A., & Pereria, M. (2014). Synergistic effect between bioactive glass foam and a perfusion bioreactor on osteogenic differentiation of human adipose stem cells. *Journal of Biomedical Materials Research Part A*, 102(3), 818-827.
- Sionkowska, A. (2011). Current research on the blends of natural and synthetic polymers as new biomaterials: Review. *Progress in Polymer Science*, 36(9), 1254-1276.
- Sivak, W. N., Pollack, I. F., Petoud, S., Zamboni, W. C., Zhang, J., & Beckman, E. J. (2008). Catalyst-dependent drug loading of LDI-glycerol polyurethane foams leads to differing controlled release profiles. *Acta Biomaterialia*, 4(5), 1263-1274.
- Smith, L. A., Liu, X., Hu, J., & Ma, P. X. (2009). The influence of three-dimensional nanofibrous scaffolds on the osteogenic differentiation of embryonic stem cells. *Biomaterials*, 30(13), 2516-2522.
- Söderberg, T. A., Sunzel, B., Holm, S., Elmros, T., Hallmans, G., & Sjöberg, S. (1990). Antibacterial effect of zinc oxide in vitro. *Scandinavian Journal of Plastic and Reconstructive Surgery and Hand Surgery*, 24(3), 193-197.
- Spaans, C., Belgraver, V., Rienstra, O., De Groot, J., Veth, R., & Pennings, A. (2000). Solvent-free fabrication of micro-porous polyurethane amide and polyurethane-urea scaffolds for repair and replacement of the knee-joint meniscus. *Biomaterials*, 21(23), 2453-2460.

- Srinivasan, S., Jayasree, R., Chennazhi, K., Nair, S., & Jayakumar, R. (2012). Biocompatible alginate/nano bioactive glass ceramic composite scaffolds for periodontal tissue regeneration. *Carbohydrate Polymers*, 87(1), 274-283.
- Sripanyakorn, S., Jugdaohsingh, R., Thompson, R. P., & Powell, J. J. (2005). Dietary silicon and bone health. *Nutrition Bulletin*, 30(3), 222-230.
- Stanić, V., Dimitrijević, S., Antić-Stanković, J., Mitrić, M., Jokić, B., Plećaš, I. B., & Raičević, S. (2010). Synthesis, characterization and antimicrobial activity of copper and zinc-doped hydroxyapatite nanopowders. *Applied Surface Science*, 256(20), 6083-6089.
- Steinbüchel, A. (2001). Perspectives for biotechnological production and utilization of biopolymers: metabolic engineering of polyhydroxyalkanoate biosynthesis pathways as a successful example. *Macromolecular Bioscience*, 1(1), 1-24.
- Stoor, P., Söderling, E., & Salonen, J. I. (1998). Antibacterial effects of a bioactive glass paste on oral microorganisms. *Acta Odontologica Scandinavica*, 56(3), 161-165.
- Stuckey, D. J., Ishii, H., Chen, Q.-Z., Boccaccini, A. R., Hansen, U., Carr, C. A., . . . Ali, N. N. (2010). Magnetic resonance imaging evaluation of remodeling by cardiac elastomeric tissue scaffold biomaterials in a rat model of myocardial infarction. *Tissue Engineering Part A*, 16(11), 3395-3402.
- Subia, B., Kundu, J., & Kundu, S. (2010). Biomaterial scaffold fabrication techniques for potential tissue engineering applications. *Tissue Engineering*, 141-157.
- Tapiero, H., & Tew, K. D. (2003). Trace elements in human physiology and pathology: zinc and metallothioneins. *Biomedicine & Pharmacotherapy*, 57(9), 399-411.
- Teplyuk, N. M., Galindo, M., Teplyuk, V. I., Pratap, J., Young, D. W., Lapointe, D., . . . Stein, G. S. (2008). Runx2 regulates G protein-coupled signaling pathways to control growth of osteoblast progenitors. *Journal of Biological Chemistry*, 283(41), 27585-27597.
- Tian, H., Tang, Z., Zhuang, X., Chen, X., & Jing, X. (2012). Biodegradable synthetic polymers: Preparation, functionalization and biomedical application. *Progress in Polymer Science*, 37(2), 237-280.
- Tsaryk, R., Peters, K., Unger, R. E., Scharnweber, D., & Kirkpatrick, C. J. (2007). The effects of metal implants on inflammatory and healing processes. *International journal of materials research*, 98(7), 622-629.

- Tsigkou, O., Hench, L., Boccaccini, A., Polak, J., & Stevens, M. (2007). Enhanced differentiation and mineralization of human fetal osteoblasts on PDLLA containing Bioglass® composite films in the absence of osteogenic supplements. *Journal of Biomedical Materials Research Part A*, 80(4), 837-851.
- Urry, D., Hugel, T., Seitz, M., Gaub, H., Sheiba, L., Dea, J., . . . Parker, T. (2002). Elastin: a representative ideal protein elastomer. *Philosophical Transactions of the Royal Society of London. Series B: Biological Sciences*, 357(1418), 169-184.
- Valappil, S. P., Ready, D., Abou Neel, E., Pickup, D. M., O'Dell, L. A., Chrzanowski, W., . . . Wilson, M. (2009). Controlled delivery of antimicrobial gallium ions from phosphate-based glasses. *Acta Biomaterialia*, 5(4), 1198-1210.
- Valappil, S. P., Ready, D., Neel, E. A. A., Pickup, D. M., Chrzanowski, W., O'Dell, L. A., . . . Knowles, J. C. (2008). Antimicrobial Gallium-Doped Phosphate-Based Glasses. *Advanced Functional Materials*, 18(5), 732-741.
- Valerio, P., Pereira, M. M., Goes, A. M., & Leite, M. F. (2004). The effect of ionic products from bioactive glass dissolution on osteoblast proliferation and collagen production. *Biomaterials*, 25(15), 2941-2948.
- Van der Mee, M., Goossens, J., & Van Duin, M. (2008). Thermoreversible covalent crosslinking of maleated ethylene/propylene copolymers with diols. *Journal of Polymer Science Part A: Polymer Chemistry*, 46(5), 1810-1825.
- Varghese, S., & Elisseeff, J. H. (2006). Hydrogels for musculoskeletal tissue engineering *Polymers for regenerative medicine* (pp. 95-144): Springer.
- Velema, J., & Kaplan, D. (2006). Biopolymer-Based Biomaterials as Scaffolds for Tissue Engineering. In K. Lee & D. Kaplan (Eds.), *Tissue Engineering I* (Vol. 102, pp. 187-238): Springer Berlin Heidelberg.
- Verma, S., Garkhal, K., Mittal, A., & Kumar, N. (2011). Biodegradable polymers for emerging clinical use in tissue engineering. *Biodegradable Polymers in Clinical Use and Clinical Development*, 565-629.
- Verron, E., Bouler, J., & Scimeca, J. (2012). Gallium as a potential candidate for treatment of osteoporosis. *Drug discovery today*, 17(19), 1127-1132.

- Verron, E., Masson, M., Khoshniat, S., Duplomb, L., Wittrant, Y., Baud'huin, M., . . . Scimeca, J. C. (2010). Gallium modulates osteoclastic bone resorption in vitro without affecting osteoblasts. *British journal of pharmacology*, 159(8), 1681-1692.
- Vieth, S., Bellingham, C. M., Keeley, F. W., Hodge, S. M., & Rousseau, D. (2007). Microstructural and tensile properties of elastin-based polypeptides crosslinked with Genipin and pyrroloquinoline quinone. *Biopolymers*, 85(3), 199-206.
- Vollenweider, M., Brunner, T. J., Knecht, S., Grass, R. N., Zehnder, M., Imfeld, T., & Stark, W. J. (2007). Remineralization of human dentin using ultrafine bioactive glass particles. *Acta Biomaterialia*, 3(6), 936-943.
- Wang, M. (2003). Developing bioactive composite materials for tissue replacement. *Biomaterials*, 24(13), 2133-2151.
- Wang, T., Zhang, J.-C., Chen, Y., Xiao, P.-G., & Yang, M.-S. (2007). Effect of zinc ion on the osteogenic and adipogenic differentiation of mouse primary bone marrow stromal cells and the adipocytic trans-differentiation of mouse primary osteoblasts. *Journal of Trace Elements in Medicine and Biology*, 21(2), 84-91.
- Wang, Y., Ameer, G. A., Sheppard, B. J., & Langer, R. (2002). A tough biodegradable elastomer. *Nature biotechnology*, 20(6), 602-606.
- Warrell, R. P. (1997). Gallium nitrate for the treatment of bone metastases. *Cancer*, 80(S8), 1680-1685.
- Watson, C., & Dark, J. (2012). Organ transplantation: historical perspective and current practice. *British journal of anaesthesia*, 108(suppl 1), i29-i42.
- Wise, S. G., Mithieux, S. M., & Weiss, A. S. (2009). Engineered Tropoelastin and Elastin-Based Biomaterials. In M. Alexander (Ed.), *Advances in Protein Chemistry and Structural Biology* (Vol. Volume 78, pp. 1-24): Academic Press.
- Woodruff, M. A., & Hutmacher, D. W. (2010). The return of a forgotten polymer—polycaprolactone in the 21st century. *Progress in Polymer Science*, 35(10), 1217-1256.
- Wren, A., Boyd, D., Thornton, R., Cooney, J., & Towler, M. (2009). Antibacterial properties of a tri-sodium citrate modified glass polyalkenoate cement. *Journal of Biomedical Materials Research Part B: Applied Biomaterials*, 90(2), 700-709.

- Wren, A., Coughlan, A., Placek, L., & Towler, M. (2012). Gallium containing glass polyalkenoate anti-cancerous bone cements: glass characterization and physical properties. *Journal of Materials Science: Materials in Medicine*, 23(8), 1823-1833.
- Wren, A., Keenan, T., Coughlan, A., Laffir, F., Boyd, D., Towler, M., & Hall, M. (2013). Characterisation of Ga₂O₃-Na₂O-CaO-ZnO-SiO₂ bioactive glasses. *Journal of materials science*, 48(11), 3999-4007.
- Wu, C., Labrie, J., Tremblay, Y., Haine, D., Mourez, M., & Jacques, M. (2013). Zinc as an agent for the prevention of biofilm formation by pathogenic bacteria. *Journal of applied microbiology*, 115(1), 30-40.
- Wu, L., & Ding, J. (2004). In vitro degradation of three-dimensional porous poly (D, L-lactide-co-glycolide) scaffolds for tissue engineering. *Biomaterials*, 25(27), 5821-5830.
- Wu, L., & Ding, J. (2005). Effects of porosity and pore size on in vitro degradation of three-dimensional porous poly (D, L-lactide-co-glycolide) scaffolds for tissue engineering. *Journal of Biomedical Materials Research Part A*, 75(4), 767-777.
- Wu, X. (2012). *Surface Modification of Polylactic Acid Nonwoven Webs*: North Carolina State University.
- Xing, Q., Yates, K., Vogt, C., Qian, Z., Frost, M. C., & Zhao, F. (2014). Increasing mechanical strength of gelatin hydrogels by divalent metal ion removal. *Scientific reports*, 4.
- Xing, Z.-C., Chae, W.-P., Baek, J.-Y., Choi, M.-J., Jung, Y., & Kang, I.-K. (2010). In vitro assessment of antibacterial activity and cytocompatibility of silver-containing PHBV nanofibrous scaffolds for tissue engineering. *Biomacromolecules*, 11(5), 1248-1253.
- Xu, H., Nguyen, K. T., Brilakis, E. S., Yang, J., Fuh, E., & Banerjee, S. (2012). Enhanced endothelialization of a new stent polymer through surface enhancement and incorporation of growth factor-delivering microparticles. *Journal of cardiovascular translational research*, 5(4), 519-527.
- Xynos, I., Hukkanen, M., Batten, J., Buttery, L., Hench, L., & Polak, J. (2000). Bioglass® 45S5 stimulates osteoblast turnover and enhances bone formation in vitro: implications and applications for bone tissue engineering. *Calcified tissue international*, 67(4), 321-329.

- Xynos, I. D., Edgar, A. J., Buttery, L. D., Hench, L. L., & Polak, J. M. (2000). Ionic products of bioactive glass dissolution increase proliferation of human osteoblasts and induce insulin-like growth factor II mRNA expression and protein synthesis. *Biochemical and biophysical research communications*, 276(2), 461-465.
- Xynos, I. D., Edgar, A. J., Buttery, L. D., Hench, L. L., & Polak, J. M. (2001). Gene-expression profiling of human osteoblasts following treatment with the ionic products of Bioglass® 45S5 dissolution. *Journal of Biomedical Materials Research*, 55(2), 151-157.
- Yamaguchi, M. (1998). Role of zinc in bone formation and bone resorption. *The Journal of Trace Elements in Experimental Medicine*, 11(2-3), 119-135.
- Yamaguchi, M., & Yamaguchi, R. (1986). Action of zinc on bone metabolism in rats: increases in alkaline phosphatase activity and DNA content. *Biochemical pharmacology*, 35(5), 773-777.
- Yamamoto, A., Honma, R., & Sumita, M. (1998). Cytotoxicity evaluation of 43 metal salts using murine fibroblasts and osteoblastic cells. *Journal of Biomedical Materials Research*, 39(2), 331-340.
- Yan, Q., & Sage, E. H. (1999). SPARC, a matricellular glycoprotein with important biological functions. *Journal of Histochemistry & Cytochemistry*, 47(12), 1495-1505.
- Yang, J., Webb, A. R., & Ameer, G. A. (2004). Novel Citric Acid-Based Biodegradable Elastomers for Tissue Engineering. *Advanced Materials*, 16(6), 511-516.
- Yang, J., Webb, A. R., Pickerill, S. J., Hageman, G., & Ameer, G. A. (2006). Synthesis and evaluation of poly (diol citrate) biodegradable elastomers. *Biomaterials*, 27(9), 1889-1898.
- You, Z., & Wang, Y. (2011). Bioelastomers in Tissue Engineering *Biomaterials for Tissue Engineering Applications* (pp. 75-118): Springer.
- Zaidman, N., & Bosnakovski, D. (2012). Advancing with ceramic biocomposites for bone graft implants. *Recent Patents on Regenerative Medicine*, 2(1), 65-72.
- Zhang, L., Jiang, Y., Ding, Y., Povey, M., & York, D. (2007). Investigation into the antibacterial behaviour of suspensions of ZnO nanoparticles (ZnO nanofluids). *Journal of Nanoparticle Research*, 9(3), 479-489.

Zhang, X.-Q., Tang, H., Hoshi, R., De Laporte, L., Qiu, H., Xu, X., . . . Ameer, G. A. (2009). Sustained transgene expression via citric acid-based polyester elastomers. *Biomaterials*, 30(13), 2632-2641.

Zhen-Ming, H., Sean, A., Stephen, K., Sandor, G. K., & Clokie, C. M. (2009). Induction of bone matrix protein expression by native bone matrix proteins in C2C12 culture. *Biomedical and Environmental Sciences*, 22(2), 164-169.

Zhou, D., Zhao, K., Li, Y., Cui, F., & Lee, I. (2006). Repair of segmental defects with nano-hydroxyapatite/collagen/PLA composite combined with mesenchymal stem cells. *Journal of Bioactive and Compatible Polymers*, 21(5), 373-384.

Zreiqat, H., Dunstan, C. R., & Rosen, V. (2015). *A Tissue Regeneration Approach to Bone and Cartilage Repair*: Springer.

University of Malaya

LIST OF PUBLICATIONS AND PAPERS PRESENTED

❖ Review article

Ehsan Zeimaran, Sara Pourshahrestani, Ivan Djordjevic, Belinda Pinguan-Murphy, Nahrizul Adib Kadri, Mark R. Towler, (2015). Bioactive glass reinforced elastomer composites for skeletal regeneration: A review. *Materials Science and Engineering: C*, 53, 175-188. doi:10.1016/j.msec.2015.04.035

Materials Science and Engineering C 53 (2015) 175–188

Contents lists available at ScienceDirect

Materials Science and Engineering C

journal homepage: www.elsevier.com/locate/msec

Bioactive glass reinforced elastomer composites for skeletal regeneration: A review

Ehsan Zeimaran^a, Sara Pourshahrestani^a, Ivan Djordjevic^{a,*}, Belinda Pinguan-Murphy^a, Nahrizul Adib Kadri^a, Mark R. Towler^{a,b}

^a Department of Biomedical Engineering, Faculty of Engineering, University of Malaya, Kuala Lumpur 50603, Malaysia
^b Department of Mechanical & Industrial Engineering, Ryerson University, Toronto M5B 2K3, ON, Canada

ARTICLE INFO

Article history:
Received 27 January 2015
Received in revised form 2 April 2015
Accepted 21 April 2015
Available online 22 April 2015

Keywords:
Elastomers
Bioactive glass
Composites
Scaffolds
Bone tissue engineering
Bioactivity

ABSTRACT

Biodegradable elastomers have clinical applicability due to their biocompatibility, tunable degradation and elasticity. The addition of bioactive glasses to these elastomers can impart mechanical properties sufficient for hard tissue replacement. Hence, a composite with a biodegradable polymer matrix and a bioactive glass filler can offer a method of augmenting existing tissue. This article reviews the applications of such composites for skeletal augmentation.

© 2015 Elsevier B.V. All rights reserved.

Contents

1. Introduction	176
2. Bioglass materials: concept and performance	176
2.1. Cellular response to bioglass materials	176
2.2. Antibacterial activity of bioglass materials	176
3. Scaffold guided tissue engineering and scaffold materials	177
3.1. Polymers: general requirements for bone regeneration	177
3.2. Elastomers as biomimetic scaffold materials	177
4. Elastomer/bioglass composite scaffolds	177
4.1. Composite scaffolds: fabrication techniques	177
4.2. Thermoplastic elastomer/bioglass composites	178
4.2.1. Poly (α -caprolactone) based thermoplastic elastomers	178
4.2.2. Poly (hydromycolanate) (PHA) based composites	180
4.2.3. Composite of polyurethane/bioglass	181
4.3. Thermoset polyester/bioglass elastomer composites	182
4.3.1. Poly (diacrylate)	182
4.3.2. Poly (glycerol sebacate)	182
5. Composite materials from natural elastomers and bioglass	183
6. The effect of filler size: polymer/bioglass nano- and micro-composites	184
7. Conclusion and future perspectives	185
Acknowledgments	185
References	186

* Corresponding author.
E-mail address: ivan.djordjevic@um.edu.my (I. Djordjevic).

<http://dx.doi.org/10.1016/j.msec.2015.04.035>
0928-4931/© 2015 Elsevier B.V. All rights reserved.

Ehsan Zeimaran, Sara Pourshahrestani, Belinda Pinguan-Murphy, Nahrizul Adib Kadri, Hussin A. Rothan, Rohana Yusof, Mark R. Towler, Ivan Djordjevic, (2015). Fabrication and characterization of poly (octanediol citrate)/gallium-containing bioglass microcomposite scaffolds. *Journal of Materials Science*, 50(5), 2189-2201. doi:10.1007/s10853-014-8782-2

J Mater Sci (2015) 50:2189–2201
DOI 10.1007/s10853-014-8782-2

Fabrication and characterization of poly(octanediol citrate)/gallium-containing bioglass microcomposite scaffolds

Ehsan Zeimaran · Sara Pourshahrestani · Belinda Pinguan-Murphy · Nahrizul Adib Kadri · Hussin A. Rothan · Rohana Yusof · Mark R. Towler · Ivan Djordjevic

Received: 22 July 2014 / Accepted: 11 December 2014 / Published online: 24 December 2014
© Springer Science+Business Media New York 2014

Abstract Bone can be affected by osteosarcomae requiring surgical excision of the tumor as part of the treatment regime. Complete removal of cancerous cells is difficult and conventionally requires the removal of a margin of safety around the tumor to offer improved patient prognosis. This work considers a novel series of composite scaffolds based on poly(octanediol citrate) (POC) impregnated with gallium-based bioglass microparticles for possible incorporation into bone following tumor removal. The objective of this research was to fabricate and characterize these scaffolds and subsequently report on their mechanical and biological properties. The porous microcomposite scaffolds with various concentrations of bioglass (10, 20, 30 wt%) incorporated were fabricated using a salt leaching technique. The scaffolds exhibited compression modulus in the range of 0.3–7 MPa. The addition of bioglass increased the mechanical properties even though porosity increased. Furthermore, increasing the concentration of bioglass had a significant influence on glass transition temperature from 2.5 °C for the pure polymer to around 25 °C for 30 % bioglass-containing composite. The ion release study revealed that composites containing 10 % bioglass had the highest ion release ratio after 28 days of soaking in

phosphate buffered saline. The interaction of bioglass phase with POC led to the formation of additional ionic crosslinks aside from covalent crosslinks which further resulted in increased stiffness and decreased weight loss. The osteoblast cells were well attached and growth on composites and collagen synthesis increased particularly with the 10 % bioglass concentration.

Introduction

Bone defects caused by tumor reconstruction, chronic infection, or traumatic bone loss create a major surgical problem [1]. The majority of fractures heal well under standard conservative or surgical therapy. However, extended bone defects following trauma or cancer resection or non-unions of fractures may require more sophisticated treatments [2]. The accepted clinical standard for bone defect treatment and nonunion is autologous bone grafting. This treatment presents serious problems with donor site morbidity, prolonged operation time, and the limited availability of graft materials [3]. Allograft bone also has concerns related to disease transmission risk and infection, explaining why synthetic bone grafts are increasingly being employed in the clinical field [1]. Certain biomaterials can repair or replace damaged or diseased tissue by mimicking the natural extracellular matrix (ECM) [4]. Bio-resorbable scaffolds degrade in situ and minimize the need for additional surgery to remove the implant [5]. An ideal scaffold should degrade at a rate compatible with the rate of bone growth, physically creating open space for new bone formation until full regeneration is achieved. From a mechanical viewpoint, an ideal bone scaffold must provide sufficient mechanical support for preserving tissue volume and consequently promotion of tissue regeneration [6].

E. Zeimaran · S. Pourshahrestani · B. Pinguan-Murphy · N. A. Kadri · M. R. Towler · I. Djordjevic (✉)
Department of Biomedical Engineering, Faculty of Engineering,
University of Malaya, 50603 Kuala Lumpur, Malaysia
e-mail: ivandjordjevic@hotmail.com

H. A. Rothan · R. Yusof
Department of Molecular Medicine, Faculty of Medicine,
University of Malaya, 50603 Kuala Lumpur, Malaysia

M. R. Towler
Department of Mechanical & Industrial Engineering, Ryerson
University, Toronto, ON M5B 2K3, Canada

➤ Research article

Ehsan Zeimaran, Sara Pourshahrestani, Ivan Djordjevic, Belinda Pinguan-Murphy, Nahrizul Adib Kadri, Anthony W. Wren, Mark R. Towler, (2016). Antibacterial properties of poly (octanediol citrate)/gallium-containing bioglass composite scaffolds. *Journal of Materials Science: Materials in Medicine*, 27(1), 1-11. doi: 10.1007/s10856-015-5620-2

J Mater Sci: Mater Med (2016) 27:18
DOI 10.1007/s10856-015-5620-2



DELIVERY SYSTEMS

Antibacterial properties of poly (octanediol citrate)/gallium-containing bioglass composite scaffolds

Ehsan Zeimaran¹ · Sara Pourshahrestani¹ · Ivan Djordjevic¹ · Belinda Pinguan-Murphy¹ · Nahrizul Adib Kadri¹ · Anthony W. Wren² · Mark R. Towler^{1,3}

Received: 9 April 2015 / Accepted: 5 November 2015 / Published online: 16 December 2015
© Springer Science+Business Media New York 2015

Abstract Bioactive glasses may function as antimicrobial delivery systems through the incorporation and subsequent release of therapeutic ions. The aim of this study was to evaluate the antimicrobial properties of a series of composite scaffolds composed of poly(octanediol citrate) with increased loads of a bioactive glass that releases zinc (Zn^{2+}) and gallium (Ga^{3+}) ions in a controlled manner. The antibacterial activity of these scaffolds was investigated against both Gram-positive (*Staphylococcus aureus*) and Gram-negative (*Escherichia coli*) bacteria. The ability of the scaffolds to release ions and the subsequent ingress of these ions into hard tissue was evaluated using a bovine bone model. Scaffolds containing bioactive glass exhibited antibacterial activity and this increased in vitro with higher bioactive glass loads; viable cells decreased to about 20 % for the composite scaffold containing 30 % bioactive glass. The Ga^{3+} release rate increased as a function of time and Zn^{2+} was shown to incorporate into the surrounding bone.

1 Introduction

The stiffness and strength of a hard tissue scaffold should be matched with those of natural bone [1]. The mechanical properties of scaffolds are highly dependent on both fabrication technique and porosity; the latter being small enough to facilitate load bearing but large enough to encourage vascularization [2]. Engineered scaffolds for self-regenerative applications not only provide a framework for tissue repair but can also act as carriers for antimicrobial agents. The scaffold should be designed to promote cell adhesion for target tissues whilst also preventing bacterial adhesion and biofilm formation. Infections associated with surgical implants require long periods of antibiotic therapy and usually implant removal and replacement is the only remedy once a mature bacterial biofilm is formed [3].

A biofilm is a microbially derived sessile community characterized by cells that are irreversibly attached to an interface or to one another. Embedded in an extracellular matrix that the attached bacteria have produced, these cells exhibit an altered phenotype with respect to growth rate and gene transcription [4]. Infections by biofilm formation, following hip joint replacement, account for 7 % of all revision surgeries [5]. Such infections are difficult to detect, are tolerant to host defense mechanisms and antibiotics, and can lead to endocarditis [6]. A strategy to prevent or inhibit biomaterial-associated infection is to use materials which are resistant to bacterial infection [7]. There is evidence to suggest that a surface engineering strategy based on a coating comprised of zinc (Zn^{2+}), where ions elute in a controlled manner to the surface could reduce infection. Many pathogenic microorganisms mediate their resistance to inhibitory substances via biofilm formation [8]. Due to both the development of resistant

✉ Mark R. Towler
mtowler@ryerson.ca

¹ Department of Biomedical Engineering, Faculty of Engineering, University of Malaya, 50603 Kuala Lumpur, Malaysia

² Inamoni School of Engineering, Alfred University, Alfred, NY, USA

³ Department of Mechanical and Industrial Engineering, Faculty of Engineering and Architectural Science, Ryerson University, 350 Victoria Street, Toronto, ON M5B 2K3, Canada

➤ Research article


Ehsan Zeimaran, Saktiswaren Mohan, Sara Pourshahrestani, Belinda Pinguan-Murphy, Nahrizul Adib Kadri, Malliga Raman Murali, Hanumantha Rao Balaji Raghavendran, Khairunnisa Hasikin, Tunku Kamarul, Mark R. Towler, (2016). Osteogenic differentiation of mesenchymal stem cells on a poly (octanediol citrate)/bioglass composite scaffold *in vitro*. *Materials & Design*, 109, 434-442. doi: <http://dx.doi.org/10.1016/j.matdes.2016.07.096>

Materials and Design 109 (2016) 434–442

Contents lists available at ScienceDirect

Materials and Design

Journal homepage: www.elsevier.com/locate/matdes

 CrossMark

Osteogenic differentiation of mesenchymal stem cells on a poly (octanediol citrate)/bioglass composite scaffold *in vitro*

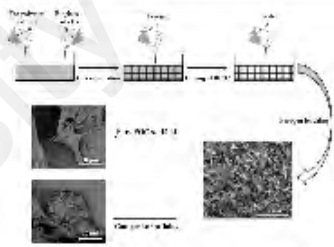
Ehsan Zeimaran ^a, Saktiswaren Mohan ^b, Sara Pourshahrestani ^a, Belinda Pinguan-Murphy ^a, Nahrizul Adib Kadri ^{a,*}, Malliga Raman Murali ^b, Hanumantha Rao Balaji Raghavendran ^b, Khairunnisa Hasikin ^a, Tunku Kamarul ^b, Mark R. Towler ^{a,c,**}

^a Department of Biomedical Engineering, Faculty of Engineering, University of Malaya, 50603 Kuala Lumpur, Malaysia
^b Biome Engineering Group (TEG), National Orthopaedic Centre of Excellence in Research and Learning (NOCEBML), Department of Orthopaedic Surgery, Faculty of Medicine, University of Malaya, 50603 Kuala Lumpur, Malaysia
^c Department of Mechanical & Industrial Engineering, Ryerson University, Toronto M5B 2K3, ON, Canada

HIGHLIGHTS

- The responses of mesenchymal stem cells to a poly (octanediol citrate)-bioglass composite scaffold were evaluated *in vitro*.
- Mesenchymal stem cells appeared to flatten on the neat scaffold while maintaining rounded shape on the composite scaffolds.
- Composite scaffolds showed enhanced osteogenic differentiation compared to the unfilled poly (octanediol citrate) scaffold.

GRAPHICAL ABSTRACT



The graphical abstract illustrates the experimental setup and results. It shows a schematic of a scaffold structure with cells on top. Below this, there are SEM images showing cells on a neat scaffold and on a composite scaffold. The composite scaffold shows cells that are more rounded and flattened compared to the neat scaffold.

ARTICLE INFO

Article history:
Received 15 June 2016
Received in revised form 14 July 2016
Accepted 18 July 2016
Available online 20 July 2016

Keywords:
Composite scaffold
Bioactive glass
Human bone marrow mesenchymal stem cells
Osteogenic differentiation
Bone tissue engineering

ABSTRACT

This study investigated the effect of composite scaffolds composed of poly (octanediol citrate) (POC) and a bioactive glass (composition, 48SiO₂-12%CaO-32%ZnO-8%Ca₂P₂O₇) on the growth and osteogenic differentiation of human bone marrow-derived mesenchymal stem cells (hBMSCs). All the scaffolds, regardless of the amount of bioglass incorporation, were able to support the growth of hBMSCs and guide their osteogenic differentiation without osteogenic media stimulation. The expression of bone-associated genes (runx-related transcription factor 2, type I collagen, bone morphogenetic protein 2, osteonectin and osteocalcin) was significantly increased by a culture time of up to 2 weeks, particularly for the composite scaffold loaded with 10% bioactive glass. The composite scaffold significantly stimulated alkaline phosphatase (ALP) activity compared to the pure POC scaffold. Cellular mineralization of the secreted extracellular matrix illustrated a higher calcium level on the composites than on the pure POC and increased with culture time. These results suggest that composite scaffolds of POC and a bioactive glass can provide favourable conditions for osteogenic differentiation of hBMSCs and can potentially be used to induce bone healing and regeneration.

© 2016 Elsevier Ltd. All rights reserved.

* Corresponding author.
** Correspondence to: M.R. Towler, Department of Biomedical Engineering, Faculty of Engineering, University of Malaya, 50603 Kuala Lumpur, Malaysia.
E-mail addresses: nahrizuladib@um.edu.my (N.A. Kadri), mtowler@ryerson.ca (M.R. Towler).

<http://dx.doi.org/10.1016/j.matdes.2016.07.096>
0254-1275/© 2016 Elsevier Ltd. All rights reserved.

- Conference paper

Ehsan Zeimaran, Sara Pourshahrestani, Ivan Djordjevic, Belinda Pinguan-Murphy, Nahrizul Adib Kadri, Mark R. Towler, (2015). Poly (octanediol citrate)/Gallium-containing bioglass microcomposite scaffolds. *Society for Biomaterials*, USA.

Poly (octanediol citrate)/Gallium-containing bioglass microcomposite scaffolds

Ehsan Zeimaran¹, Sara Pourshahrestani¹, Ivan Djordjevic¹, Belinda Pinguan-Murphy¹, Nahrizul Adib Kadri¹, Mark R. Towler^{1,2}

¹Department of Biomedical Engineering, Faculty of Engineering, University of Malaya, Kuala Lumpur 50603, Malaysia.

²Department of Mechanical & Industrial Engineering, Ryerson University, Toronto M5B 2K3, ON, Canada.

Statement of Purpose: Bone defects caused by tumor reconstruction, chronic infection or traumatic bone loss create a major surgical problem [1]. In recent years development of bioresorbable tissue engineering scaffolds has advanced due to their ability to support the formation of newly grown tissue. Gallium compounds have utility in the treatment of diseases characterized by accelerated bone loss [2]. This paper describes a novel composite scaffold fabricated from poly (octanediol citrate) (POC) and gallium-containing bioglass.

Methods: Composite scaffolds were prepared by employing a salt-leaching method. The POC pre-polymer was dissolved in dioxane to obtain a 20% solution. Then, different concentrations (10, 20 and 30 wt%) of melt derived bioactive glass (0.48SiO₂-0.12CaO-0.32ZnO-0.08Ga₂O₃, molar fraction) with particle size below 45 μm were added to the solution. Following that, sieved NaCl (200-300 μm) was added and the mixture was stored at 80°C for one week. Then, NaCl was washed for 4 days in distilled water. Once the washing was completed, the resultant scaffolds were frozen at -80 °C and lyophilized using a freeze-dryer. Scaffold morphology was investigated by field emission scanning electron microscopy (FESEM, Zeiss-Auriga laser, Germany). The samples were placed on aluminum stubs (8 mm diameter) and images were recorded at various magnifications using an accelerated voltage of 15 kV. The cylindrical scaffolds were subsequently evaluated mechanically using an Instron 5544 (USA) mechanical tester, fitted with a 2 KN load cell. Samples were compressed to 50% of initial volume.

Results: Table 1 reports the compression modulus (E_c) of the scaffolds which were seen to increase with the addition of bioglass. Figure 1 shows the porous structure of the scaffolds.

Table 1: Compression modulus of POC-BG scaffolds.

Property	POC	POC-BG-10%	POC-BG-20%	POC-BG-30%
E _c (MPa)	0.31 ± 0.10	2.60 ± 0.69	4.00 ± 1.00	6.78 ± 1.62

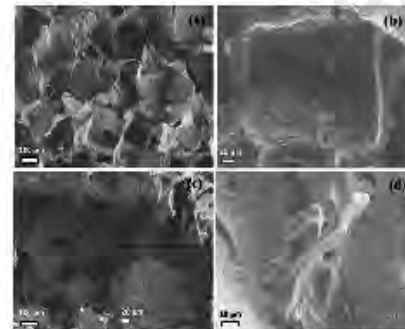


Figure 1: Microstructure of scaffolds observed by FESEM: (a) POC; (b) POC-BG-30%; (c) POC-BG-20%; and (d) POC-BG-10%.

Conclusions: The objective of the study was to fabricate gallium-containing composite scaffolds for potential scaffolding applications in human bone.

The observation of the porous structure of the scaffolds by FESEM demonstrated the glass particles were well-dispersed and the scaffolds had interconnected pores with pore size ranging from 200-300 μm suitable for cell migration and tissue growth [3]. However large particles were not fully embedded into the matrix which can be readily debonded and consequently reduce the composite strength [4].

Addition of bioglass to the polymer had a significant influence on the compression moduli as a result of enhanced physical crosslinks (metallic carboxylic bonds).

Although stiffness of materials increased by addition of bioglass, it is still lower than natural cancellous bone. Thus, the composite scaffolds have only potential to be used as filling in hard tissue surgery where there is an external support [5].

References:

- [1] Nishida, J. and Shimamura, T. *Medical Science Monitor Basic Research*. 2008;14:RA107-RA113.
- [2] Warrell, R. P. *Cancer*. 1997;80:1680-1685.
- [3] Bose, S. et al. *Trends in biotechnology*. 2012;30:546-554.
- [4] Fu S. Y. et al., *Composites Part B: Engineering*. 2008;39:933-961.
- [5] Ródenas-Rochina, J. et al. *Journal of Materials Science: Materials in Medicine*. 2013;24:1293-1308.

- Conference paper

Ehsan Zeimaran, Sara Pourshahrestani, Belinda Pinguan-Murphy, Nahrizul Adib Kadri, Mark R. Towler, (2016). Osteoblast responses of Poly (octanediol citrate)/Gallium-containing bioglass composite scaffolds *10th World Biomaterials Congress*, Canada.

Osteoblast responses of Poly (octanediol citrate)/Gallium-containing bioglass composite scaffolds

Ehsan Zeimaran¹, Sara Pourshahrestani¹, Belinda Pinguan-Murphy¹, Nahrizul Adib Kadri¹, Mark R. Towler^{1,2}

¹Department of Biomedical Engineering, Faculty of Engineering, University of Malaya, Kuala Lumpur 50603, Malaysia.

²Department of Mechanical & Industrial Engineering, Ryerson University, Toronto M5B 2K3, ON, Canada.

Introduction: Engineered scaffolds for self-regenerative applications should provide the necessary support for cells to attach, proliferate and facilitate ingrowth [1]. Gallium compounds have shown to inhibit resorption and differentiation of osteoclast without negatively affecting osteoblast activity as well as increasing the synthesis and content of type I collagen [2, 3]. This work considers the osteoblast-like cells responses of composite scaffolds made up poly (octanediol citrate) (POC) and gallium-containing bioglass.

Materials and Methods: Composite scaffolds of POC and different portions (10, 20 and 30 wt%) of a melt-derived bioglass (0.48SiO₂-0.12CaO-0.32ZnO-0.08Ga₂O₃, molar fraction) were prepared by employing a salt-leaching method. The scaffolds were sterilised and human Osteoblast cells were cultured for 7 days into the scaffolds (1×10⁷/scaffold) and then fixed with 3% glutaraldehyde. After that, the scaffolds were washed with PBS and dehydrated in a serial ethanol. Then the samples were freeze-dried, sputtercoated with gold and observed under SEM (HitachiS-530). Real-Time PCR was carried out using Syber green™ fluorescent dye (Applied Biosystems, USA) to evaluate the expression of genes of interest. The primers used as follows: type I collagen (COL1-F-5-CCTGGATGCCATCAAAGTCT-3 and COL1-R-5-GAATCCATCGGTCATGCTCT-3) and type III collagen (COL3-F-5-CTAAAGGGGAAGATGGCAAG-3 and COL3-R-5-TTCCCATCACTTCCTGGTC-3). After 7 days in culture indirect Immunostaining was performed using a mouse antibody specific to type I collagen (abcam, USA, cat. # ab90395) or type III collagen (abcam, USA, cat. # ab3610). The mouse antibodies were added separately and the cells were incubated overnight at 4°C. The cells were washed with PBS and incubated for 30 min with an anti-mouse IgG labeled with FITC fluorescent dye (Invitrogen, USA, cat. # 62-6511).

Results and discussion: Figure 1a shows the cell morphology on the scaffold seeded for 7 days. The results indicate that the cells are well-adhered and spread throughout the surface and the walls of pores of POC-BG-10% and formed a confluent cells sheet on the scaffold. Figure 1b exhibits the comparison of osteoblast type I and III collagen expression for composite scaffolds. The POC-BG-10% composite showed a remarkably higher expression of type I and III collagens compared to the other composites.

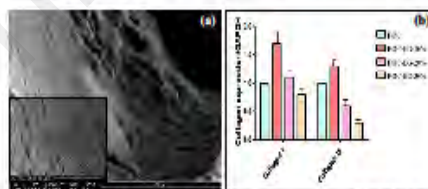


Figure 1: (a) SEM image of osteoblast attachment on POC-BG-10%, and (b) gene expression of collagen I and collagen III on composite scaffolds in comparison to POC scaffold used as control after 7 days in culture.

The green fluorescence indicated the expression of both type I and III collagen proteins (Figure 2). Although all the scaffolds cultured by

osteoblasts positively expressed both type I and III collagens, the staining had significantly higher intensity and distribution for POC-BG- 10 % for both collagen types. This can be attributed to the ionic dissolution products of bioglass which may upregulate the gene expression and enhance the collagen synthesis [4].

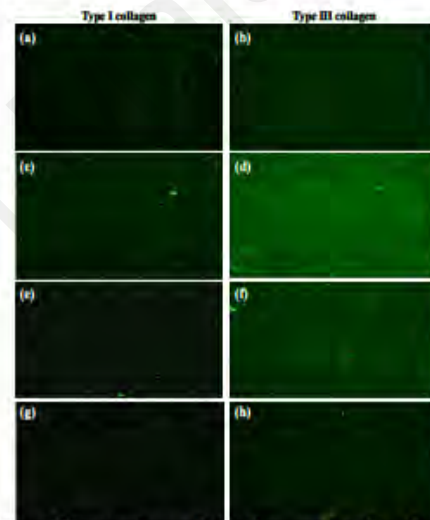


Figure 2: Fluorescent images of indirect immunostaining of type I and III collagen synthesis on composite scaffolds: (a,b) pure POC, (c,d) POC-BG-10%, (e,f) POC-BG-20%, and (g,h) POC-BG-30%.

Conclusions: This paper proposes that gallium can positively influence osteoblast responses. Composite scaffolds had favorable influence on collagen formation by seeded osteoblast cells. However composite containing 10% bioglass indicated enhanced both type I and III collagen expression in comparison to the other samples. Thus it can be concluded that there is a threshold for bioglass concentration in which osteoblast cell attachment and collagen secretion increase.

References:

- [1] Zeimaran, E., et al., *Materials Science and Engineering: C*, 2015, 53: p. 175-188.
- [2] Warrell, R.P., *Cancer*, 1997, 80(S8): p. 1680-1685.
- [3] Verrou, E., et al., *British journal of pharmacology*, 2010, 159(8): p. 1681-1692.
- [4] Xynos, I.D., et al., *Biochemical and biophysical research communications*, 2000, 276(2): p. 461-465.

